Transcriptional gene silencing mutants in *Arabidopsis thaliana* and their impact on nuclear architecture and heterochromatin organization

Friedrich Miescher Institut

Inauguraldissertation

zur

Erlangung der Würde eines Doktors der Philosophie

vorgelegt der

Philosophisch-Naturwissenschaftlichen Fakultät der Universität

Basel

von

Aline Valeska Probst

aus Deutschland

Basel, 2004

TABLE OF CONTENTS

I. Mittelsten Scheid, O., Probst, A.V., Afsar, K., and Paszkowski, J. (2002). Two regulatory levels of transcriptional gene silencing in Arabidopsis. Proc Natl Acad Sci U S A 99, 13659-13662.
II. Probst, A.V., Fransz, P.F., Paszkowski, J., and Mittelsten Scheid, O. (2003). Two means of transcriptional reactivation within heterochromatin. Plant J 33, 743-749.
III. Tariq, M., Saze, H., Probst, A.V., Lichota, J., Habu, Y., and Paszkowski, J. (2003). Erasure of CpG methylation in Arabidopsis alters patterns of histone H3 methylation in heterochromatin. Proc Natl Acad Sci U S A.
IV. Takeda, S., Tadele, Z., Hofmann, I., Probst, A.V., Angelis, K.J., Kaya, H., Araki, T., Mengiste, T., Mittelsten Scheid, O., Shibahara, K., Scheel, D., and Paszkowski, J. (2004). BRU1, a novel link between responses to DNA damage and epigenetic gene silencing in Arabidopsis. Genes Dev 18, 782-793.
V. Probst, A.V., Fagard, M., Proux, F., Mourrain, P., Boutet, S., Earley, K., Lawrence, R.J., Pikaard, C.S., Murfett, J., Furner, I., Vaucheret, H., and Mittelsten Scheid, O. (2004). Arabidopsis histone deacetylase HDA6 is required for maintenance of transcriptional gene silencing and determines nuclear organization of rDNA repeats. Plant Cell 16, 1021-1034.

1. SUMMARY

The epigenetic regulation of gene expression is defined by covalent modifications of DNA and histone tails as well as by chromatin structure and nuclear architecture. Maintenance of epigenetic states therefore requires proteins engaged in chromatin remodeling, histone modifications, DNA replication and methylation. Using Fluorescence *In Situ* Hybridization, immunolocalization, genetic as well as molecular biology techniques I investigated chromatin structure and properties in *Arabidopsis* mutants impaired in the maintenance of transcriptional gene silencing (TGS). I showed that silencing of a multicopy transgenic locus results in neo-heterochromatin formation, accompanied by hypermethylation of DNA and of histone H3K9, two modifications enriched also in constitutive heterochromatin. Loss of the SWI2/SNF2 chromatin-remodeling factor DDM1 involved in maintenance of DNA methylation patterns, but also lack of functional protein MOM1 release silencing from specific repetitive targets. While the reactivation in *ddm1* mutants is accompanied by a significant decondensation of heterochromatin and changes in histone modification patterns, *mom1* allows transcription within a heterochromatic environment without disturbing DNA and histone methylation. An analysis of epistasis revealed that the nuclear MOM1 protein is part of a novel, methylation-independent pathway. Therefore decondensation of heterochromatin may accompany transcriptional activation, but it is not an obligate prerequisite. However, both pathways may act synergistically, as shown by the additive effects of reactivation, chromatin and phenotype aberrations in *mom1/ddm1* double mutants. Within the methylation-based pathway, the different chromatin modifications are interrelated since the correct setting of H3K9 methylation marks depends on CpG methylation. In the complete absence of CpG methylation, histone H3 methylated at K9 becomes redistributed away from the chromocenters. Heterochromatin structure at the chromocenters, however, can be maintained even in the absence of both modifications previously assumed to be essential for heterochromatin formation and maintenance. In addition to the factors influencing chromatin properties globally, other components seem to have more specific targets, as loss of functional histone de-acetylase 6 results in hyperacetylation and DNA methylation changes preferentially at rDNA loci.

In general, the work presented here revealed several connections between chromatin shape and modifications at transgenic and endogenous parts of the genome and added to our insight into the complexity of epigenetic transcriptional regulation in *Arabidopsis*.

2. ABRREVIATIONS

aa:	amino acids
ASF1:	Anti-Silencing Factor 1
ATP:	Adenosine Triphosphate
AXE:	Auxin-inducible Expression
BAC:	Bacterial Artificial Chromosome
BRU1:	Brushy 1
BSA:	Bovine Serum Albumin
CAF-1:	Chromatin Assembly Factor 1
CaMV:	Cauliflower Mosaic Virus
ChIP:	Chromatin Immunoprecipitation
CHS:	Chalcone Synthase
CMT3 :	Chromomethylase 1
Col:	Columbia
CTP:	Cytidine triphosphate
DAPI:	4'-6-diamidino-2-phenylindole
DDM1:	Decrease in DNA Methylation1
DEPC:	Diethyl pyrocarbonate
DIG:	Digoxigenin
DMSO:	Dimethyl Sulfoxide
DRM:	Domain Rearranged Methyltransferase
DSB:	Double Stranded Break
FISH:	Fluorescent In Situ Hybridization
FITC:	Fluorescein isothiocyanate
FLC:	Flowering Locus C
GFP:	Green Fluorescent Protein
GTP:	Guanine Triphosphate
GUS:	Glucuronidase
HA:	Influenza A virus hemagglutinin
HAT:	Histone Acetyltransferase
HDAC:	Histone De-Acetylase
HP1:	Heterochromatin Protein 1
HPT:	Hygromycin Phospho Transferase
HR:	Homologous Recombination

HRP:	Horse Reddish Peroxidase
KYP:	KRYPTONITE
LBR:	Lamin B Receptor
Ler:	Landsberg erecta
LSH:	Lymphoid specific helicase
MAR:	Matrix Attachment Region
MBD:	Methyl-DNA Binding Domain
MES:	(N-morpholino)ethanesulfonic acid)
MFP1:	MAR binding filament-like protein 1 (MFP1)
MMS:	Methyl Methane Sulfonate
MOM1:	Morpheus Molecule1
MS:	Murashige and Skoog
NHEJ:	Non-Homologous End Joining
NLS:	Nucleus Localization Sequence
NOR:	Nucleolus Organizer Region
NPT:	Neomycine Phoshotransferase
NTP:	Nucleotide Triphosphate
OD:	Optical Density
PBS:	Phosphate-buffered saline
PCNA:	Proliferating Cell Nuclear Antigen
PCR:	Polymerase Chain Reaction
PEG:	PolyEthylene Glycol
PEV:	Position Effect Variegation
PFA:	Paraformaldehyde
PIPES:	Piperazine-N,N'-bis[2-ethanesulfonic acid]
PMSF:	Phenylmethyl Sulphonyl Fluoride
PTGS:	Post-Transcriptional Gene Silencing
RCAF:	replication-coupling assembly factor
RIP:	Repeat-Induced Point Mutations
RISC:	RNA Induced Silencing Complex
RITS:	RNA-induced Initiation of Transcriptional Gene Silencing
RPD3:	Reduced Potassium Dependency 3
RT:	Room Temperature
RTS1:	RNA-mediated Transcriptional Silencing
SDS:	Sodium Dodecyl Sulfate

SET:	Su(*var*)3-9, E(Z) and Trithorax
SIL1:	modifier of silencing 1
SIR:	Silent Information Regulator
SSC:	Sodium chloride/sodium citrate
SUP:	SUPERMAN
T-DNA:	Transfer-DNA
TE:	Tris-EDTA
TEMED:	N,N,N',N'-tetramethylethylenediamine
TGS:	Transcriptional Gene Silencing
TPCK:	L-1-Chloro-3-[4-tosylamido]-4-phenyl-2-butanone
TSI:	Transcriptionally Silent Information
TTP:	Thymine Triphosphate
UV:	Utra Violet
WS:	Wassilewskija
ZH:	Zürich

3. INTRODUCTION

In eucaryotic cells, most of the genetic material is organized in a complex structure termed chromatin, derived from the Greek *khroma*, denoting color, and packaged into a membrane-surrounded organelle, the nucleus. The nucleus contains the machinery responsible for essential processes like DNA replication, condensation and separation of the chromosomes into daughter cells during mitosis, as well as for the regulation of gene expression. Since every cell of an organism carries the same complement of genes, patterns of gene expression must be defined to allow differentiation and to assure proper reaction to changing environmental conditions. The expression of genes is not only determined by *cis*-acting DNA regulatory elements (e.g. enhancers and promoters) specified by nucleotide sequence, but also depends on additional mechanisms involving DNA and histone modifications and high order chromatin structure. These processes that contribute to heritable changes in gene expression and cannot be accounted for by changes in the DNA sequence were termed *epigenetic* mechanisms, '*epi*; meaning 'in addition'.

I. The functional significance of nuclear architecture

Since the early days of cytological investigations evidence existed that the interphase nucleus is characterized by a well-defined architecture (Comings, 1968; Comings, 1980). Nuclear staining techniques e.g. with DAPI (4',6'-diamidino-2-phenylindole) that forms fluorescent complexes with natural double-stranded DNA, reveals three distinct chromatin domains in the interphase nucleus: the nucleolus, heterochromatin and euchromatin (see also *Figure 2A*). Within the nucleolus, devoid of staining, ribosomal RNA genes and their products are separated from the rest of the genome. The nucleoli develop during telophase at the site of the chromosomal nucleolus organizer regions (NORs), which contain the tandemly arrayed rRNA genes. Heterochromatin, cytologically defined as chromatin that remains condensed throughout the cell cycle except during its replication (Heitz, 1928), is intensely stained, because of its high degree of condensation. Euchromatin is faintly labeled and partially decondensed. The distinction of eu- and heterochromatin was initially inferred from staining properties. Later these two compartments were characterized by their difference in gene density, content of repetitive

DNA, meiotic recombination frequency, replication timing, chromatin composition, nucleosome spacing and accessibility to nucleases (Henikoff et al., 2000).

The recent development of fluorescence *in situ* hybridization (FISH) and immunolocalization techniques as well as the use of fluorescent proteins has defined many more nuclear subcompartments, e.g. PMG, Cajal and PML bodies (Spector, 2001), and has allowed characterizing the position of single loci relative to those (Brown et al., 1997). Many non-random chromatin arrangements have been described ranging from association between NORs (Schwarzacher and Wachtler, 1983), centromeric and telomeric associations (Haaf and Schmid, 1989; Nagele et al., 2001), ectopic pairing of constitutively heterochromatic regions (Schmid et al., 1975) to somatic pairing of homologous chromosomes (Comings, 1980). FISH techniques with probes covering whole chromosomes (chromosome painting) showed that individual chromosomes occupy compact non-overlapping domains within the interphase nucleus, termed chromosome territories (Schermelleh et al., 2001). In certain plant species with larger genomes (e.g. barley and wheat) as well as in *Drosophila* polytene salivary gland nuclei (Hochstrasser et al., 1986) chromosomes are arranged in the so-called Rabl conformation (Rabl, 1885) with centromeres clustered at one and telomeres at the opposite pole (Abranches et al., 1998) (*Figure 1A*). The Rabl-orientation is possibly a relict of anaphase movement, when centromeres disjoin and move to opposite poles with chromatids and telomeres dragging behind. It suggests an interaction of both centromeres and telomeres with peripheral nuclear structures. In contrast, vertebrate chromosomes are arranged in a more complex fashion (*Figure 1B*).

Is this chromosome arrangement of functional significance and can nuclear architecture influence gene expression? Active and inactive regions of the genome as well as protein factors involved in the activation or repression of gene expression could be compartmentalized within the nucleus. Indeed, within a chromosome territory distinct active and inactive domains exist, with potentially active genes preferentially located at the periphery of the territory or extending in form of chromatin loops outwards into the intra-chromosomal domain (Volpi et al., 2000). An interesting observation is the fact that chromosomes 18 and 19 of human fibroblasts occupy relatively peripheral versus central locations (Schermelleh et al., 2001). These two chromosomes are similar in size, but differ significantly in their estimated gene content, establishing a correlation between gene density and nuclear localization: The gene-poor chromosome 18 is preferentially located at the nuclear periphery, while chromosome 19 is found in the interior of the nucleus (*Figure 1C*). A comparison of the radial distribution of human chromosome 18- and 19-

homologous chromatin in seven primate species revealed that gene-density-correlated chromatin arrangements are preserved during higher-primate genome evolution (Tanabe

Figure 1

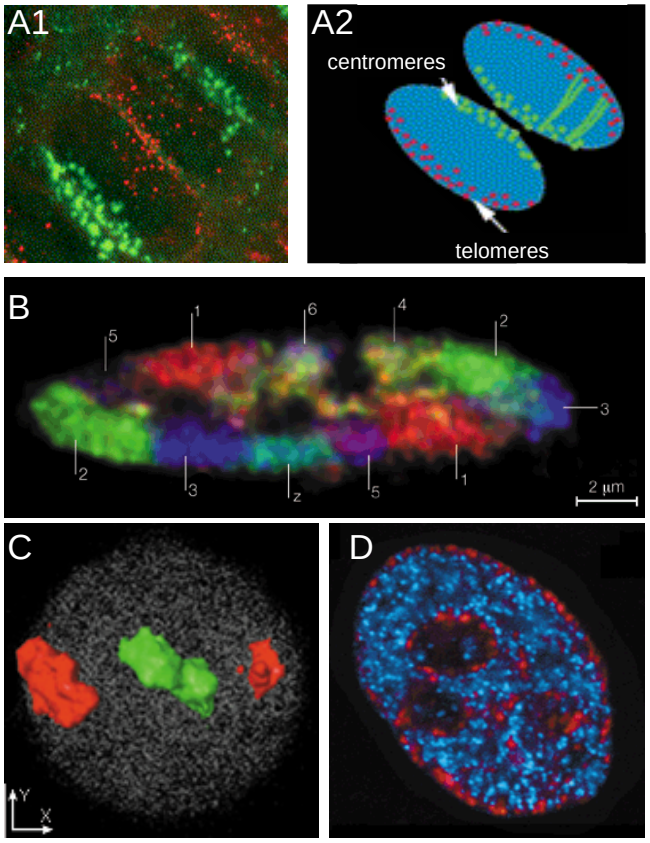

Figure 1. Chromatin arrangements in interphase nuclei
Wheat root tissue double-labeled by fluorescence in situ hybridization with probes to the centromeres (green) and telomeres (red, **A1**). Diagram showing the organization of the chromosomes as the Rabl configuration (**A2**). The chromosomes are parallel to one another, with the centromeres clustered on one side of the nuclear periphery, and the telomeres somewhat more dispersed on the other side of the nuclear periphery. (Image modified from Shaw et al, 2002). Mid-plane light optical section through a chicken fibroblast nucleus shows mutually exclusive chromosome territories (CTs) with homologous chromosomes seen in separate locations (**B**). Three-dimensional reconstructions of chromosome 18 (red; gene-poor) and 19 (green; gene-rich) territories painted in the nucleus of a human lymphocyte. Chromosome 18 territories were typically found at the nuclear periphery, whereas chromosome 19 territories were located in the nuclear interior (**C**). Mid-plane light optical section through the nucleus of a neuroblastoma cell fixed 20 h after direct two-color labeling of DNA with Cy3- and Cy5-conjugated nucleotides at early and mid-S-phase, respectively, shows typical early- (blue) and mid-replicated chromatin (red, **D**). Images B – D taken from (Cremer et al., 2001).

et al., 2002). Even between mammals and the simple polyp Hydra, two species separated at least 600 million years ago, basic features of higher order chromatin arrangements are conserved (Alexandrova et al., 2003). A correlation also exists between defined positions of chromatin and replication timing. Using replication pulse-labeling techniques it was shown that early replicating chromatin localizes in the nuclear interior while later-replicating chromatin concentrates at the nuclear periphery and around the nucleoli (*Figure 1D*) (Sadoni et al., 1999; Schermelleh et al., 2001). Similar nuclear genome architecture exists also in plants (Mayr et al., 2003). Distinct higher order compartments with DNA characterized by specific replication timing are stably maintained during all interphase stages and can be clonally inherited (Sadoni et al., 1999). Furthermore, replication pulse labeling patterns indirectly indicate the spatial organization of transcriptional activity in the nucleus, since early replicating chromatin is potentially transcriptionally active and late replicating chromatin often silenced (Sadoni et al., 1999; Schubeler et al., 2002). Changes in transcriptional activity at particular loci that occur during cellular differentiation correlate with changes in nuclear localization. Genes that become transcriptionally silent during B and T-cell development undergo dynamic repositioning in the nucleus and are localized to pericentromeric heterochromatin (Brown et al., 1997). In accord with this observation the β-globin locus is relocated away from heterochromatin compartments in the nucleus upon its activation during erythroid differentiation (Francastel et al., 2001). In Drosophila, the insertion of heterochromatin into a euchromatic gene, which results in position-effect variegation (PEV), causes the aberrant association of the gene and its homologous copy with heterochromatin (Csink and Henikoff, 1996). Genetic modifiers of PEV can affect the repression phenotype and the cytological association with heterochromatin. This suggests that heterochromatin and proteins involved in its formation provide a structural framework for the interphase nucleus. In *S. cerevisiae*, the perinuclear chromatin domains constitute areas of transcriptional repression. These domains prone to silencing are defined by the presence of perinuclear telomere clusters (Galy et al., 2000). Tethering a reporter gene flanked by an HMR silencer to the nuclear periphery enhances transcriptional repression of the reporter gene (Andrulis et al., 1998; Feuerbach et al., 2002).

If nuclear compartmentalization contributes indeed to gene expression patterns in a particular cell lineage, the clonal transmission of cell identity would require the transfer of the spatial organization of interphase through DNA replication, chromatin assembly and unpacking after mitosis to the daughter cells. Selective photobleaching of nuclei labeled via incorporation of histone H2B-GFP fusion proteins revealed a conservation of the

bleaching pattern in daughter nuclei (Gerlich et al., 2003), indicating that global chromosome positions can be transmitted through mitosis.

II. Chromosome structure and nuclear architecture in *Arabidopsis thaliana*

Arabidopsis has 5 chromosomes per haploid genome ranging in their physical length from 17 to 29 Mbps, with a size in mitotic metaphase from 1.5 –1.8μm (Koornneef et al., 2003). Compared to the average human chromosome territory with 130Mbp and ~1700 genes, an *Arabidopsis* chromosome contains three times more genes confined in only ~25Mpbs. In contrast to wheat and barley where the majority of the DNA consists of tandem repeats and transposable elements located in heterochromatic segments, the relative heterochromatin fraction in *Arabidopsis* nuclei is only ~10-15%, matching the percentage of repetitive sequences in the *Arabidopsis* genome (ArabidopsisGenomeInitiative, 2000). The heterochromatin in *Arabidopsis* is predominantly confined to the pericentromeric regions of all chromosomes and the NORs on distal ends of chromosome 2 and 4, which comprise the ribosomal 18S, 5.8S, and 25S units, together known as 45S rDNA. Pericentromeric regions and NORs contain all major tandem repeats of the *Arabidopsis* genome (Heslop-Harrison et al., 2003). Each NOR spans 3.5-4.0 Mbps in the ecotype Columbia (Col) (Copenhaver and Pikaard, 1996). In addition 1000 copies of 5S rDNA genes are located within the centromeric regions of chromosome 3, 4 and 5 (Cloix et al., 2000). Some ecotypes, e.g. Wassilevskija (WS) and Col, also contain a heterochromatic knob on the short arm of chromosome 4 that originated from the pericentromere after an inversion event (Fransz et al., 2000). The *Arabidopsis* centromeric region consists of a core accommodating the functional centromere comprising large tandem arrays of 180bp repeats. These repeats are embedded in a recombination-deficient heterochromatic region formed largely by retrotransposons and other moderately repetitive sequences (ArabidopsisGenomeInitiative, 2000; Haupt et al., 2001). This tripartite organization, a central domain of satellites that mediates spindle attachment flanked by pericentromeric heterochromatin, conforms to a general model of the structure of centromeric regions (Choo, 2001). In comparison, the centromere region of Drosophila also displays three domains, where the central and flanking domains are referred to as α- and β-heterochromatin (Miklos and Cotsell, 1990). The estimated size of the 180bp domains varies from 1.1-2.9Mb. Sequencing of part of the central domain of chromosome 5 revealed nearly equal amounts of 180bp repeats and interspersed Athila derivatives, plus 4% other sequences (Kumekawa et al., 2000). The 180bp repeats at one end of the core

were oriented oppositely to those at the other end, similar to the organization in *S. pombe* centromeres (Chikashige et al., 1989).

Figure 2

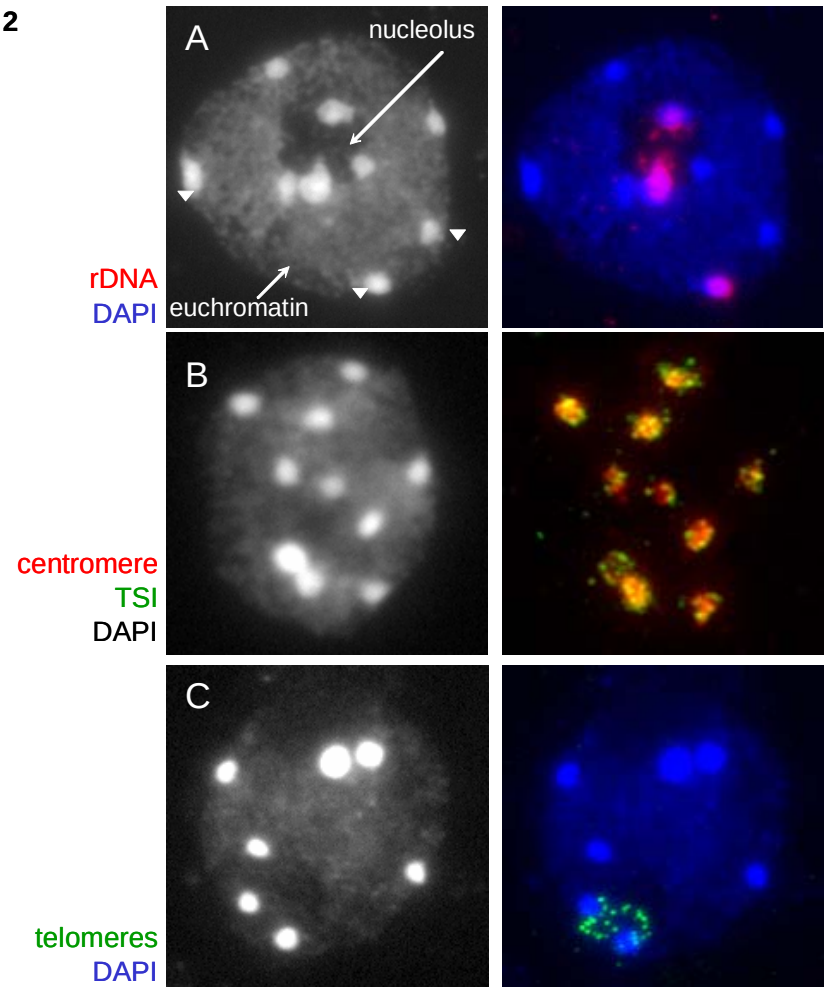

Figure 2. Distribution of the major repeats in *Arabidopsis* as revealed by Fluorescence *in situ* hybridization (FISH)
FISH for ribosomal DNA (red, **A**), the 180bp repeat probe (red, **B**), which labels the core centromeric regions of all chromosomes (Murata et al., 1994; Haupt et al., 2001), TSI (for Transcriptionally Silent Information) specific to pericentromeric repeats (red, **B**, Steimer et al., 2000), and a telomeric probe (**C**, Weiss and Scherthan, 2002). DNA is visualized by DAPI staining. Arrowheads in **A** depict the heterochromatic chromocenters.

Combining DNA staining and fluorescent *in situ* hybridization (FISH) the arrangement of the major repeats in the *Arabidopsis* genome can be visualized. In DAPI stained nuclear spreads a single nucleolus can be identified, free of DNA except single threads protruding into the nucleolar compartment. The chromocenters are DAPI bright (*Figure 2A*, arrowheads), because of the specificity of DAPI for AT clusters, enriched in pericentromeric repeats in *Arabidopsis* and mammals. The NORs (*Figure 2A*, left panel in red) are part of the chromocenters and those actively involved in rRNA transcription associate with the nucleolar compartment. In contrast, the 180bp repeats are the predominant repeats clustered in each chromocenter (*Figure 2B*, left panel), but also pericentromeric repeats are confined in the chromocenter (*Figure 2B*, exemplified by TSI repeats (Steimer et al., 2000). The chromocenters align mainly at the nuclear periphery and have the tendency to fuse, so in a diploid *Arabidopsis* plant the majority of nuclei show 8 or 9 chromocenters (Fransz et al., 2002). Telomeres are clustered around the nucleolus (*Figure 2C*). With this arrangement the *Arabidopsis* nucleus differs substantially from plants with large genomes having their chromosomes arranged in the Rabl configuration or from yeast, where the telomeres localize to the nuclear periphery and centromeres show a high incidence of clustering (Jin et al., 1998). *Arabidopsis* chromosomes also occupy nuclear territories (Lysak et al., 2001) (*Figure 3A*), with their chromocenters as organizing point and emanating euchromatic DNA loops (*Figure 3B*) (Fransz et al., 2002). The euchromatic loops range in size from 200kb up to an entire chromosome arm, since the telomeres-near NORs on chromosome 2 and 4 colocalize with the chromocenter formed by the centromeric and pericentromeric repeats of their respective chromosome (*Figure 3C*) (Fransz et al., 2002).

The formation of the described higher order chromatin structure, however, requires epigenetic modifications directly placed onto DNA and the histone proteins involved in packaging of nuclear DNA.

III. Epigenetic Modifications of DNA and Histones

III.1. DNA Methylation

Nuclear DNA can be modified by post-replicative methylation of its cytosine residues. This is the case in plants (Bender, 2004), mammals (Attwood et al., 2002), and *Neurospora crassa* (Selker et al., 2003), while in yeast, Drosophila and *C. elegans* very little or no DNA

Figure 3

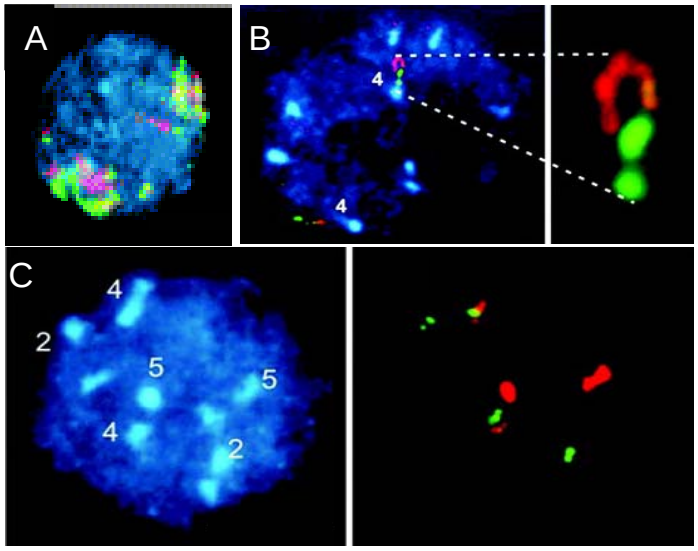

Figure 3. Chromosome territories in *Arabidopsis thaliana*
Arabidopsis chromosomes form territories. Fluorescence *in situ* hybridization (FISH) with the BACs specific for the long arm of chromosome 4 (**A**). Individual interphase chromosomes are organized as a heterochromatic chromocenter with emanating euchromatic loops. FISH with 2 BACs adjacent to the centromere of chromosome 4 reveals the formation of a small loop structure (**B**). The NOR on chromosome 4 colocalizes with the chromocenter formed by the centromeric and pericentromeric repeats, including 5S, of its respective chromosome; FISH with 5S (red) and 45SrDNA (green) (**C**). Images modified from Lysak et al., 2001 (**A**) and Fransz et al., 2002 (**B** and **C**).

methylation is found. Recent evidence indicates that DNA methylation is an important epigenetic mark essential for normal development in mammals and plants, implicated in gene silencing, imprinting, as well as transposon and X-chromosome inactivation (Heard et al., 1997; Feil and Khosla, 1999; Martienssen and Colot, 2001). In mammals and other vertebrates, methylation occurs predominantly at symmetrical CpG sites, which can be faithfully maintained through replication. Besides CpG methylation, plants also show extensive CpNpG as well as asymmetric methylation. Methylation is preferentially targeted to repeated sequences including centromere-associated repeats, rDNA and transposable elements. For this reason the 5metC content correlates with the repeat content. While in maize a quarter of all cytosines are methylated, in *Arabidopsis* only 6% carry this modification (Kakutani et al., 1999). Immunostaining experiments using *Arabidopsis* nuclei with an antibody directed against methylated cytosines reveal that most of it colocalizes with repetitive DNA clustered in the chromocenters (*Figure 5A*).

In mammals DNA methylation patterns are reprogrammed during germ cell development and in preimplantation embryos (Reik et al., 2001). In plants, however, DNA demethylation seems to occur mainly via passive de-methylation in the context of DNA replication (Saze et al., 2003), even though local, active de-methylation activity has recently been reported to play a role in imprinting (Choi et al., 2002). DNA methylation can suppress gene transcription either directly, by blocking the binding of transcription factors to the promoter or indirectly, through proteins that bind methylated DNA resulting in deacetylation of nearby histones and decreased transcription (Jones et al., 1998). The mammalian genome encodes three active methyltransferases, Dnmt1, Dnmt3a and Dnmt3b. Dnmt1, the maintenance methyltransferase, acts preferentially on hemimethylated substrates and localizes to DNA replication foci (Leonhardt et al., 1992). Mice that are homozygous for a deletion in Dnmt1 die early in development (Lei et al., 1996), and also the two *de novo* DNA methylases Dnmt3a/b are essential enzymes (Okano et al., 1999). In *A. thaliana*, three different classes of DNA methyltransferases exist, MET1, the Dnmt1 ortholog, the plant specific CMT3 (CHROMOMETHYLASE 3) and two *de novo* methyltransferases DRM (DOMAINS REARRANGED METHYLTRANSFERASE). In addition, DNA methylation patterns in *Arabidopsis* were found to depend on the presence of DDM1, a SWI2/SNF2 chromatin remodeling factor (Jeddeloh et al., 1999). SNF2 family members have seven conserved helicase motifs involved in ATP binding and hydrolysis. They allow for the physical movement of nucleosomes along the DNA driven by ATP hydrolysis to alter accessibility of chromatin to regulators of replication, transcription and repair (Yan et al., 2003).

III.2. Histone Tail Modifications

DNA methylation, although essential for those organisms that have evolved this epigenetic mark, is not found in every species known to be subject to epigenetic regulation. Chromatin proteins are good candidates to function as additional carriers of epigenetic information: In chromatin, 147bp of DNA are wrapped in 1 3/4 superhelical turns around a histone octamer forming a structure termed nucleosome. The histone octamer consists of two molecules each of histone proteins H2A, H2B, H3 and H4 with their N-terminal tails protruding from the globular domains (*Figure 4A*) (Luger et al., 1997). Linker DNA connects the neighboring histone octamers, serving as binding site for histone H1 in some organisms (Zhou et al., 1998). For many years it was believed that the role of histones is constraint to their packaging function (*Figure 4B*), that non-histone proteins carry the instructions for the activity of chromatin and that changes in gene expression are regulated by the synthesis, modification and compartmentalization of these proteins. However, in recent years it became clear that the nucleosome core particle contributes to the dynamic remodeling of chromatin during gene activation and repression and carries important epigenetic information. This information resides primarily in the histone tails, which are subject to various covalent modifications, including acetylation, methylation, phosphorylation, ubiquitination, sumoylation and ADP-ribosylation (*Figure 4C*) (Jenuwein and Allis, 2001; Berger, 2002). It has been suggested that the specific tail modifications and their combinations constitute a histone code that defines actual or potential transcriptional states (Berger, 2002). The histones are evolutionary highly conserved proteins not only in their globular domain but also in their protruding ends and their covalent modifications. This suggests that the role of histones as mediator of epigenetic information as well as the mechanism of subsequent ‘translation’ of this message into actual transcriptional activation or repression might be evolutionary conserved. In principle, despite the presence of certain species-specific details, insights gained from the study of one model organism can be conferred to other systems.

Acetylation of lysine residues was one of the first histone modifications described to correlate with transcriptional activity (Allfrey et al., 1964). Acetylation influences transcription by neutralizing the positive charge of the histone tails and decreasing their affinity for DNA, however, there is growing evidence that acetylation also helps shape the binding surface for activators and repressors (Kurdistani and Grunstein, 2003). The hypoacetylated histone H3 and H4 tails, for example, serve as a binding site for Sir3 and

Figure 4

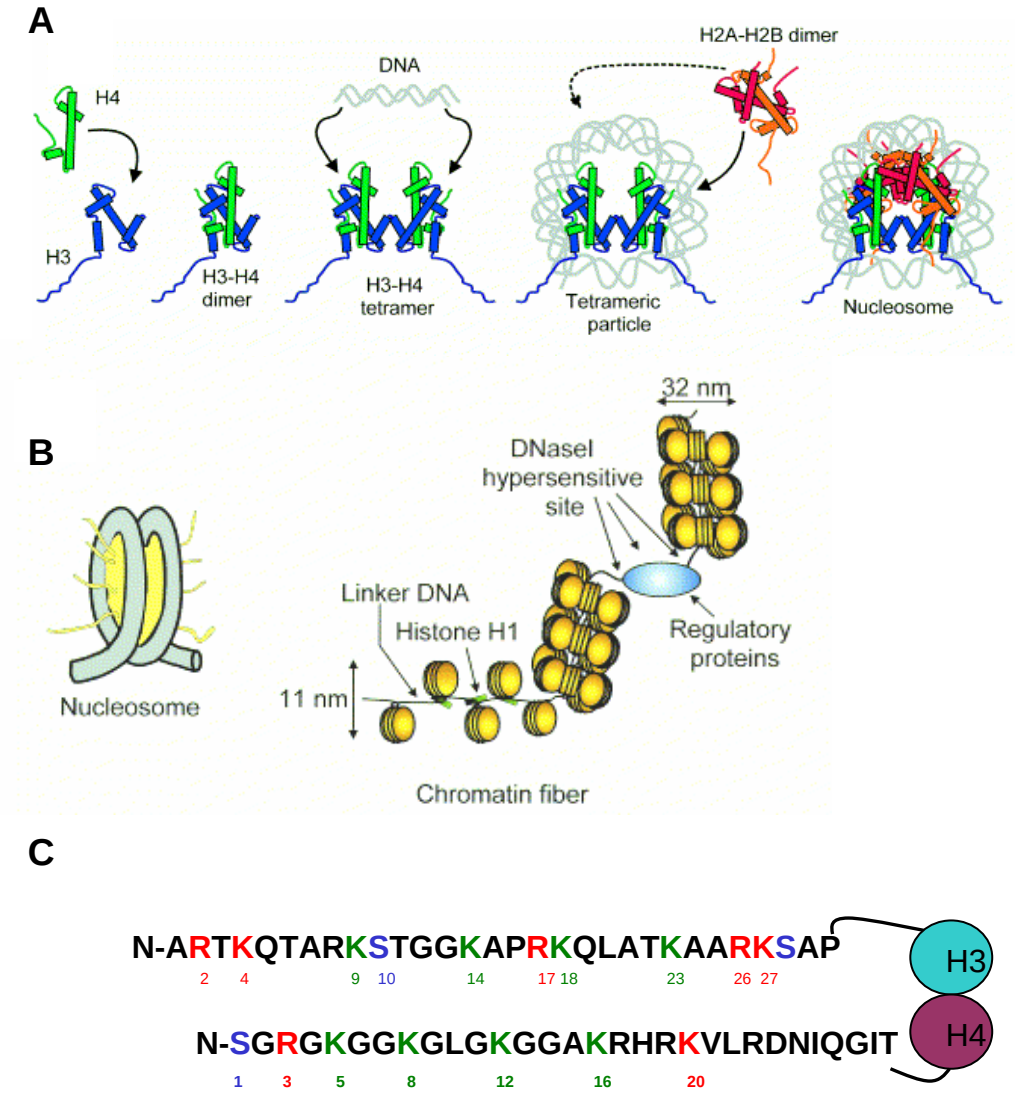

Figure 4. Structure of chromatin and covalent histone modifications Structure and assembly of the nucleosome (**A**). Organization of the chromatin fiber (**B**). Histone modifications of the N-terminal tails of histone H3 and H4 (**C**); phosphorylation sites are marked in blue, methylation sites in red and acetylation sites in green. Figure A and B are taken from Morales et al., 2001.

Sir4 proteins, which mediate heterochromatin formation at telomeres and mating type loci in *S. cerevisiae* (Hecht et al., 1995).

Histone H3 can be acetylated at lysine 9, 14, 18 and 23, while for histone H4 acetylation at lysine 5, 8, 12, 16 and 20 was described (*Figure 4*). Examples of histone acetylation are the modification of H4 K5 and K12 in the histone H3.H4 tetramere deposited into newly replicated DNA (Sobel et al., 1995) or the acetylation of H4K16 involved in dosage compensation of the male X-chromosome in *Drosophila* (Turner et al., 1992). Hypoacetylated isoforms of H4 locate to heterochromatin regions in many organisms and are involved in transcriptional gene silencing (Jeppesen and Turner, 1993; Braunstein et al., 1996; Jasencakova et al., 2000). Antibodies raised against a tetra-acetylated isoform of H4 specifically label the eurchromatic compartment in *Arabidopsis* (*Figure 5B*), clearly excluding the heterochromatic chromocenters. Staining with antibodies directed against a single acetylated lysine revealed a cell cycle dependent acetylation for H4K16 and H3K18, whereas acetylation at K5, K8 and K12 of histone H4 was always correlated with gene-rich euchromatin in *Arabidopsis* (Jasencakova et al., 2003). Acetylated lysines in the context of H3 and H4 tail sequences are recognized by the bromodomains found in many chromatin-associated proteins, e.g. in nearly all known nuclear histone acetyltransferases (HATs) and in some components of the SWI/SNF ATP-dependent chromatin remodeling complexes.

Patterns of H4 acetylation are set in part during post-replicative chromatin assembly through targeting of specific histone acetyltransferases (HATs) and de-acetylases (HDACs) to the replication fork, but reversible alterations of histone acetylation also take place during interphase (Belyaev et al., 1997). HATs are transcriptional co-activators and components of large multisubunit complexes e.g. SAGA, NuA4 (Grant et al., 1998; Sterner and Berger, 2000), and HDACs are found associated with sequence-specific regulatory factors like Sin3, NuRD, and CoREST (Ahringer, 2000; You et al., 2001). HDACs can also be recruited by high DNA methylation levels, via association with methyl-DNA binding domain (MBD) containing proteins such as MeCP2 and MBD2 (Bird and Wolffe, 1999) or directly, via recruitment by the maintenance DNA methyltransferase itself (Fuks et al., 2000). Evaluation across kingdoms indicates that HDAC families comprise conserved as well as highly divergent members (Pandey *et al.,* 2002). The large number of different HATs and HDACs suggests that they have evolved to have specific and/or overlapping roles concerning their targets. In addition, HDACs are regulated in various ways, by subcellular compartmentalization, post-transcriptional modification and interacting proteins

Figure 5

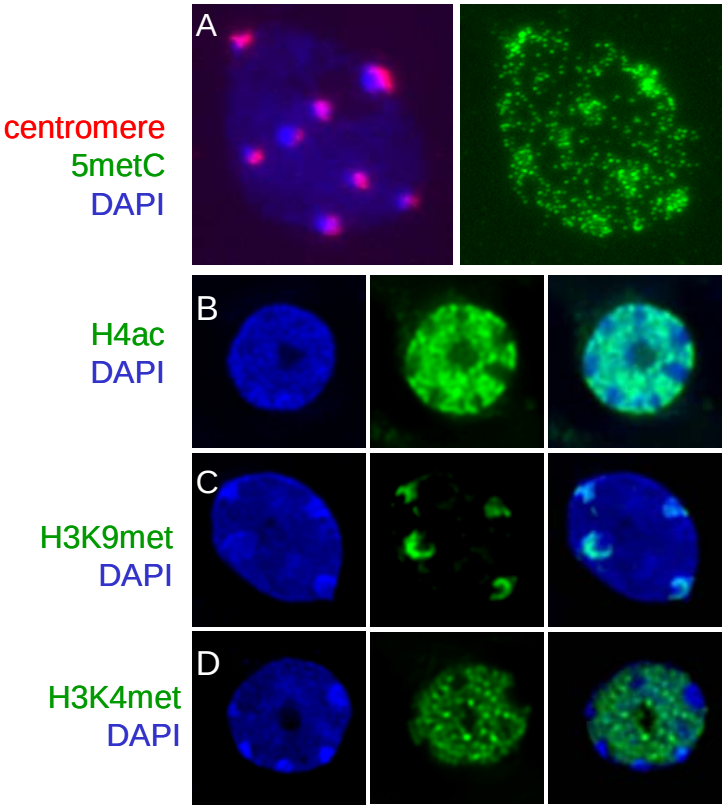

Figure 5. Distribution of 5metCytosine and histone modifications in interphase nuclei of *Arabidopsis thaliana*

FISH for 180bp repeats and immunolocalization of methylated Cytosines show that chromocenters comprise highly methylated DNA (**A**). Antibodies against H3 dimethylated at K9 specifically label the DAPI bright chromocenters, (**C**). This nearly exclusive labeling of microscopically detectable heterochromatin was specific to plant species with genome size of 500Mbp or less (Houben et al., 2003). Antibodies against tetra-acetylated H4 (**B**) and methylated H3K4 (**D**) stain euchromatin and chromocenters remain unlabeled. Extensive methylation of K9 and hypomethylation of K4 of histone H3 appear to be specific features of heterochromatin in *Arabidopsis*.

(Yang and Seto, 2003). The *Arabidopsis* genome encodes a total of 12 and 16 potentially functional histone acetyltransferases and deacetylases, respectively (Pandey *et al.,* 2002).

In contrast to acetylation, the methylation of a lysine residue, which can accommodate up to three methyl groups, is usually a stable modification (Zhang and Reinberg, 2001) and no demethylation activity has been described so far. Histone methylation affects not only lysine residues (K4, 9, 27, 79 of H3 and K20 of H4), but also arginine residues (R2, 17, 26 of H3 and R3 of H4, *Figure 4C*). Methylation of H3K9 and H3K27 have been linked to epigenetic silencing. Histone H3 methylated at lysine9 is enriched in heterochromatin and has the potential to initiate chromatin condensation and silencing (Peters et al., 2001) in part through its ability to bind proteins like HP1 via their chromodomain (Bannister et al., 2001; Lachner et al., 2001). Chromodomains characterize proteins like HP1, involved in heterochromatin formation, Polycomb proteins or chromatin remodeling factors (Mi-2) and the CMT3 DNA methyltransferase. At lower levels H3K9 methylation is found in mammalian euchromatin where it is involved in transcriptional repression (Tachibana et al., 2002). H3K27 methylation in contrast is specifically recognized by Polycomb proteins to mediate gene silencing of developmentally regulated genes (Fischle et al., 2003). In *Arabidopsis*, mono- and di-methylated H3K9 are enriched in centromeric and pericentromeric repeats (Gendrel et al., 2002; Jackson et al., 2004) (*Figure 5C*). While in mammals trimethylated H3K9 is specifically localized to pericentromeric repeats (Lehnertz et al., 2003), *Arabidopsis* chromatin seems to be devoid of this modification (Jackson et al., 2004). Both H3K9 and K27 methylation are involved in silencing of the FLC locus during the vernalization response in *Arabidopsis* (Bastow et al., 2004; Yan et al., 2004). Histone methylation is catalyzed by SET domain containing proteins; Su(var)3-9 in Drosophila, SUV39H in humans and Clr4 in *S. pombe*. In *Arabidopsis* several proteins with homology to SUV39H have been identified, with KRYPTONITE (KYP) being the predominant histone methyltransferase (Jackson et al., 2002; Jackson et al., 2004). The *kyp* mutant was identified in a mutant screen for suppressors of gene silencing at the *Arabidopsis thaliana* SUPERMAN (SUP) locus. It shows loss of cytosine methylation at CpNpG sites and reactivation of endogenous retrotransposon sequences.

In contrast to methylation of H3K9 and K27, H3K4 methylation is linked to transcriptional activity. In yeast, H3K4met was predominantly found in coding regions suggesting that H3K4met plays an important role in the elongation stage of transcription, rather than its initiation. In this case H3K4 trimethylation serves as a “short term memory” for actively transcribed genes (Santos-Rosa et al., 2002; Ng et al., 2003), probably maintaining their transcriptional potential and protecting them from long term silencing by inhibition of

binding of the NuRD complex (Zegerman et al., 2002) and methylation of H3K9. Interestingly, the set of the H3K4 mark during transcription elongation requires the ubiquitination of K123 of H2B mediated by Rad6. Staining of *Arabidopsis* nuclei with antibodies raised against di-methylated K4 of H3 showed that H3K4 methylation is exclusively localized to euchromatin (*Figure 5D*), with the heterochromatic chromocenters being devoid of staining. Mutations in *ddm1* resulting in loss of H3K9 at target genes in the heterochromatic knob also induced increased association with H3 methylated at K4 (Gendrel et al., 2002), suggesting a reciprocal effect on epigenetic gene regulation of these two modifications.

Like H3K4 methylation arginine methylation of H3 and H4 correlates with transcriptional activation, e.g. the methylation of H4R3 facilitates subsequent acetylation of H4 (Zhang and Reinberg, 2001). The phosphorylation of H3 serine 10 is also linked to transcriptional activation (Lo et al., 2000) that precedes K14 methylation but negatively affects H3K9 methylation (Rea et al., 2000). Furthermore, together with phosphorylation at serine 28 of H3 this modification is involved in mitosis and chromosome condensation (Wei et al., 1999).

Many of the different histone modifications are located close enough together on the histone tail to influence the ability of enzymes to further modify histones. Hence, the implication of a specific histone modification depends on the modifications that surround it and the time point of its setting. For example the Drosophila Ash1 protein specifically methylates H3K4 and K9 as well as H4K20 thereby creating a distinct signal for binding of the Brahma complex (Beisel et al., 2002).

In addition to the canonical histones, the genome of many organisms also encodes specific histone variants. The H3.3 variant of histone H3 for example is enriched in transcriptional active domains and replaces H3 (methylated at K9) in a replication-independent manner (Ahmad and Henikoff, 2002; Janicki et al., 2004) upon transcriptional activation. H3.3 differs from H3 only in few residues. Another histone variant specific for centromeres shows significant differences in the N-terminal tail. Named SpCENP-A in *S. pombe* (Takahashi et al., 2000)), Cid in Drosophila (Henikoff et al., 2000), CenP-A in humans (Sullivan et al., 1994) and HTR12 in *Arabidopsis* (Talbert et al., 2002), it contributes to centromere organization and function. The histone H2A.Z variant is involved in transcriptional regulation (Santisteban et al., 2000), while the macroH2A, that has a 25kDa non-histone fold domain added to its C-terminus, is found to be enriched in the inactive mammalian X chromosome.

IV. Initiation of Transcriptional Repression

What is the signal that targets certain regions of the genome for transcriptional silencing and heterochromatin formation? Evidence accumulates that small RNAs might be the critical players in guidance of DNA and chromatin modifications. Small interfering RNAs have been first detected in plants expressing a reporter gene subject to post-transcriptional gene silencing (PTGS) (Hamilton and Baulcombe, 1999). During PTGS mRNAs undergoes rapid, sequence specific degradation triggered by homologous double stranded RNA through the RNA interference pathway. The degradation is catalyzed by the RNA-induced silencing complex (RISC), which contains as one of the components the RNA binding protein Argonaute, which is highly conserved between plants, yeast and animals (Fagard et al., 2000). Small RNAs of 21-23 nucleotides in size confer specificity to this multiprotein complex. These small RNAs are generated from double-stranded precursors through the enzymatic activity of the Dicer enzyme, an RNaseIII helicase. Interestingly, if double stranded RNA is synthesized from a hairpin construct with homology to a promoter region, RNA directed DNA methylation and transcriptional gene silencing was observed (Mette et al., 2000; Sijen et al., 2001), providing the first evidence for involvement of an RNA component in chromatin modifications. In contrast to PTGS, TGS is stably inherited not only through mitotic, but also through meiotic divisions. Mutations in the ARGONAUTE4 protein of *Arabidopsis* also interfere with H3K9 and DNA methylation at the SUP locus (Zilberman et al., 2003). In fission yeast, the expression of a synthetic hairpin dsRNA homologous to a reporter gene is sufficient to silence and to induce assembly of silent chromatin at the target locus (Schramke and Allshire, 2003). In fission yeast overlapping transcripts are generated from the outer repeats of the centromeres. If any of the components involved in the RNAi machinery is lacking, silencing and heterochromatin formation are impaired at the outer repeats, interfering with centromere function (Volpe et al., 2002). In *Arabidopsis* small RNAs homologous to transposons, retrotransposons and centromeric repeats have been identified (Xie et al., 2003), suggesting a similar mechanism of RNA-mediated heterochromatin formation. The recent identification of the RNA-induced initiation of transcriptional gene silencing (RITS) complex directly links the RNAi machinery in heterochromatin assembly (Verdel et al., 2004). Two subunits of the RITS complex are specifically associated with heterochromatic DNA regions, suggesting that it uses siRNAs to recognize and to bind to specific chromosome regions so as to initiate heterochromatic gene silencing (Verdel et al., 2004). Once the transcriptionally silent state is established through specific DNA and histone

modifications, it needs to be clonally transmitted. The inheritance of epigenetic modifications at the level of DNA and histones seems to be tightly linked to DNA replication. The chromatin assembly complex CAF-1 is targeted to replication forks via its interaction with the proliferating cell nuclear antigen (PCNA) (Shibahara and Stillman, 1999). This three-component complex is a histone chaperone involved in DNA synthesis-dependent histone deposition. CAF-1 mutants in *S. cerevisiae* are deficient in stable inheritance of gene silencing at mating-type loci and telomeres (Gerbi and Bielinsky, 2002) and *Arabidopsis* CAF-1 mutants are impaired in the maintenance of transcriptional gene silencing (Kaya et al., 2001). In mammals Dnmt1 associates with sites of DNA synthesis recruited by PCNA (Vertino et al., 2002). Dnmt1 interacts with HDACs (Fuks et al., 2000; Rountree et al., 2000), HP1 and histone methyltransferases (Burgers et al., 2002; Fuks et al., 2003), thereby targeting a whole set of epigenetic regulators to the replication forks and assuring inheritance of silenced states in the daughter cells.

V. Objective of This Study

Genetic screens for mutants involved in the maintenance of transcriptional gene silencing at transgenic loci or endogenous repeats have identified several components of the regulatory network involved in epigenetic regulation in the model plant *Arabidopsis*. The aim of this work was to analyze the nuclear structure as well as DNA and histone modifications in *Arabidopsis* and to investigate the impact of these TGS mutants on nuclear architecture. All of the studied mutants are either directly involved in the establishment of DNA methylation patterns (*met1*, *cmt3*, *drm2* and *ddm1*) or affect DNA replication (*fas1*, *fas2* and *bru1*), histone deacetylation (*axe1*) or release silencing by an unknown mechanism (*mom1*). More specifically I investigated the relationship between DNA methylation at CpG sites and histone H3K9 methylation and asked whether DNA methylation might be dispensable for heterochromatin formation. We also asked if MOM1 controls the arrangement and the degree of heterochromatinization of the targets reactivated in the mutant and compared the results to plants lacking the chromatin-remodeling factor DDM1. Further I studied the release of transcriptional gene silencing in a histone deacetylase mutant and investigated its role in maintenance of nuclear organization at rDNA repeats, as well as the effect of mutations impaired in DNA

replication on heterochromatin structure. Using an epistasis analysis I investigated whether MOM1 acts downstream of a silencing pathway delineated by DNA methylation and histone deacetylation or whether MOM1 is part of an independent pathway of epigenetic control.

4. MATERIALS AND METHODS

I. Material

I.1. Plant Material

In this study *Arabidopsis thaliana* wild type plants of the ecotypes Zürich (ZH), Col (Columbia), Wassilewskija (WS), Nossen (No), Enkheim (En) and Landsberg erecta (L*er*) were used. Line A, carrying a silent multicopy HPT transgene (Mittelsten Scheid et al., 1991), is derived from ecotype ZH. The mutants *mom1-2*, *met1-3* (*MET1,* isolated by Hidetoshi Saze), *axe1-1*, *axe 1-4* and *axe1-5* (*HDA6* mutant alleles, provided by Jane Murfett), as well as *bru1-2* and *bru1-3* (Takeda et al., 2004) are in the Col background. The mutants *mom1-1*, *ddm1-5* (*som8*) were isolated in the lineA background (Mittelsten Scheid et al., 1998; Amedeo et al., 2000); *sil1* (provided by Ian Furner, (Furner et al., 1998)) as well as the *fas2-1* allele (Leyser and Furner, 1992) are in the L*er* background, *fas1-1* (Reinberg et al., 1966) and *fas2-2* (Kaya et al., 2001) are derived from ecotypes Enkheim and Nossen, respectively. The *bru1-1* mutant (originally isolated by Zerihun Tadele) is in the Wassilewskija background.

I.2. Plant Tissue Culture Media

Solid germination medium (Masson and Paskowski, 1992) contains MS macroelements (KNO_3 (0.95 g/l), NH_4NO_3 (0.825 g/l), $CaCl_2xH_2O$ (0.22 g/l), $MgSO_4x7H_2O$ (0.185 g/l) and KH_2PO_4 (85 mg/l) final concentration), B5 microelements ($MnSO_4xH_2O$ (10 mg/l), H_3BO_4 (3 mg/l), $ZnSO_4x7H_2O$ (2 mg/l), KJ (0.75 mg/l), $Na_2MoO_4x2H_2O$ (0.25 mg/l), $CuSO_4x5H_2O$ (25 μg/l) and $CoCl_2x6H_2O$ (25 μg/l)), 0.005% ammonium iron citrate, 1% sucrose, and 0.8% agar-agar (Merck). The pH was adjusted with KOH to pH5.6 and buffered with 0.07% MES. The antibiotics Kanamycin (50 μg/ml) or Hygromycin (10 μg/ml) were added for selection of plants containing T-DNA inserts from *Agrobacterium* mediated transformation; Cefotaxime (250 μg/ml) and Vancomycine (250 μg/ml) to eliminate *Agrobacterium* growth in plant tissue culture.

I.2. Bacterial Strains

Escherichia coli DH5α was used for all cloning procedures. For plant transformation the *Agrobacterium tumefaciens* strain C58CIRifR containing the non-oncogenic Ti plasmid pGV3101 was used.

I.3. Bacterial Growth Media

E. coli and *A. tumefaciens* were grown in liquid LB medium (Luria-Bertani medium: 1% Bacto-tryptone, 0.5% (w/v) Bacto yeast extract, 0.5% (w/v) NaCl) or on LB plates (supplemented with 1.5% Bacto-agar). The antibiotics Ampicillin (100 μg/ml), Kanamycin (50 μg/ml), Rifampicin (10 μg/ml) or Gentamycin (25 μg/ml) were added for selection of plasmids.

I.4. Plasmid Vectors

For cloning and plant transformation purposes the plasmid vectors pCambia1300, pBluescript SK- (Stratagene) and pGEM-7Zf(+) (Promega) were employed.

I.5. Enzymes and Reagents

The enzymes used in this study were purchased form Roche Diagnostics (Rotkreuz, Switzerland), New England Biolabs (Beverly, MA, USA), Amersham Pharmacia Biotech (Buckinghamshire, UK), Gibco BRL (Grand Island, NY, USA), Promega (Madison, WI, USA) and Stratagene (La Jolla, CA, USA). Chemicals were obtained from Fluka (Buchs, Switzerland), Merck (Darmstadt, Germany), Sigma (St. Louis, MO, USA), and Bio-Rad (Hercules, CA, USA) and were of analytical grade. Radioactively labeled ^{32}P was obtained from Amersham Pharmacia Biotech.

Antibodies for FISH, Immunostaining and ChIP experiments were obtained from Sigma, Molecular Probes (Eugene, OR, USA), Vector Laboratories (Burlinghame, CA, USA), Eurogentec (Seraing, Belgium), and Upstate Biotechnology (Lake Placid, NY, USA); the HRP-conjugated secondary antibody was purchased from DAKO A/S, Denmark.

I.6. Oligonucleotides

Oligonucleotides were designed with help of Vector NTI PCR amplification and were synthesized by Microsynth (Balgach, Switzerland).

II. Methods

II.1. Plant Growth

Seeds for *in vitro* culture were sterilized for 10 min in 5% sodium-hydrochlorite containing 0.1% Tween80, followed by 3 washes with sterile ddwater. The seeds were dried and

plated on germination medium to allow growth under axenic culture conditions with 16 h light of 100 $\mu Em^{-2}s^{-1}$ (Osram Natura de Luxe) at 22.5°C and 8 h darkness at 16°C.
Seeds were otherwise directly sown on soil, and plants grown in a phytotron under short day (12 h light/21°C and 12 h darkness/16°C) or under long day conditions (16 h light/21°C and 8 h darkness/16°C) with 80% humidity and a light intensity of 3000-4000 lux. All seeds were stratified after sowing for 2-4 days at 4°C.

II.2. Plasmid Construction

II.2.1. pBluescript 180bp

The original clone containing the conserved 180bp repeat as a *Hind*III fragment was obtained from Eric J. Richards (Richards, et al., 1991). It was subcloned into pBluescript and a clone containing a tandem repeat of the 180bp repeat was selected.

II.2.2. MOM-GFP fusion construct

For transient expression of a MOM1-GFP fusion protein in *N. plumbaginifolia* protoplasts the pUC based plasmid pCK GFP S65C was used, in which the GFP coding region had been replaced by the one of eGFP (enhanced GFP) and the *Nde*I site in the lacZ gene was removed (Habu personal communication). The vector was linearized with *Nco*I and a linker was introduced (5'-CAT GCA TAT GAT GTT CCT GAT TAT GC-3' and 5'-CAT GGC ATA ATC AGG AAC ATC ATA TG-3') to generate a new *Nde*I site. MOM1 cDNA was cut as *Nde*I fragment from the p2HAPA vector (provided by Yoshiki Habu) and then cloned in frame to eGFP.

II.3. Generation of Competent Bacteria

To generate heat-shock competent bacteria the "Ultra-competect *E.coli* method" was applied (Inoue et al., 1990). Therefore, 250 ml SOB (2% (w/v) bacto-tryptone, 0.5% (w/v) yeast extract, 10 mM NaCl, 2.5 mM KCl, 10 mM $MgCl_2$ and 10 mM $MgSO_4$ pH6.7-7.0) was inoculated from an overnight culture to OD_{600}=0.05-0.08. The culture was grown to an OD_{600} of 0.6 at 18°C, incubated on ice for 10 min and resuspended gently in 80 ml ice-cold transformation buffer (10 mM PIPES, 55 mM $MnCl_2$, 15 mM $CaCl_2$, 250 mM KCl, pH6.7). The cells were collected by centrifugation (2500g, 10 min, 4°C), resuspended in 20 ml transformation buffer and incubated on ice for 10 min. After the addition of DMSO to a final concentration of 7%, the cells were again incubated on ice for 10 min, aliquoted and frozen in liquid nitrogen.

Electrocompetent *Agrobacterium tumefaciens* were prepared by inoculating 500 ml LB with 5 ml of a fresh saturated culture and incubation at 28°C with agitation (210 rpm). When the culture reached an OD_{600} of 0.5-0.8, the cells were chilled in ice-water and pelleted by centrifugation (4000g, 10 min, 4°C). The bacteria were resuspended in 500 ml of ice-cold ddwater. Centrifugation and resuspension were repeated twice and the cells resuspended in a final volume of 250 ml and 50 ml, respectively. After an additional centrifugation the bacteria were resuspended in 5 ml of 10% (v/v) ice-cold sterile glycerol, aliquoted and frozen in liquid nitrogen.

II.4. Bacterial transformation

Competent *E.coli* cells were transformed with plasmid DNA or ligated plasmid products using the heat shock transformation protocol: After thawing the competent cells on ice and incubation with an appropriate amount of plasmid DNA for 15 min on ice, the cells were heat shocked at 42°C for 90 sec and transferred to ice for 5 min. 800 µl of LB-medium was added and the cells incubated at 37°C for 1 hour before plating on appropriate selection medium. Alternatively, electrocompetent *E. coli* (Invitrogen) or *A. tumefaciens* were transformed using the BioRad *E. coli* pulser at a voltage of 1.8kV according the manufacturer's instructions.

II.5. *Agrobacterium tumefaciens* mediated plant transformation

Arabidopsis mom1-1 plants were transformed according to the germ-line transformation protocol using the floral dip method (adapted from Clough and Bent, 1998): *Agrobacterium* cultures were initiated by inoculation of 15 ml LB medium supplemented with Rifampicin (10 µg/ml), Gentamycin (25 µg/ml) and Kanamycin (50 µg/ml) to select for cells containing the plasmids. After 48 h at 28°C, the cultures were transferred to 1 l flasks containing 500 ml LB with Kanamycin (50 µg/ml) and grown to an OD_{600} of 1.8-2.0. The bacteria were harvested by centrifugation at 400 rpm for 20 min at RT, the pellet resuspended in 500 ml infiltration medium (5% sucrose), and Silwet L-77 was added to 0.05%. Plants with inflorescences at the early flowering stage were dipped into the bacterial solution for 30 sec. After infiltration, plants were covered with a polyethylene foil, kept horizontally for 24 h in a growth chamber and then grown to maturation. Seeds were sterilized with ethanol in addition to sodium-hydrochlorite and transformants were selected on plates containing 250 µg/ml cefotaxime, 250 µg/ml vancomycine and 50 µg/ml kanamycin.

II.6. Genotyping of *Arabidopsis* mutants

One *Arabidopsis* leaf frozen in liquid nitrogen was ground to fine powder in the presence of 1.7 – 2.0 mm glass beads (Roth) with help of a Silamat S5 (Vivadent), vortexed in 400 µl of buffer (0.2 M Tris-HCl pH7.5, 0.25 M NaCl, 25 mM EDTA, 0.5%SDS) and centrifuged for 5 min (13000 rpm) at RT. The DNA in the supernatant was precipitated with an equal volume of isopropanol and centrifuged for 5 min (13000 rpm) at RT. The pellet was washed in 70% ethanol, dried and resuspended in 50 µl ddwater. 1 µl was added to 20 µl of a standard PCR mix (1x Polymerase buffer supplemented with $MgCl_2$ to 1.5 mM and KCl to 5 mM, 0.25 mM dNTPs, 0.5 µM of each primer and 0.75 units Taq polymerase, Roche).

To genotype the *mom1-1* mutant the T-DNA insertion can be amplified using 5'-GTG GTT ACT GAT CAA GTC TCG-3' and 5'-GTG AAG GGC AAT CAG CTG TTG-3', giving rise to a 600 bp fragment. The wildtype allele can be amplified with a combination of 5'-CAC TTT CCG ATT TCG ATT CTC G-3' and 5'-CAT GAC TCC CCC AGC CAG TAG-3' resulting in a 260 bp fragment.

To identify the *ddm1-5* mutant allele we made use of the 82 bp insertion in the 5′ region of the *DDM1* gene. Using the primer pair DDM+ (5′-CGC TCT CGA AAT CGC TCG CTG TTC-3') and DDM- (5′-AAA GGA CCC ATT TAC AGA ACA C-3') amplification of the wild type locus results in a band of 332 bp, while the mutant locus gives rise to band of 414 bp.

For genotyping of the *axe1-1* locus we exploited the fact that the single nucleotide exchange in this mutant (C to A, 337 bp downstream of the ATG) abolishes an *Msp*I site. A 259 bp fragment was amplified (5'- CGG AAT CTA TGG GCG ATC C-3' and 5'- CCA GAA TCC CTA GCA CGA TGT C-3'), PCR purified and subjected to an *Msp*I digest.

II.7. DNA isolation and Southern Blot analysis

II.7.1 Genomic DNA Isolation from *Arabidopsis*

DNA from *Arabidopsis thaliana* leaf tissue was isolated with help of the nucleon extraction and purification kit (Amersham) according to the manufacturer's instructions and resuspended in a final volume of 30 µl ddwater.

II.7.2 Gel Electrophoresis and Southern Blot Analysis

DNA was digested overnight with the required restriction enzyme and electrophoretically separated on a 1% agarose gel. The gel was than treated with 250 mM HCl for 10 min, the DNA denatured in denaturation solution (500 mM NaOH, 1.5 M NaCl) for 30 min and

treated with neutralization solution (500 mM Tris-HCl pH7.2, 1.5 M NaCl and 1 mM EDTA) twice for 15 min. The DNA was transferred overnight by capillary transfer onto a Hybond N membrane (Amersham) using 20x SSC (1.5 M NaCl, 0.3 M $C_6H_5Na_3O_7$-$2H_2O$) as transfer buffer. After transfer, the DNA was cross-linked to the membrane by UV (1.2 kJ/m^2, Stratalinker UV Crosslinker, Stratagene).

II.8. Total RNA Isolation and Northern Blot Analysis

II.8.1 RNA Isolation

RNA was isolated using the Trizol Reagent (Gibco BRL) according to the manufacturer's instructions. In brief, 2-3 *Arabidopsis* leaves, frozen in liquid nitrogen, were ground to fine powder in the presence of 1.7 – 2.0 mm glass beads (Roth) with help of a Silamat S5 (Vivadent). After adding 1 ml of Trizol Reagent the suspension was vortexed and incubated at RT for 5 min. Subsequently 0.2 ml of chloroform was added and each sample was vortexed for 15 sec. Following centrifugation (12000 g, 5 min, 4°C) the aqueous phase was transferred to a fresh tube, the RNA precipitated with 0.5 ml isopropanol for 10 min at RT and collected by centrifugation (12000 g, 10 min, 4°C). The RNA pellet was washed once in 75% Ethanol, air-dried and resuspended in 50 µl of DEPC treated ddwater (10 min, 55°C).

II.8.1. RNA Electrophoresis and Northern Blot Analysis

5-20 µg of RNA was dried in a speed vac and resuspended in 50% DMSO, 10 mM sodiumphosphate, pH7.0 and 6% glyoxal pH5.5-6.0 by incubation for 1 h at 50°C. 4 µl of sample buffer (50% glycerol, 0.4% bromophenolblue, 10 mM Na_2HPO_4/NaH_2PO_4, pH7.0) was added and the RNA separated on a 1.5% agarose gel in 10 mM Na_2HPO_4/NaH_2PO_4, pH7.0. The gel was stained in Radiant Red RNA Gel Stain (BioRad, diluted 1:1000 in 10 mM Na_2HPO_4/NaH_2PO_4, pH7.0), and the RNA blotted by capillary transfer overnight onto a Hybond N membrane with 20x SSC (3 M NaCl, 0.3 M $C_6H_5Na_3O_7$-$2H_2O$) as transfer buffer. The membrane is washed briefly in 2x SSC, dried and cross-linked by UV (see above).

II.9. Hybridization with radioactive probe

DNA fragments were labeled with ^{32}P by random oligonucleotide-primer synthesis (Feinberg and Vogelstein, 1983). The DNA fragment (50 ng in 7 µl of water) was denatured by boiling for 3 min, followed by cooling down on ice for 5 min. Then 11.5 µl of labeling solution (LS, Feinberg and Vogelstein, 1983), 1 µl of BSA, 0.5 µl (2.5U) Klenow fragment of polymerase I, and 5 µl of [α-^{32}P] dATP (2 MBq) were added, mixed and

incubated at RT for 2-4 h. The labeled DNA was separated from unincorporated radioactive precursors by chromatography on a NICK™ Column (Pharmacia Biotech) following the manufacturer's instructions. Membranes were pre-hybridized in hybridization buffer (0.5 M $NaHPO_4$ pH7.2, 7%SDS, 1 mM EDTA) for 1-3 h at 65°C (RNA membranes were washed before in 0.1% boiling SDS). The radioactive probe was denatured (95°C, 5 min), cooled down on ice and added to 15 ml of fresh hybridization solution. The hybridization was carried out overnight at 65°C in a hybridization oven. The membranes were washed 10 min at 65°C, twice for 20 min at 60°C in washing solution (0.5 M $NaHPO_4$ pH7.2, 1%SDS), dried, rapped in polyethylene foil and either exposed to a phosphoimager screen (BioRad) at RT or autoradiographed at -80°C. To allow hybridization of the same membrane with a different radioactive probe, the membranes were stripped using 0.1% boiling SDS.

II.10. Reverse-Transcription (RT-PCR)

5 μg of RNA was treated with 4 μl of DNase RQ1 (Promega) for 75 min at 37°C in the presence of 1 μl of RNase inhibitor (Invitrogen), 0.1 μl of 1 M DTT, and 1x RQ buffer in a total volume of 50 μl. The treated RNA was phenol-chloroform extracted, precipitated with 1/10 volume of NaAc and 2.5 volumes of Ethanol and washed in 70% Ethanol. The RNA pellet was resuspended in 10 μl of DEPC treated water by incubation for 10 min at 65°C in a heating block with agitation. The 10 μl were divided into 2 PCR tubes and incubated either with or without 1 μl of AMV reverse transcriptase (Roche) in 1x AMV buffer with 0.67 mM dNTPs, and 0.167 μM RT-primer in a total volume of 15 μl. cDNA synthesis was allowed to proceed for 1 h at 42°C, followed by a denaturation step (95°C, 5 min). 2 μl of the cDNA was used in a standard PCR reaction.

II.11. Transfection of *Nicotiana plumbaginifolia* protoplasts

Protoplasts at a concentration of $6x10^5$/ml competent for transfection were obtained from Matthias Müller (FMI). In a 15 ml falcon tube 10 μg of plasmid DNA, 0.3 ml of protoplast suspension and 0.3 ml of 40% PEG 6000 were mixed. After 5 min of incubation at RT, 4 ml of K3 medium (Nagy et al., 1976, provided) was added. The protoplasts were incubated at 25°C in the dark for 4 h to overnight and GFP fluorescence was analyzed using the Leitz DMR Fluorescence Microscope.

II.12. Isolation of histones and Western blot analysis

Fresh leaf tissue (5 g) was ground in liquid nitrogen, transferred to extraction buffer (0.25 N HCl, 10 mM Tris-HCl pH7.5, 2 mM EDTA, 20 mM β-mercaptoethanol, 0.2 mM PMSF) and treated with ultra-sound. Following centrifugation (10 min, 12000 g) soluble proteins were precipitated with trichloracetic acid (TCA, 25% final concentration) and collected by centrifugation at 17000 g for 20 min. The pellet was washed two times in acetone, air dried and resuspended in 1x SDS loading buffer (75 mM Tris-HCl pH6.8, 0.6% SDS, 15% glycerol, 0.0009% bromophenol blue and 1.075 M β-mercaptoethanol). The proteins were separated electrophoretically by means of a 14% SDS page (stacking gel: 3.9% acrylamide, 0.1%bisacrylamide, 125 mM Tris-HCl pH6.8, 0.1% SDS, 0.05% ammonium persulfate, 6.6 mM TEMED; separating gel: 14% acrylamide, 0.37% bisacrylamide, 375 mM Tris-HCl pH8.8, 0.1% SDS, 0,033% ammonoium persulfate, 4.4 mM TEMED) in Lämmli Buffer (3% Tris base, 14.4% glycine, 1% SDS). Subsequently the proteins were blotted onto a Hybond ECL membrane (Amersham) in blotting buffer (20% methanol, 25 mM Tris, 200 mM glycine) using the Mini Trans-Blot electrophoretic transfer cell (Bio-Rad). The membrane was blocked with 3% dry milk in western basic buffer (20 mM Tris-HCl pH7.5, 150 mM NaCl, 0.05% Tween 20) and incubated overnight at 4°C with α-tetra-acetylated H4 or α-H3K4met (from Upstate, 1:2000 in western basic buffer supplemented with 1% BSA). After washing, the primary antibody was detected with secondary anti-rabbit HRP coupled antibody (1:7500, Amersham, diluted in western basic buffer) at RT for 45 min. Visualization was achieved using the ECL Western detection kit (Amersham) according to the manufacturer's instructions. For loading control a gel was stained in Coomassie solution (50% (v/v) methanol, 0.1% (w/v) Coomassie brilliant blue R-250, and 10% (v/v) acetic acid) and destained in 15% methanol/10% acetic acid (v/v).

II.13. Fluorescence *in situ* hybridization (FISH)

The protocol for fluorescence *in situ* hybridization (FISH) was adapted from (Fransz et al., 1998). Young rosette leaves (1-1.5 cm) were fixed in 3:1 ethanol-acetic acid and stored at -20°C until use. After two washes in ddwater and 1x citrate buffer (10 mM $C_6H_8O_7$ and 10 mM $Na_3C_6H_5O_7$ pH4.8) the leaf tissue was digested with a combination of cellulase, pectolyase and cytohelicase (Sigma, 0.3% w/v) in citrate buffer. A piece of the digested leaf was transferred to a clean microscope slide and the tissue tapped to form a fine suspension. After adding 20 µl of 60% acetic acid the suspension was stirred for 1 min on a heating block set to 45°C, and the spread nuclei fixed in ethanol-acetic acid 3:1.

Following a post-fixation in 2% paraformaldehyde in PBS, the slides were air-dried. Subsequently the slides were baked at 60°C, treated with RNase (100 μg/ml in 2x SSC) at 37°C for 1 hour, followed by a pepsin treatment (10 μg/ml in water with pH2) at 37°C for 20 min. After 3 washes in 2x SSC, the slides were post-fixed in 2% PFA in PBS and washed again in 2x SSC, followed by a dehydration via an ethanol series (70%, 90%,100%, each for 2 min). The slides were air-dried for at least 1 hour.

Biotin labeled probes complementary to the 180bp repeat region were generated by PCR from a cloned tandem repeat in pBluescript using T3 and T7 standard primers and 0.1 mM dATP, dCTP, dGTP, 0.065mM dTTP and 0.035 mM Biotin-dUTP (Roche). TSI-probes were produced by PCR from a vector containing a 1.5 kb fragment of TSI A2 (Hide, Andrea) with primers 5'-GTT AAT CCA AGT AGC TGA CTC TCC–'3 and 5'-TTT AAC AAC TAA GGT TCC TG-3' using the Dig DNA labeling kit. The amplified sequence corresponds to region 68442 - 68869 of BAC F7N22 (GenBank AF058825). To ensure incorporation the extension time was set to 1 min.

Probes for the *HPT* locus were obtained by labeling the pGL2 plasmid with the digoxygenin-dUTP nick translation kit (Roche), rDNA probes were obtained with the biotin nick translation kit (Roche) using 18S- and 25S-rDNA-containing plasmids (courtesy of Hanna Weiss-Schneeweiss) following the manufacturers instructions. Telomere-specific labeling with digoxygenin was achieved in a primer extension PCR (5' 95°C, followed by 5 cycles (1' 95°C, 40''55°C, 2' 72°C) and 25 cycles (1' 95°C, 40'' 60°C, 2' 72°C)) with 5'-TTT AGG G-3' and 5'-CCC TAA A-3' oligonucleotides using the digoxygenin-dUTP DNA labeling mix (Roche).

For hybridization 1 μl of the PCR reaction or 3 μl of the nick translation mix were added to 20 μl hybridization mix (50% deionized formamide, 2x SSC, 50 mM sodium phosphate pH7.0, 10% dextran sulfate). The probe and the nuclear DNA were denatured for 2 min at 80°C. After hybridization for about 15 h in a wet chamber, slides were washed for 5 min in 2x SSC, 5 min in 0.1x SSC, 3 min in 2x SSC at 42°C and 5 min in 2x SSC/0.1 % Tween20 at RT; for telomere detection the slides were washed twice for 5 min in 0.3x SSC, 3 min in 2x SSC at 42°C and 5 min in 2x SSC/0.1 % Tween 20 at RT.

The Biotin labeled probe was detected with Texas Red conjugated avidin (5 μg/ml, Vector Laboratories), followed by a biotinylated goat-anti-avidin antibody (5 μg/ml, Vector Laboratories) and once more Texas Red avidin. The Digoxygenin probe was detected with mouse anti-digoxigenin antibody (0.2 μg/ml, Roche), followed by a rabbit anti-mouse antibody coupled to FITC (28 μg/ml, Sigma) and subsequently Alexa 488-conjugated goat

anti-rabbit antibody (10 μg/ml, Molecular Probes). The antibody incubations were performed for 30 min at 37°C in a wet chamber and followed by 3 x 5 min washes in 4T (4x SSC, 0.05% Tween20) or TNT (100 mM Tris-HCl pH7.5, 150 mM NaCl, 0.05% Tween-20) at RT. DNA was counterstained with DAPI (2 μg/ml) in Vectashield Mounting Medium (Vector Laboratories). Images were analyzed with a Leitz DMR Fluorescence Microscope and documented with a SPOT RT camera (Diagnostic Instruments) or a Zeiss Axioplan Microscope equipped with a CoolSNAP–HQ camera (Visitron). Images were merged and processed using Adobe Photoshop 7.0 or analyzed with the MetaMorph Imaging Software.

II.14. Immunolocalization

The immunolocalization procedure was modified from *http://www.arabidopsis.org/info/protocols.jsp*). Protoplasts were isolated from young leaves by digestion with 1% cellulase and 0.25% macerozyme in MES buffer (10 mM MES, pH5.7, 0.4 M mannitol, 30 mM $CaCl_2$, 5 mM β-mercaptoethanol and 0.1% BSA). The protoplasts were washed 3 times in wash solution (4 mM MES, pH5.7, 2 mM KCl, 0.5 M mannitol), attached to poly-lysine coated slides, fixed in 2% paraformaldehyd (PFA) in PHEM buffer (6 mM Pipes, 25 mM Hepes, 10 mM EGTA, 2 mM $MgCl_2$, pH6.9) for 10 min, permeabilized in 0.5% NP40 in PHEM buffer, and post-fixed in methanol-acetone 1:1 at –20°C. Following rehydration in PBS, slides were blocked in 2% BSA in PBS (30 min, 37°C) and incubated with antibodies against tetra-acetylated H4 (dilution 1:100), K9 dimethylated H3 (1:100) or lysine4-di-methylated H3 (1:500) (all from Upstate) in blocking solution or 1% BSA in PBS (1 h, 37°C or overnight at 4°C). To detect the MOM1-GFP fusion protein an anti-GFP antibody (courtesy of Uli Mueller) was diluted (1:1000 to 1:10 000) in 1% BSA in PBS. The detection was carried out with an anti-rabbit~FITC-coupled antibody (Molecular Probes, 1:100, 37°C, 45 min) in 0.5% BSA in PBS. Between each antibody incubation the slides were washed in PBS, PBS supplemented with 0.1% NP-40 and PBS, 5 min each. The DNA was counterstained with DAPI (2 μg/ml) in Vectashield Mounting Medium (Vector Laboratories). Images were analyzed with the Deltavision Deconvolution Microscope (Applied Precision, LCC). The WoRx software supplied with the Deltavision system was applied for deconvolution of the image stacks and single layers were chosen for illustration.

II.15. Immuno-FISH

To combine immunostaining and FISH for specific DNA sequences the slides were first processed as for immunostaining experiments. After incubation with the secondary antibody and subsequent washes, the slides were dehydrated in an ethanol series (2 min in 70%, 2 min in 90% and 2 min in 100%), air-dried and baked at 60°C for 30 min. Following an RNase treatment (100 μg/ml in 2x SSC) for 1 h at 37°C, the slides were washed in PBS, post-fixed in 4% PFA in PBS for 20min at 4°C, washed again in PBS, dehydrated in an ethanol series and air-dried. Hybridization, washing and detection of the labeled probe were carried out exactly as for FISH on spread nuclei. Images were analyzed with the Deltavision Deconvolution Microscope.

II.16. Chromatin Immunoprecipitation (ChIP)

Chromatin Immunoprecipitation (ChIP) and PCR analysis were performed as described (Gendrel *et al.,* 2002; Johnson *et al.,* 2002) with minor modifications. In brief, 1.5 g of leaf tissue derived from 3-week old plants grown in soil was vacuum-infiltrated with 1% formaldehyde in buffer 1 (0.4 M sucrose, 10 mM Tris-HCl pH8.0) for 10 min. The reaction was stopped by the addition of glycine to a final concentration of 125 mM and vacuum application for another 5 min. The leaves were then rinsed with ddwater, dried briefly, ground to fine powder in liquid nitrogen, and resuspended in ice-cold buffer 1 supplemented with 5 mM β-mercaptoethanol, 1 mM PMSF and protein inhibitors (Aprotinin, Pepstatin A, Leupeptin, Antipain, TPCK and Benzamidine, all at 1 μg/ml), filtered and centrifuged (4000 rpm, 20 min, 4°C). The pellet was dissolved in buffer 2 (0.25 M sucrose, 10 mM Tris-HCl pH8.0, 10 mM $MgCl_2$, 1% Triton X-100, 5 mM β-mercaptoethanol and protein inhibitors) and transferred to a 1.5 ml eppendorf tube. After centrifugation (12000 g, 10 min, 4°C), the crude nuclear pellet was resuspended in buffer 3 (1.7 M sucrose, 10 mM Tris-HCl pH8.0, 2 mM $MgCl_2$, 0.15% Triton X-100, 5 mM β-mercaptoethanol, 1 mM PMSF and protein inhibitors) and layered on top of an equal amount of buffer 3. Centrifugation (16000 rpm, 1 h, 4°C) resulted in a nuclear pellet that was finally resuspended in nuclei lysis buffer (50 mM Tris-HCl pH8.0, 10 mM EDTA, 1% SDS), incubated for 15 min on ice, diluted with ChIP dilution buffer (1.1% Triton X-100, 1.2 mM EDTA, 16.7 mM Tris-HCl pH8.0, 167 mM NaCl) and sonicated 4 times for 20 sec, at 70% amplitude using a Branson Digital Sonifier. The sheared chromatin was pre-cleared with salmon sperm DNA/protein-A agarose (Upstate) for 1 h and the histone-DNA complexes were immunoprecipitated with α-H4ac and α-H3K4met antibodies (Upstate)

overnight with gentle agitation. The immuno-complexes were then collected by incubation with protein-A agarose for 3 hours at 4°C. The beads were then washed 5 times: once in wash buffer 1 (20 mM Tris-HCl pH8.0, 150 mM NaCl, 1% TritonX-100, 2 mM EDTA), once in wash buffer 2 (20 mM Tris-HCl pH8.0, 500 mM NaCl, 1% TritonX-100, 2 mM EDTA), once in wash buffer 3 (10 mM Tris-HCl pH8.0, 250 mM LiCl, 1% NP40, 1% sodium deoxycholate, 1 mM EDTA) and twice in TE buffer and collected by centrifugation (12000 g, 2 min, 4°C) between the washes. Finally, the chromatin was eluted with 0.1 M $NaHCO_3$ and 1% SDS. Cross-linking was reversed overnight at 65ºC in the presence of 0.2 M NaCl, and samples were treated with proteinase K (42 μg/ml) for 3 hours. After phenol-chloroform extraction the DNA was resuspended in TE supplemented with RNase A to 10 μg/ml. The immunoprecipitated DNA was analyzed by PCR as described (Johnson *et al.,* 2002). Amplification of the *Actin2/7* gene (Tariq et al., 2003) was performed for 40 cycles, the rDNA repeats for 25 cycles using the primers 5'-GAT TCC CTT AGT AAC GGC G-3' and 5'- CGG TAC TTG TTC GCT ATC GG -3' (95°C 5 min, [95°C 30 sec, 60°C 30 sec, 72°C 30 sec], 72°C 4 min).

5. RESULTS

I. Components Involved in Epigenetic Control of Chromatin Organization and Transcription in *A. thaliana*

I.1. DNA Methyltransferases

I.1.1. MET1

The symmetric CpG methylation in *Arabidopsis* is maintained by the mammalian *Dnmt1* homologue: *MET1*. Four *MET1* genes are encoded in the *Arabidopsis* genome (*MET1, 2, 3* and *MetIIb*, see also Chromatin data base), however so far in any screen affecting DNA methylation (Vongs et al., 1993) or gene silencing (Saze et al., 2003) solely mutations in one of the four genes, *MET1*, were discovered. The function of *MET1* and the role of DNA methylation in regulation of gene expression have been studied expressing an antisense*MET1* construct, resulting in up to 90% reduction in DNA methylation levels in certain lines (Finnegan et al., 1996). The plants with reduced methylation exhibit a number of phenotypic and developmental abnormalities including decreased fertility, altered plant size, leaf shapes and flowering time. Partial loss of function mutations like *met1-1* and *met1-2* (Vongs et al., 1993; Kankel et al., 2003) with missense mutations affecting the catalytic domain were also described. Recently a complete loss-of-function mutant allele was identified in a screen for insertion mutants impaired in transcriptional gene silencing (Saze et al., 2003). The 7.1kb T-DNA insert in the *met1-3* locus disrupts the conserved DNA methyltransferase motif. The DNA methylation status at the centromeric 180bp repeats in the mutant plant was determined by Southern Blot and bisulfite sequencing: CpG methylation was reduced from 90% in wildtype to 1.3%, while CpNpG methylation was reduced from 45.6% to 26.3% and asymmetric methylation from 14.1% to 10.3%, revealing the major impact of this DNA methyltransferase on the maintenance of symmetric CpG methylation (Saze et al., 2003). Mutations in *MET1* however do not only affect repeat sequences, but also single copy genes (Rap2.1 and FWA, (Saze et al., 2003)). Segregation analysis revealed that the transmission frequency of the mutant *met1-3* allele to the progeny was lower than expected. Siliques of heterozygous plants showed seed abortion and homozygous *met1-3* plants were recovered only with very low

frequency (Saze et al., 2003). However, when a homozygous mutant plant was obtained, the phenotype was rather subtle, mainly showing a late flowering phenotype and reduced seed set (Saze et al., 2003).

We were interested in studying the effect of a near complete removal of DNA methylation on heterochromatin, chromatin structure and epigenetic modifications of histones. Conflicting data existed to what extend DNA methylation is determined by histone modifications (Johnson et al., 2002) or whether genomic DNA methylation is in fact the stable epigenetic mark determining N-terminal histone modifications (Soppe et al., 2002). Therefore, we performed Chromatin Immunoprecipitation (ChIP) on 3-week old homozygous *met1-3* plants using targets like the Ta2 retrotransposon, hypothetical genes and transposons residing within the heterochromatic knob on chromosome 4, and the 180bp repeat (Tariq et al., 2003). ChIP revealed that H3K9 methylation is consistently lost or reduced at all targets examined, while all targets except the 180bp repeat sequences gain methylation at H3K4. In addition, enrichment in acetylated histone H4 was observed, which correlated with transcriptional reactivation of the target sequences in the mutant. Western analysis revealed total H3K9 methylation as well as histone H4 acetylation levels to be unaffected in *met1-3* plants. Total H3K4 methylation levels, however, are increased as a result of CpG methylation loss.

Using the same antibodies employed in the ChIP experiments, I performed immunostaining on nuclei of *met1-3* mutant plants (Tariq et al., 2003). Surprisingly, DAPI staining revealed the chromocenters to be well discernible and most of the mutant nuclei were indistinguishable from those in wildtype plants. In wildtype nuclei the antibody directed against di-methylated H3K9 specifically labels chromocenters (*Figure 6A*, left). Chromocenters mainly consist of the 180bp repeat sequence and pericentromeric repeats and are hypermethylated, as revealed by immunostaining with an anti-5^{met}Cytosine antibody on chromatin spreads (*Figure 6D*, left). In *met1-3* nuclei however, the chromocenters detectable by DAPI staining remained unlabeled by the anti-H3K9met antibody, only dispersed signals were observed (*Figure 6A*, right). In wildtype nuclei, the antibodies specific for H3K4 methylation or tetra-acetylated H4 stain euchromatin and exclude the chromocenters (*Figure 6B* and *C*, left part). The distribution of these histone modifications is unaltered in *met1-3* mutant nuclei (*Figure 6B* and *C*, right part). This corroborates the ChIP results that did not reveal an increase in H3K4 methylation at the 180bp repeats. The staining with the anti-5^{met}Cytosine antibody on chromosome spreads of the mutant showed as expected a strong reduction in DNA methylation. Interestingly however, most of the nuclei retained the condensed heterochromatic structure of the

chromocenters and FISH analysis for the 180bp repeat sequence did not show dispersion of centromeric heterochromatin.

Figure 6

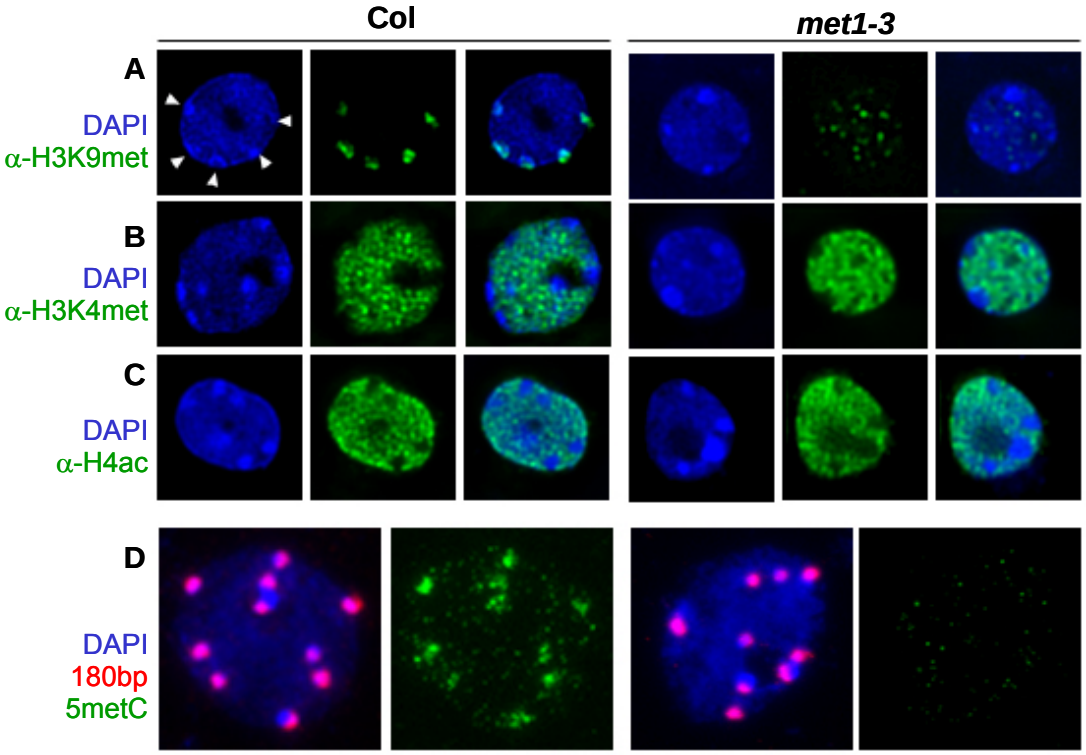

Figure 6. Effect of ^{met}CpG depletion on histone modifications and chromatin structure

Distribution of H3K9 **(A)** and H3K4 methylation **(B)** and histone H4 acetylation **(C)** revealed by DAPI staining of DNA (blue, left panel) and immunodetection with an antibody specific for H3K4dimet, H3K9dimet and tetra-acetylated histone H4, (green, middle panel) in nuclei of control line Col and mutant *met1-3*. Right panels show merged images. Chromocenters are visible as light blue, densely DAPI-stained structures marked by arrowheads in **(A)**. Fluorescence *in situ* hybridization using 180bp repeats (red, left panel) counterstained with DAPI (blue, left panel), right panels show immunodection of 5^{met}Cytosine **(D)**. Images **A** – **C** show single layers selected from deconvoluted image stacks.

I.1.2. CMT3 and DRM2

CMT3 encodes a plant specific cytosine methyltransferase containing a chromodomain inserted between motif II and IV of the methyltransferase domain. *Arabidopsis* mutants in *CMT3* show a decreased CpNpG (N = A, T and C) methylation in all sequence contexts analyzed including retrotransposons, the 180bp repeat and ribosomal sequences (Lindroth et al., 2001). *cmt3* mutants also have reduced asymmetric methylation at certain loci, however do not loose CpG methylation. A null allele, *cmt3-7,* reactivates TSI (Steimer et al., 2000) and the Ta3 retrotransposon, but shows no phenotypic abnormalities (Lindroth et al., 2001).

Two genes homologous to the mammalian Dnmt3 *de novo* methylases exist in the *Arabidopsis* genome: DRM1 and DRM2 (Cao and Jacobsen, 2002a). The two genes show strong sequence similarity, but DRM2 is expressed at much higher levels and seems to be the predominant *de novo* methylase in *Arabidopsis*. *DRM2* is required for the establishment but not the maintenance of gene silencing at FWA and SUP loci and was shown to mediate *de novo* methylation of CpG, CpNpG and asymmetric DNA methylation (Cao and Jacobsen, 2002a).

We were interested in investigating the effect of a mutation in *CMT3* or *DRM2* on centromeric heterochromatin organization. Two mutant alleles were available: the *cmt3* mutant in the WS background has an intron II acceptor mutation and was supplied by Judith Bender (Bartee et al., 2001). The *drm2* mutant in the Col background was obtained from the SALK collection (N150863). This *drm2* allele carries a T-DNA insertion in the last exon reducing the mRNA to undetectable levels and shows de-methylation of the medea intergenic repeat sequence (Sally Adams, personal communication) as described for the *drm2* allele isolated in the WS background (Cao and Jacobsen, 2002b).

In a preliminary experiment I performed fluorescence *in situ* hybridization (FISH) analysis on nuclear spreads. I used the 180bp repeat as probe and evaluated in more than 130 nuclei the fraction of nuclei showing highly condensed heterochromatin organization (type A), slightly decondensed (type B) or strongly affected repeat structures (type C, *Figure 7A*). The results are assembled in *Figure 7B*. Two slides derived from separate leaves of different mutant plants were analyzed for each mutation. Both wildtype ecotypes show only a very limited number of nuclei, in which the 180bp centromeric repeats are not tightly condensed into chromocenters. In the *cmt3* mutation heterochromatin organization is not significantly affected. However this preliminary investigation suggests that the methylation

changes caused by a mutation in the *de novo* methylase DRM2 affect heterochromatin organization.

Figure 7

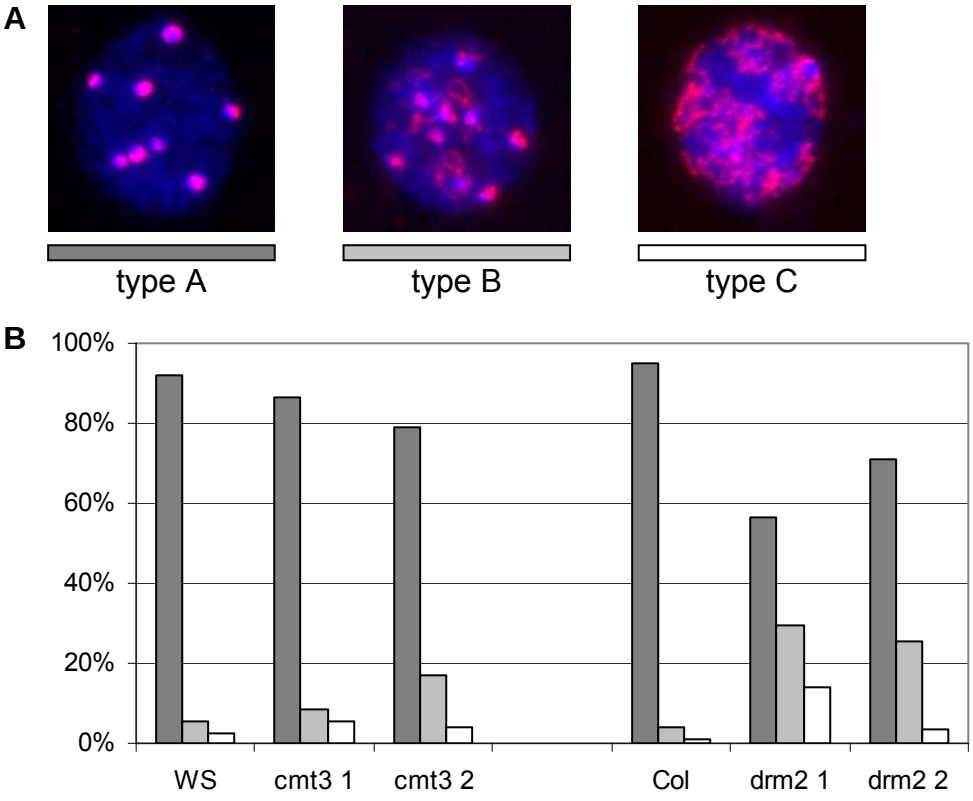

Figure 7. Centromeric heterochromatin organization in *cmt3* (WS) and *drm2* (Col) mutants
Organization of 180bp centromeric repeats was analyzed using FISH on nuclear spreads of WS, Col, *cmt3* and *drm2*. Nuclei were scored according to their phenotype into tightly organized chromocenters (dark gray), dispersion of single repeats (light gray) and severely affected organization (white) (**A**). For each mutant two independent slides were analyzed, the number of scored nuclei per slide is >131(**B**).

I.2. SWI2/SNF2 Chromatin Remodeling Factor DDM1

Mutations in the *DDM1* gene encoding a SWI2/SNF2-like chromatin remodeling factor of the DEXD/H-ATPase superfamily (Vongs et al., 1993; Jeddeloh et al., 1999) have been identified in several independent mutant screens: The first screen was based on Southern blot analysis aiming to discover mutants impaired in the maintenance of DNA methylation at the 180bp centromere repeats (Vongs et al., 1993) and the identified mutants were called *ddm1* for "decrease in DNA methylation". Additional alleles were found to release transcriptional gene silencing in the transgenic line A (Mittelsten Scheid et al., 1998). Line A contains a complex locus with multiple copies of the hygromycine phosphotransferase (HPT) gene, stably silenced over several generations (Mittelsten Scheid et al., 1991). Here I used the *ddm1-5* allele (former *som8*) in a background isogenic to line A that reactivates silencing of the *HPT* locus. This allele carries an 82bp insertion that forms two stop codons in the DDM1 reading frame terminating translation after 30 or 53 aa, respectively. A possible reinitiation of translation at the first downstream start codon would result in a frameshift. However, although detectable in wild-type plants, no *DDM1* mRNA was found in *ddm1–5*, suggesting its decreased stability (Mittelsten Scheid et al., 2002).

The *ddm1* mutation is recessive when maintained as heterozygote, but interestingly the demethylation phenotype arising in homozygotes persists when outcrossed to wildtype plants. The early generations of homozygotes display demethylation primarily of pericentromeric sequences, but the severity of the phenotypic abnormalities and the demethylation increase with successively selfed generations of homozygous *ddm1* plants, affecting – in later generations - single copy sequences as well. DDM1 deficiency induces loss of DNA methylation at transposons and causes new transposition events (Kato et al., 2003; Hiroshika, et al., 2000; Steimer et al., 2000). In addition to reduced DNA methylation levels, the *ddm1* mutant also shows altered patterns of H3K4 and H3K9 methylation as revealed by Chromatin Immunoprecipitation (ChIP) (Gendrel et al., 2002).

The human or mouse orthologue of DDM1 is the Lsh (Lymphoid specific helicase) protein (Jarvis et al., 1996). Homologues in *S. cerevisiae* and *A. fumigatus* were identified, however sequencing of the *Drosophila* and the *C. elegans* genome did not reveal DDM1-like proteins. Mice deficient in Lsh die in the perinatal period with defects in peripheral T cells and kidney abnormalities (Dennis et al., 2001). A recent biochemical analysis of recombinant *Arabidopsis* DDM1 protein confirmed its ATPase dependent nucleosome remodeling activity (Brzeski et al., 2003). Since mutations in *DDM1* affect different epigenetic marks suggested being compulsory for transcriptional gene silencing and

Figure 8

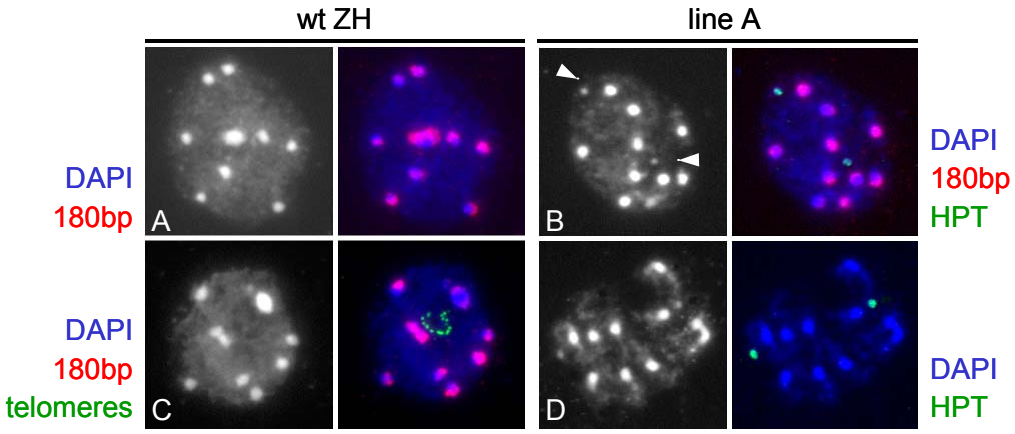

Figure 8. Organization of heterochromatin and formation of new transgenic heterochromatin

Nuclear spreads of wild type (ecotype Zürich) and transgenic line A, stained with DAPI (black and white in left panel, blue in merged image on the right panel) and hybridized with fluorescent probes for centromeric repeats (180bp **A-C**, red), telomeric repeats (**C**, green) or *HPT* vector DNA (**B, D**, green). The transgenic *HPT* locus forms an independent heterochromatic knob (**B, D**, white arrows) that localizes apart from centromeric heterochromatin, as revealed in interphase nuclei (**B**) and on chromosome spreads of an early prophase (**D**).

heterochromatin formation we were interested to investigate the effect of a *DDM1* null mutation on chromatin structure and heterochromatin organization. Before assessing possible global changes in chromatin organization associated with TGS release by the *ddm1-5* mutation, it was necessary to make sure that nuclei of the transgenic *Arabidopsis* line A, the genetic background of the *ddm1-5* mutant allele, are identical to wildtype nuclei. I combined DAPI staining of DNA with detection of 180bp repeats, *TSI*, ribosomal DNA and telomeres by fluorescent *in situ* hybridization (FISH) (*Figure 8* and *9*). In line A the bright DAPI-stained heterochromatic chromocenters mainly comprised of 180bp repeats *(Figure 8A-C*) predominantly align at the nuclear periphery, in the same way as observed in wildtype Zürich nuclei. The pericentromeric TSI repeats, located in pericentromeric regions of all chromosomes, as visualized on pachytene chromosomes and confirmed by localization on the *Arabidopsis* physical map (Steimer *et al.,* 2000), are tightly associated with the chromocenters both in line A and wildtype ZH (*Figure 9C* and data not shown). Those chromocenters, that include one of the four nucleolus organizer regions (NORs), were found close to the nucleolus (*Figure 8A-C*) and telomeres were clustered around this subnuclear compartment ((Armstrong *et al.,* 2001) and *Figure 8C*; *9E*). Although the images of line A and the corresponding wild type Zürich (ZH) are very similar, I detected one or two additional DAPI-bright spots in nuclei of line A plants hemizygous or homozygous for the transgenic locus respectively (*Figure 8B, 9A*). To investigate whether they reflect a chromatin condensation acquired *de novo* at the silent transgenic locus, we combined DAPI staining with two-color FISH using *HPT* and 180bp repeats as probes. The *HPT* signals indeed co-localized with the two neo-chromocenters (*Figure 8B*). This implies that the insertion of a complex transgene and its consecutive silencing triggered the formation of an additional, neo-heterochromatic knob. It has been observed that formation of repressive chromatin at silenced transgenes is enhanced by neighboring heterochromatic regions (Dorer and Henikoff, 1994). However, the *HPT* locus seems to be located distant to preexisting centromeric heterochromatin in interphase nuclei (*Figure 8B, 9A*) and on chromosome spreads (*Figure 8D*).

Since the overall structure of the nucleus of the transgenic line A was identical to the wildtype except for the additional heterochromatic knob, I carried on to examine the consequences of the *ddm1* mutation on the nuclear organization and structure of the reactivated transgenic locus. DAPI staining of the *ddm1-5* nuclei revealed a striking decondensation of chromocenters (*Figure 9B, D*). The number of clearly stained chromocenters was reduced and those visible were considerably smaller than in line A. FISH analysis of centromeric repeats revealed their expansion in the form of loops into

Figure 9

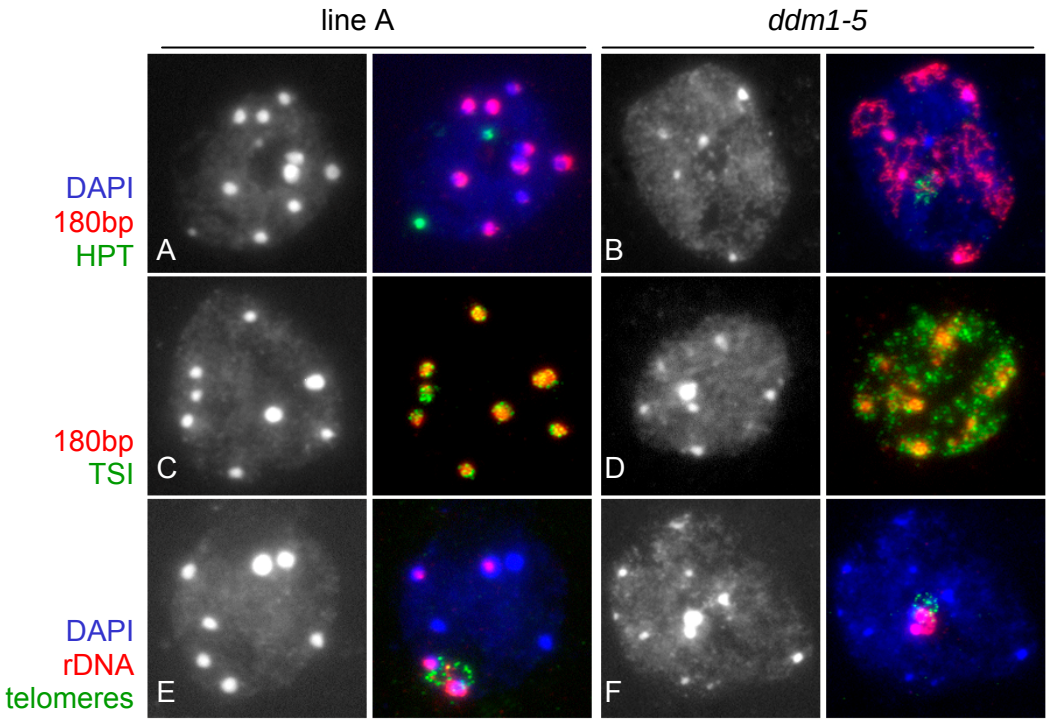

Figure 9. Organization of heterochromatin in line A and *ddm1-5*
Interphase nuclear spreads of transgenic line A and *ddm1-5,* stained with DAPI (black and white in left panel, blue in merged image on the right panel) and hybridized with fluorescent probes for centromeric repeats (180bp, **A-D**, red), *HPT* vector DNA (**A,B**, green), pericentromeric TSI repeats (**C, D**, green), telomeric repeats (**E, F**, green) or rDNA repeats (**E, F**, red).

territory usually occupied by euchromatin (*Figure 9B*). The neo-heterochromatin associated with the transgenic *HPT* locus was likewise decondensed (*Figure 9B*). The *ddm1-5* mutant had been backcrossed to wild type to promote recovery from the progressive developmental effects, and the illustrated donor plant for the nuclei, though homozygous for the mutation, is hemizygous for the transgenic locus. Moreover, the TSI templates lost the tight association with the centromeric DNA. This was clearly visible also in nuclei that still had remnants of chromocenters (*Figure 9D*), suggesting that decondensation and looping out of the pericentromeric repeats precedes a similar process occurring at centromeres and results in disappearance of chromocenters. Interestingly, telomeres were largely unaffected and remained clustered around the nucleolus, and the rDNA was associated with remnants of chromocenters where these were still present (*Figure 9F).*

In plants and mammals, heterochromatic DNA contains a significant amount of 5-methylCytosine (Johnson et al., 2002). *ddm1* mutants are characterized by a substantial hypomethylation of the repetitive pericentromeric sequences (Vongs *et al.*, 1993) and of the reactivated transgenic loci (Mittelsten Scheid et al., 1998). By immunolocalization of modified cytosines, the DNA in chromocenters in line A was found to be hypermethylated, while the remaining DNA showed low methylation (*Figure 10A*). The additional small heterochromatic knobs associated with the transgenic loci were also hypermethylated (*Figure 10A*, arrows). In *ddm1-5* nuclei, methylation signals were reduced and rather uniformly distributed (*Figure 10B*). The methylation changes visualized by immunostaining were clearly correlated with the decondensation of the centromeric heterochromatin and its relocation away from the chromocenter remnants (*Figure 10B*). It was described that *ddm1* affects histone modifications at silenced loci (Grendel et al., 2002; Johnson et al., 2002). Therefore, I investigated the effect of DDM1 depletion on the global distribution of particular histone modifications, namely H4 acetylation, H3K4 and H3K9 methylation. These three modifications were well characterized in other organisms and their involvement in either activation or silencing established. H4 acetylation patterns in line A and *ddm1-5* were visualized by immunostaining with an antibody directed against a tetra-acetylated isoform of H4. Euchromatin of line A was intensely stained (*Figure 10C*), but the chromocenters lacked any signal. In contrast, nuclei of *ddm1-5* plants were almost evenly labeled (*Figure 10D*). Since *ddm1-5* nuclei have dispersed heterochromatic regions, the loss of DDM1 appears to have at least an indirect influence on the distribution of acetylated histones, which now become associated also with centromeric and pericentromeric DNA. Whereas histone acetylation marks transcriptionally active

Figure 10

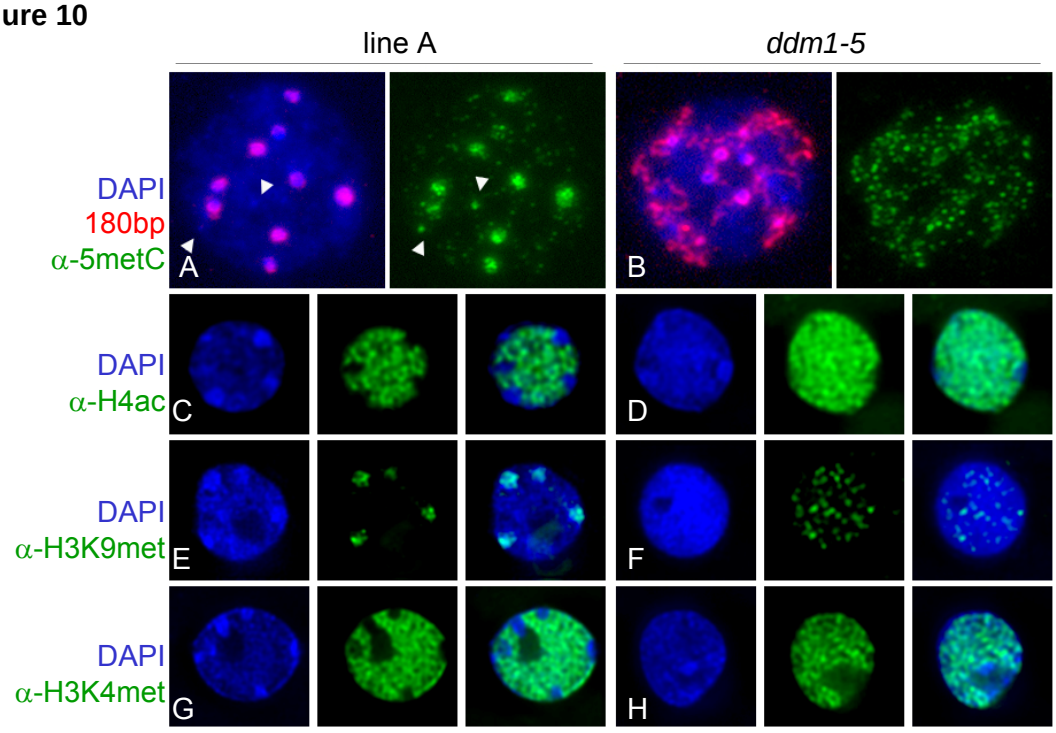

Figure 10. DNA and chromatin modification in transgenic line A and the *ddm1-5* mutant

A, B: Distribution of DNA methylation revealed by DAPI stain (blue) and FISH with probes for centromeric repeats (180bp, red, left panel) and immunodetection with an antibody specific for 5-methylcytosine (green, right panel). The newly formed heterochromatic knob is marked by white arrowheads in **A**.

C-H: Distribution of histone modifications revealed by DAPI stain (blue, left panels) and immunodetection with an antibody specific for tetra-acetylated histones (green, middle panel **C, D**), histone H3 di-methylated at lysine 9 (**E, F**) and histone H3 di-methylated at lysine 4 (**G, H**). Right panels show merged images. Images **C-H** show single layers selected from deconvoluted image stacks.

euchromatin, methylation of histone H3 at position K9 denotes silent heterochromatin. I labeled nuclei of line A and *ddm1-5* with an antibody directed against di-methylated H3K9. Methylated histones in nuclei of line A were clustered at chromocenters while the remaining nucleus showed only a weak signal (*Figure 10E*). In contrast to line A, H3K9 methylation signals at the chromocenter-remnants were dispersed and weak in *ddm1-5* (*Figure 10F*). This is in accordance with the loss of H3K9 methylation at 180bp repeats and transposons in *ddm1-2* (Johnson et al., 2002). In contrast to H3K9met, the methylation of histone H3 at lysine 4 (H3K4 met) marks euchromatin (Jenuwein and Allis,

2001). Immunostaining of line A for H3K4met revealed a pattern similar to that of acetylated histones H4, namely uniform euchromatic staining and exclusion of the chromocenters and the nucleolus (*Figure 10G*). In *ddm1-5*, an increase in H3K4met, detected by chromatin immunoprecipitation, has been observed at selected transposons and single copy genes (Gendrel *et al.*, 2002). A global enrichment in H3K4met could not be clearly visualized by immunostaining of the *ddm1-5* nuclei (*Figure 10H*). Interestingly, the chromocenter remnants remained unlabeled. Therefore, loss of H3K9met does not automatically induce replacement by H3K4met in these chromosomal regions.

I.3. MOM1 – Morpheus Molecule

The *mom1-1* mutation was identified in a T-DNA mutant screen designed to recover mutations reactivating the silenced multicopy *HPT* locus in line A (Amedeo et al., 2000). The T-DNA insertion induced a 1980bp deletion at the mutant locus, affecting the C-terminal part of the *MOM1* gene. *MOM1* encodes a multidomain protein of 2001aa with homology to the ATPase domain of SWI2/SNF2 chromatin remodeling factors, however spanning only motifs IV, V and VI of a helicase unit normally composed of two distinct domains separated by a cleft (Amedeo et al., 2000). MOM1 carries three putative nuclear localization sequences (NLSs), localizes to the nucleus in transient expression assays (Amedeo et al., 2000) and shows homology to the actin binding region of tensin. The *MOM1* gene is conserved among plants like tobacco, brassica and rice, however it does not have any homologues outside the plant kingdom. In contrast to *ddm1*, *mom1* mutant plants do not show any phenotypic alterations, even after many generations of inbreeding, and challenged by different abiotic stresses, hormones or DNA damaging agents (Paolo Amedeo, Dissertation). Loss of MOM1 function reactivates silencing from other complex transgenic loci e.g. the 35S::GUS locus (Morel et al., 2000), pericentromeric repeats (TSI, (Steimer et al., 2000)) and several single copy genes, like Cyclophilin-40 (*CyP40*, Jerzy Paszkowski unpublished results). Interestingly, again in contrast to *ddm1,* DNA methylation is not affected at the reactivated targets, as determined by Southern blot analysis and bisulfite sequencing of the 35S promoter of the *HPT* transgene (Amedeo et al., 2000). *mom1-1* is a recessive mutation, and immediate re-silencing of the reactivated targets is observed in the F1 generation when the *mom1* mutant is backcrossed to wildtype plants.

Figure 11

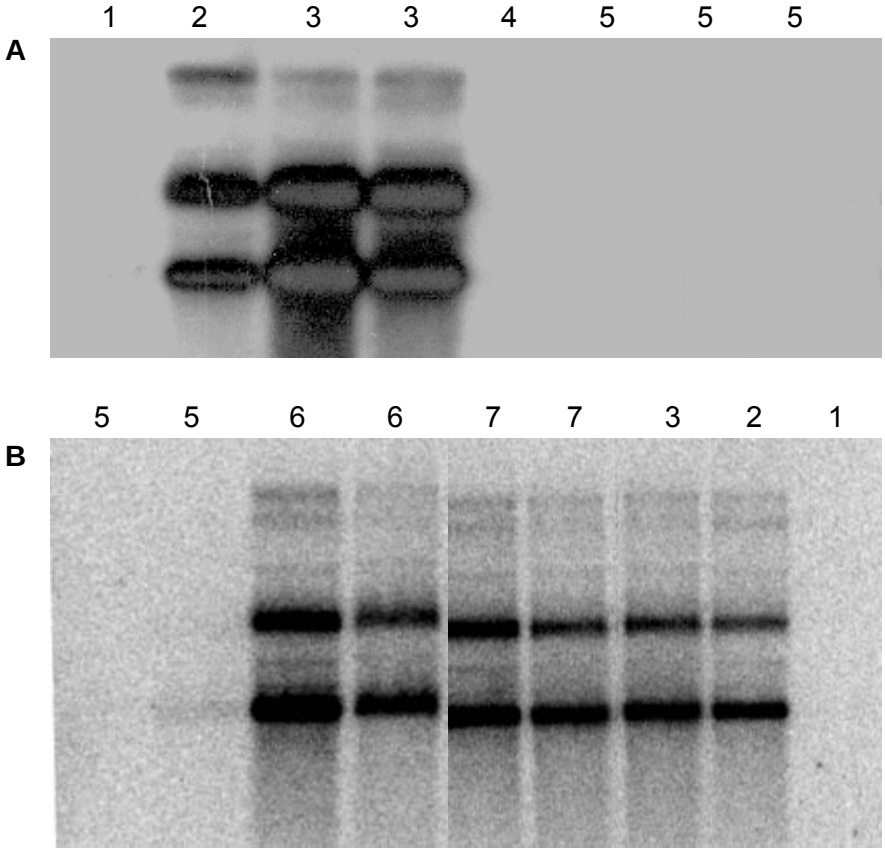

Figure 11. MOM1-HA fusions expressed from a genomic construct under its endogenous promoter complement the TSI expression phenotype, while expression of MOM1-HA cDNA from a constitutive 35S promoter fails to silence TSI

Different MOM1-HA fusion constructs introduced into the *mom1-1* mutant were tested for functional complementation by Northern Blot analysis using a probe for TSI repeats, reactivated in *mom1-1* mutant plants; genomic construct (**A**) and 35S::cDNA MOM1 (**B**)

line A (1), *mom1-1* (2), *mom1-1* with empty vector (3), *mom1-1* with a genomic MOM construct (4), *mom1-1* expressing a MOM1-HA protein fusion under the endogenous promoter (5), *mom1-1* expressing HA-MOM1 cDNA under control of the 35S promoter (6), *mom1-1* expressing MOM1-HA cDNA under control of the 35S promoter (7).

I.3.1. Subcellular Localization of MOM1 Protein

In order to study the subcellular localization of MOM1 protein, a tagged version of the protein was expressed in *A. thaliana*. Therefore, *mom1-1* mutant plants were transformed with genomic constructs expressing MOM1-HA or MOM1-GFP fusion proteins from its endogenous promoter, as well as a construct expressing a MOM1-HA fusion protein from

Figure 12

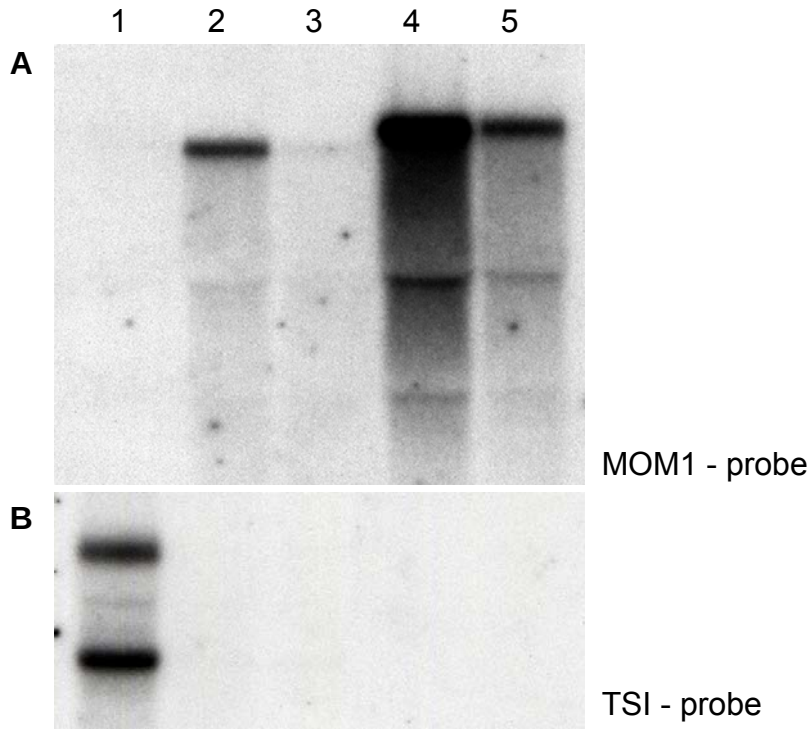

Figure 12 Expression of *MOM1* and *TSI* transcripts in *mom1-1* mutant, wildtype and a line complementing the *mom1-1* mutation with a genomic MOM1-GFP construct

(A) Northern Blot hybridized with a *MOM1* probe reveals the lack of a *MOM1* transcript in leaves of the *mom1-1* mutant (1). Line 2 and 3 show expression of *MOM1* RNA in wt flowers and leaves, respectively. Line 4 and 5 show expression of a transgenic MOM1-GFP construct under control of the endogenous MOM1 promoter (Tariq, unpublished results) in the *mom1-1* mutant background in flowers (4) and leaves (5). **(B)** The blot was reprobed with the TSI pA2 fragment, demonstrating that the MOM1-GFP fusion is functional in silencing the expression of TSI.

its cDNA under control of the 35S promoter (Yoshiki Habu, personal communication). By Northern Blot analysis I tested the functionality of the fusion proteins upon their ability to repress TSI, reactivated in *mom1-1*. While the genomic constructs expressing MOM1 or a MOM1-HA fusion protein successfully complement the *mom1-1* phenotype (*Figure 11A*), the expression of MOM1 from the 35S promoter failed to complement (*Figure 11B*). It was not investigated whether this was due to silencing of the 35S promoter, the failure to form

a stable transcript in the absence of introns or the failure to tissue specifically and developmentally regulate the expression. However, prior attempts to generate plants over-expressing the MOM1 protein have failed (Yoshiki Habu, personal communication), suggesting that high levels of MOM1 are detrimental for plant growth and development. A transgenic line expressing a MOM1-GFP fusion protein in the *mom1-1* background was also generated (Muhammed Tariq, Dissertation). *Figure 12B* shows that even a C-terminal fusion to the 27kDa GFP protein still complements the TSI expression phenotype.

In wildtype plants the *MOM1* transcript is expressed to higher levels in flowers compared to leaves (*Figure 12 A*, lane 2 and 3, see also Chromatin Data Base). The *MOM1-GFP* transcript is present at ~5 times higher levels, however the tissue-specific expression pattern is preserved, showing the functionality of the promoter.

To investigate the subnuclear localization of MOM1 protein, I first expressed a MOM1-GFP fusion protein transiently in *Nicotiana plumbaginifolia* protoplasts. Transient expression of MOM1-GFP reaches a maximum at about 5-6 hours after transformation. At later time points only protoplasts transformed with a control plasmid expressing GFP alone are observed, while no more protoplasts expressing MOM1-GFP were detected. This again confirms the notion that over-expression of MOM1 by the 35S promoter might be harmful to plant cells. GFP alone is identified in the nucleus and the cytoplasm (*Figure 13A*, upper panel), while the MOM1-GFP fusion protein is exclusively located in the nucleus (*Figure 13A*, lower panel). Even though protoplasts were analyzed at different time points after transformation, it was impossible to detect a specific subnuclear localization of the fusion protein, especially since it is not feasible to counterstain the nucleus of living protoplasts with DAPI. Since the transient expression system has, in addition, the drawback of being a heterologous system, I used the complementing lines expressing the MOM1-HA or MOM1-GFP fusion protein under control of the endogenous promoter for further studies. I performed immunolocalization experiments with anti-HA and anti-GFP antibodies (courtesy of Uli Mueller) on mesophyll protoplasts of 3-week old seedlings. Staining with the anti-HA antibody was not successful, probably due to the small tag that might be buried within the large MOM protein when fixed with formaldehyde in its native conformation. With the anti-GFP antibody however I observed many speckles throughout euchromatin (*Figure 13B*). This distribution was surprising, since I expected to detect at least part of the protein in the heterochromatic region of the chromocenters. These results must be taken with caution, since not only the GFP-tag could interfere with the proper localization of the MOM1 protein, but also the expression levels of the fusion protein are

higher than wildtype levels bearing the possibility that its natural binding sites are saturated.

Figure 13

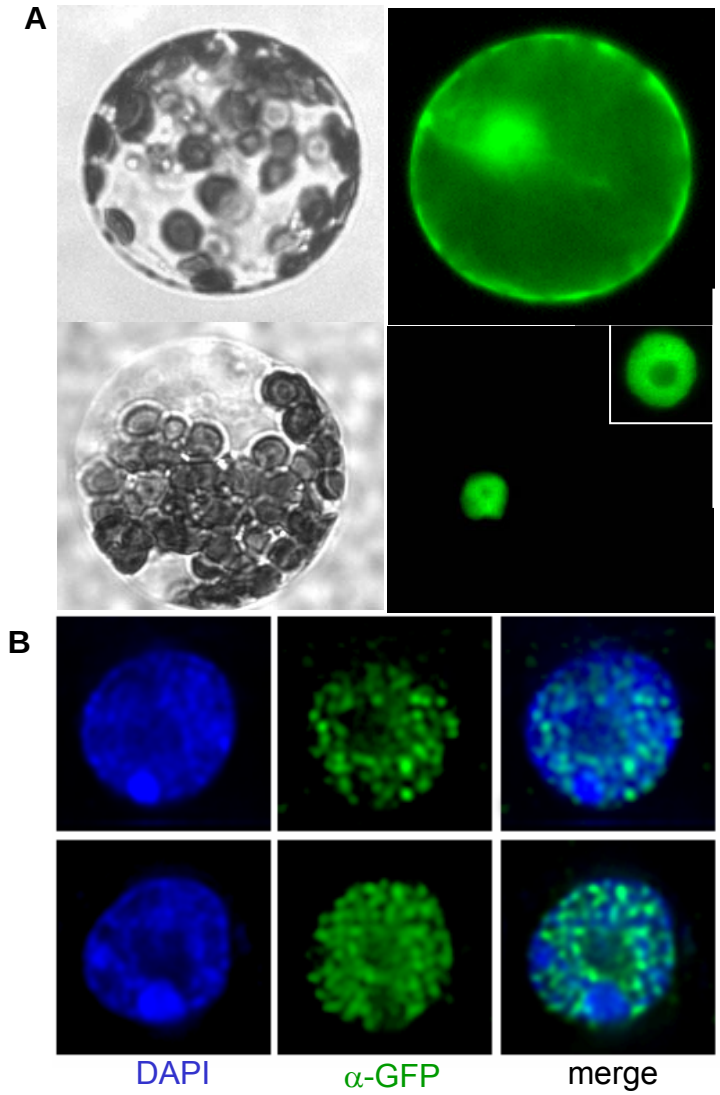

Figure 13. MOM1 is a nuclear protein and localizes to speckles in the euchromatin
(**A**) Transient expression of GFP (top) and the MOM1-GFP fusion protein (bottom) under control of a 35S promoter in *Nicotiana plumbaginifolia* protoplasts. Images were taken at 50x or 100x magnification (insert in lower panel) 5 hours post-transfection. Right panels show a light image of a *N. plumbaginifolia* protoplasts, left panels fluorescence GFP images. (**B**) DAPI staining of DNA (blue, left panel) and immunodetection using an anti-GFP antibody (green, middle panel, Uli Mueller personal communication) in nuclei of *mom1-1* mutant plants expressing a MOM1-GFP fusion protein from the endogenous MOM1 promoter. Right panels show merged images. Two layers of the same nucleus were selected from a deconvoluted image stack.

I.3.2. Chromatin Structure and Distribution of Histone Modifications are not affected in *mom1-1*

So far, the mechanism by which MOM1 establishes transcriptional gene silencing is not described. One hypothesis suggests that MOM1 establishes transcriptional repression by a mechanism involving histone tail modifications at certain loci marked for TGS. These marks might be DNA methylation or a specific sequence context e.g. the repetitive nature of (foreign) DNA. MOM1 could as well be responsible for a certain arrangement of the target loci into nuclear sub-compartments e.g. the nuclear periphery or the nucleolar compartment, thereby facilitating silencing in analogy to phenomena observed in yeast.

I was interested to test these hypotheses using fluorescence *in situ* hybridization and immunolocalization techniques. First I examined nuclear spreads of line A and *mom1-1* mutant plants, using FISH to target 180bp repeats, rDNA, *HPT*, *TSI* and telomeric sequences. In contrast to *ddm1*, the nuclear structure of the *mom1* mutant in general and of the pericentromeric heterochromatin in particular was not altered compared to line A the isogenic background of *mom1-1* (*Figure 14A-D*). In addition, and despite reactivation of the *HPT* gene, the heterochromatic nature of the transgenic locus was also retained (*Figure 14A, B*). The localization of the transcriptionally activated TSI DNA in relation to the core centromeric 180-bp repeats and the chromocenters also remained unchanged: TSI repeats were still closely associated with centromeric sequences and were part of the DAPI bright chromocenters (*Figure 14C, D*). Telomeres were also located around the nucleolus and the structure of rDNA was unaltered (*Figure 14E, F*).

Although the *mom1* mutation does not change the methylation of reactivated target sequences like *HPT* or *TSI* or modify methylation of centromeric repeats, it is still possible that other chromosomal regions suffer methylation changes. In clear contrast to the distorted methylation patterns in the *ddm1-5* mutant, immunostaining with a 5^{met}Cytosine antibody revealed no changes in methylation levels or its distribution in *mom1* (*Figure 15E, F*), corroborating previous observations (Amedeo *et al.,* 2000). Next I studied the effect of MOM1 depletion on the global distribution of particular histone modifications, namely H4 acetylation, H3K4 and H3K9 methylation. Euchromatin of both line A and the *mom1* mutant was intensely stained with an antibody directed against the tetra-acetylated isoform of H4 (*Figure 15C, D*), while the chromocenters lacked any signal. The identical distribution was observed for an antibody detecting the euchromatic mark H3K4 methylation (*Figure 15G, H*), revealing likewise no change in the *mom1-1* mutant. Methylation of histone H3 at position K9 denotes silent heterochromatin; this modification

Figure 14

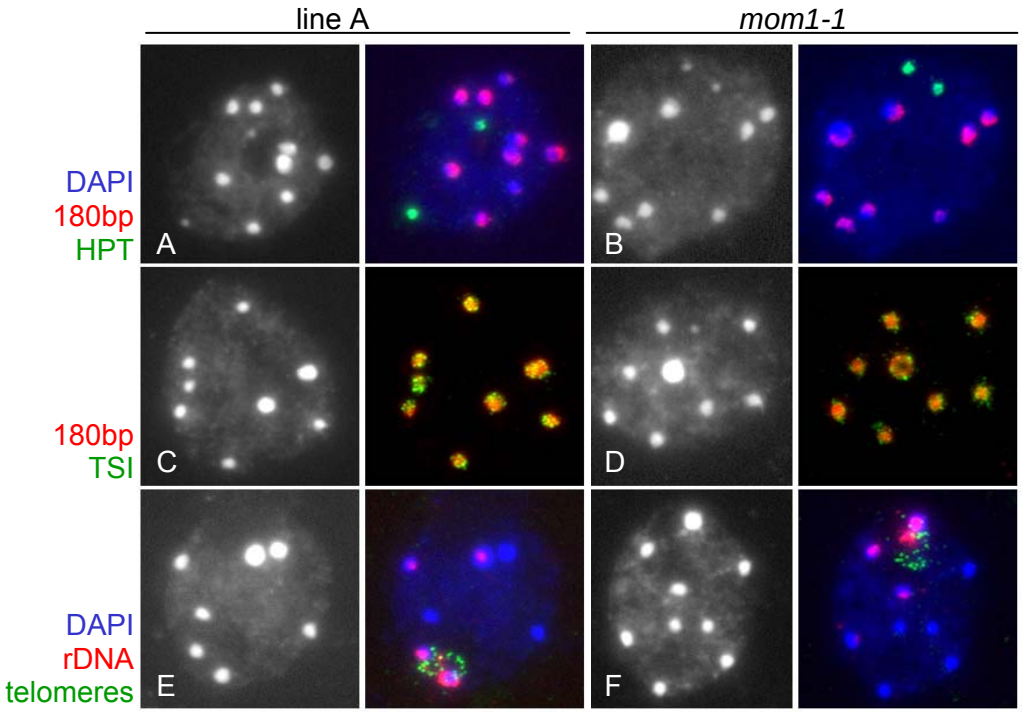

Figure 14. Organization of heterochromatin in line A and *mom1-1*
Interphase nuclear spreads of transgenic line A and *mom1-1,* stained with DAPI (black and white in left panel, blue in merged image on the right) and hybridized with fluorescent probes for centromeric repeats (180bp, **A**-**D**, red), *HPT* vector DNA (**A, B**, green), pericentromeric TSI repeats (**C, D**, green), telomeric repeats (**E, F**, green) or rDNA repeats (**E, F**, red).

is especially enriched at chromocenters (*Figure 15E*). In the *mom1* mutant, although TSI sequences as part of the chromocenters were transcribed, H3K9 methylation remained specifically localized to the chromocenters as in line A (*Figure 15F*). In summary, the *mom1-1* mutation does not affect heterochromatin structure of the reactivated transgenic locus or the arrangement of reactivated TSI sequences into chromocenters. The DNA methylation pattern is unaltered as is the global distribution of the well-defined epigenetic marks H3K4 and H3K9 methylation and the acetylation status of H4.

The inactivation of B-cell specific genes during development is linked to a change in nuclear organization involving an enhanced centromeric association of inactivated loci (Brown *et al.,* 1997). We hypothesized that a similar mechanism, requiring MOM1 protein,

Figure 15

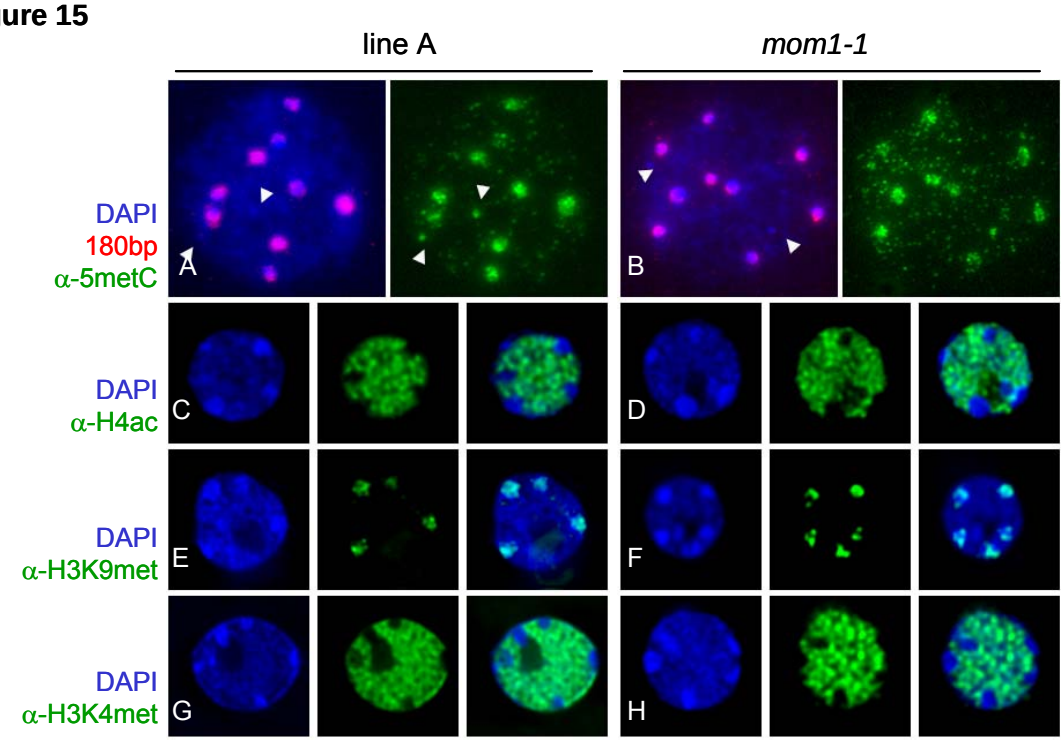

Figure 15. DNA and chromatin modification in transgenic line A and mutant *mom1-1*

A, B: Distribution of DNA methylation revealed by DAPI stain (blue) and FISH with probes for centromeric repeats (180bp, red, left panel) and immunodetection with an antibody specific for 5-methylcytosine (green, right panel). The newly formed heterochromatic knob is marked by white arrowheads in **A**.

C-**H**: Distribution of histone modifications revealed by DAPI stain (blue, left panels) and immunodetection with an antibody specific for tetra-acetylated histones (green, middle panel **C, D**), histone H3 di-methylated at lysine 9 (**E, F**) and histone H3 di-methylated at lysine 4 (**G, H**). Right panels show merged images. Images **C**-**H** show single layers selected from deconvoluted image stacks.

might be necessary to maintain the silenced state of the transgenic locus in line A. For this reason we compared the frequency of centromeric association of the *HPT* locus in nuclei of line A and *mom1* (*Figure 16*). We grouped the nuclei into different types, showing either two or only one heterochromatic knob and scored, whether both, one or none of the *HPT* loci were associated with chromocenters represented by centromeric heterochromatin

(*Figure 16*). However, no significant differences of its localization could be found between the silenced state of the locus in line A and its transcriptionally activated state in *mom1-1*. The same result was obtained if the association was calculated per locus (47.4% in close vicinity of chromocenters in line A versus 45.3% in *mom1-1*). Therefore, MOM1 seems to play no role in the spatial organization of the transgenic locus relative to constitutive heterochromatin domains. However, to confirm this statement it would be necessary to study nuclei with a conserved three-dimensional structure, since a protein-mediated association might be disrupted when the nuclei are spread for FISH analysis.

Figure 16

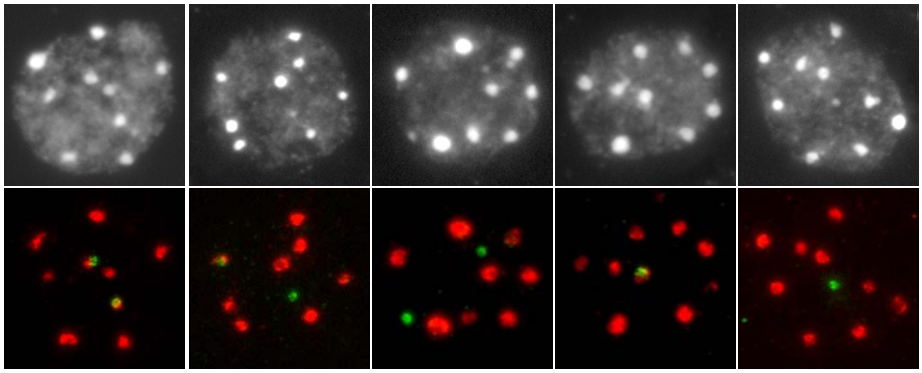

	A	B	C	D	E
line A	15.6%	30.1%	24.5%	19.7%	10.0%
mom1-1	13.5%	36.1%	29.0%	17.2%	4.2%

Figure 16. Frequency of association of the *HPT* locus with chromocenters is not changed in the *mom1-1* mutant
Localization of the transgenic heterochromatic knob in relation to chromocenters revealed by DAPI stain (black and white, upper panel) and FISH with probes for centromeric repeats (180bp, red) and the *HPT* locus (green, lower panel). Observed nuclei were grouped into 5 types: with 2 heterochromatic knobs (**A-C**), thereby showing both (**A**), one (**B**) or none (**C**) of the loci associated with chromocenters; or one knob (**D-E**) in close association (**D**) or localizing apart from chromocenters (**E**). The frequency of the association with centromeric heterochromatin was calculated from > 265 nuclei per genotype.

I.4. Histone De-Acetylase HDA6

In the *Arabidopsis* genome a total of 16 potentially functional histone deacetylases have been identified and these can be classified into three families (Pandey *et al.,* 2002); see also http://chromdb.biosci.arizona.edu): 10 belong to the RPD3/HDA1 superfamily, 2 are members of the SIR2-like family and 4 belong to the plant-specific HD2–like histone deacetylases originally identified as acidic nucleolar phosphoproteins from corn (Lusser *et al.,* 1997). Interference of HDAC functions in plants has been studied using inhibitors such as trichostatin A, SAHA or butyrate and using transgenic plants containing antisense or over-expressing constructs. These approaches have provided evidence that HDACs are involved in regulation of histone acetylation and thereby gene expression, with consequences for plant morphology and development (Chen and Pikaard, 1997; Wu *et al.,* 2000; Tian and Chen, 2001). Dissecting the function of individual HDAC members is problematic in these studies. Therefore the analysis of loss-of-function mutations of individual HDAC genes should add valuable information on specific roles. Mutants in an *Arabidopsis* RPD3-like HDAC gene, *AtHDA6* were found in three independent mutant screens based upon their effects on specific transgene expression (Murfett et al., 2001; Aufsatz et al., 2002). The *HDA6* mutant alleles *axe1* lead to higher expression from a marker gene with an auxin-responsive promoter element (Murfett *et al.,* 2001), while the *rts1* alleles of the locus interfere with double-stranded RNA-directed transcriptional silencing (Aufsatz *et al.,* 2002). The mutant *sil1* (modifiers of silencing 1, Furner *et al.,* 1998) was identified in a screen for mutations releasing silencing of the complex, rearranged transgenic locus C, containing the chalcone synthase gene (*CHS*) and the resistance marker genes neomycin phosphotransferase (*NPT*) and hygromycin phosphotransferase (*HPT*). The *sil1* mutation reactivates mainly the resistance marker genes, while the homology-dependent silencing of the endogenous and transgenic *CHS* copies are only weakly affected (Furner *et al.,* 1998).

I studied the effect of the *HDA6* mutant on the release of transcriptional silencing and the impact on chromatin structure of heterochromatic regions, especially rDNA repeats. Thereby, I concentrated on two alleles, *axe1-5* and *sil1* (*Figure 17A)*. The mutant allele *axe1-5* does not produce an *HDA6* transcript of the expected size, but shorter and longer mRNAs due to a splice-site mutation (Murfett *et al.,* 2001). This allele resides in the Col background and in all experiments the transgenic line DR5, carrying the pDR5 plasmid insertion, was used as wt control. The second allele *sil1* carries a point mutation in the very N-terminal part of the protein, which leads to a single amino acid

Figure 17

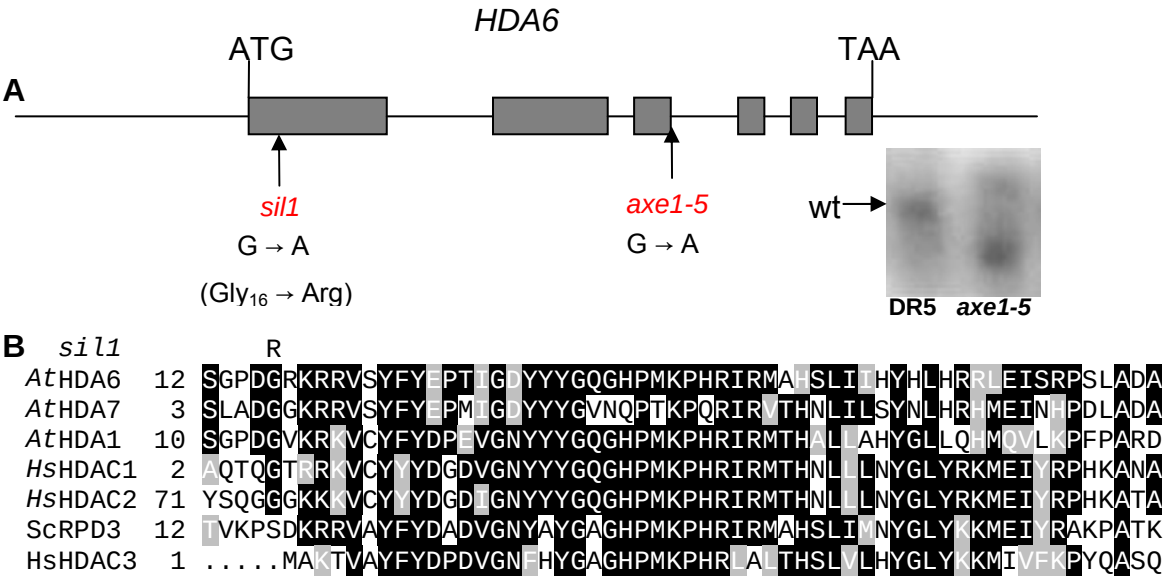

Figure 17. *sil1* has a mutation in the *AtHDA6* gene
Sequencing of the *HDA6* gene in the *sil1* mutant reveals a point mutation, 46 bases after the ATG initiation codon, leading to the replacement of Gly_{16} by Arginine. The *axe1-5* mutant has a base substitution at position 1635 downstream of the ATG at the third exon-intron junction. Alignment of *At*HDA6 with *Arabidopsis* (At), human (Hs) RPD3-like HDACs and yeast (Sc) RPD3 reveals a conservation of Gly_{16} in plant and human RPD3-like HDACs.

exchange of glycine at position 16 to an arginine. This glycine is conserved in the *Arabidopsis* homologues HDA7 and 19, as well as in the human HDAC1 and 2, however in the yeast homologue Rpd3p this specific glycine is replaced by a serine (**Figure 17B***)*. In the experiments described I used the *sil1* mutation in the Ler background. Neither mutant allele results in a strong phenotypic alteration. However, I observed a significant delay in the onset of flowering (**Figure 18**). In later generation of the *axe1-5* mutant infrequently plants with homeotic flower mutations were observed (data not shown).

Figure 18

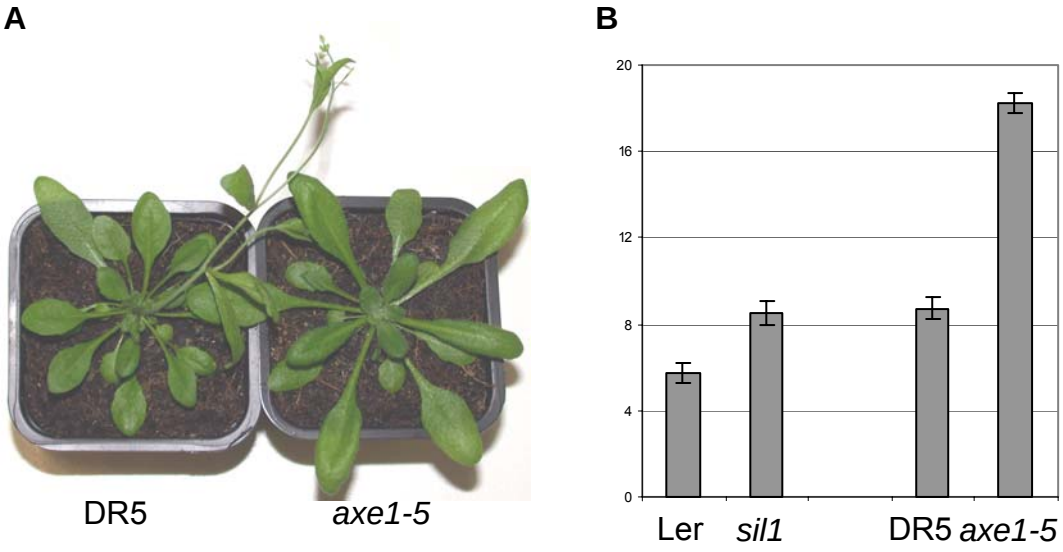

Figure 18. *HDA6* mutant alleles show a delayed flowering phenotype
Both *HDA6* mutant alleles *sil1* and *axe1-5* (illustrated in **A**) show delayed flowering compared to Ler and DR5 wildtype plants, respectively. Flowering time difference was quantitatively assessed by counting the number of rosette leaves formed by onset of flowering by Ler, *sil1*, DR5, and *axe1-5* plants (**B**).

I.4.1. Effect of *HDA6* Mutations on Maintenance of Transcriptional Gene Silencing

The C locus (reactivated by the mutant *sil1*) and the genomic insertions formed by pDR5 and p2xD0 integration (reactivated by the *axe1* mutants) are all very complex transgenic loci, consisting of multiple, rearranged and methylated transgene copies. These features made it likely that the loci were transcriptionally inactivated, and that the *HDA6* mutations interfered with transcriptional gene silencing (TGS). To verify this assumption, we crossed

alleles of *HDA6* mutant plants (*sil1, axe1-1, axe1-3, axe1-4 and axe1-5)* to a well-established TGS test line. This transgenic line, L5 (Morel *et al.,* 2000) is homozygous for an insert carrying multiple and methylated copies (**Figure 19A**) of a transgene consisting of the CaMV35S promoter and the *GUS* marker gene. The 35S::GUS transgene is silenced at the transcriptional level, as determined by Northern blot (**Figure 19B**) and transcriptional run-on assays (**Figure 19C**).

Figure 19

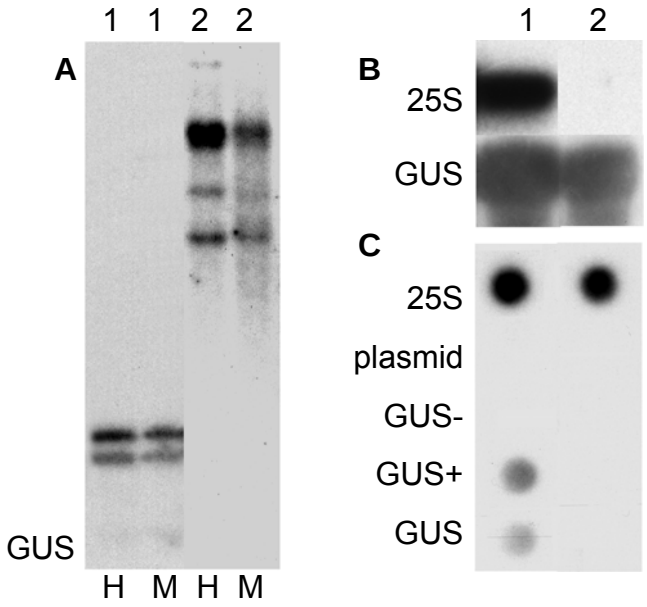

Figure 19. The 35S-GUS transgene at the L5 locus is methylated and transcriptionally silenced

A transcriptionally active transgenic line Hc1 (1) and the silenced line L5 (2) were characterized by a combination of **(A)** Southern blot, **(B)** Northern blot and **(C)** nuclear run–on analysis. The presence of high molecular weight fragments observed after digestion by the methylation-sensitive restriction enzymes *Hpa*II (H) and *Msp*I (M) and hybridization with radio-labeled 35S and GUS probes indicate that the entire insert in line L5 is strongly methylated **(A)**. Hybridization of 10 μg total RNA with a probe corresponding to the GUS coding region (upper panel) or a 25S rDNA probe reveals the absence of GUS cytoplasmic transcript in line L5 **(B).** Run-on experiments using labeled RNA extracted from leaf nuclei of adult plants for hybridization of dot blots demonstrate the lack of nascent GUS transcript in line L5. Dots contain 2μg DNA each of the 25S rDNA-containing plasmid (25S), single-stranded pBluescript KS+ (plasmid), and GUS containing plasmids (GUS- : sense single-stranded, GUS+ : antisense single-stranded, GUS : double-stranded) **(C).**

F_2 seeds derived from the crosses were grown under axenic conditions, and seedlings were stained for GUS activity one week after germination. Approximately 19% of each F_2 progeny expressed the GUS marker gene. This corresponds to the expected 3/16 ratio of F_2 plants homozygous for an *HDA6* mutation and carrying one or two copies of the L5 insert. Conversely, none of 150 F_2 seedlings resulting from a cross between a wild-type plant and line L5 expressed GUS, indicating that the maintenance of TGS at the L5 insert requires the *HDA6* gene product and is unaffected by crossing.

I also tested the effect of the *HDA6* mutations on silencing of endogenous pericentromeric repeats, *TSI*. We detected reactivation of *TSI* repeats by Northern blots in the *axe1-5* and *sil1* mutant (*Figure 20A*). The Northern blot was reprobed for the constitutively expressed RNA of RAN (small GTP binding protein, Haizel et al., 1997) as loading reference (*Figure 20B*).

Figure 20

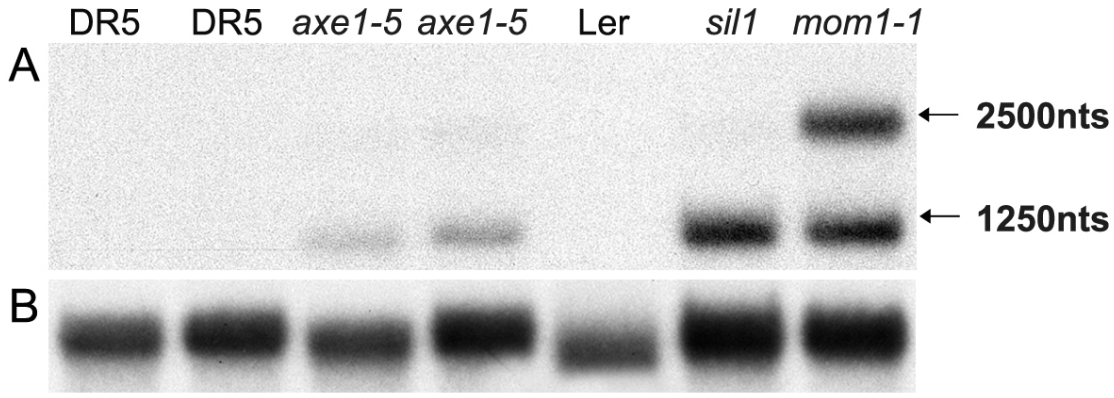

Figure 20. *sil1* and *axe1-5* alleles release silencing of an endogenous transcriptionally silent information (TSI) sequence
(A) Northern Blot analysis using the TSI pA2 fragment as probe reveals TSI transcripts in the two *HDA6* mutant alleles *axe1-5* and *sil1***.** Lane 1, 2 and 5 show silencing of the endogenous TSI repeats in the transgenic background of the *axe1-5* mutants (DR5) and the Ler ecotype; while lane 3, 4, 6 and 7 show reactivation of TSI in the two *HDA6* mutant alleles and the *mom1-1* mutant respectively. Predominantly, two transcripts are expressed – a longer, polyadenylated one (Steimer *et al.,* 2000), as well as a shorter transcript. **(B)** The blot was reprobed with RAN (small GTP binding protein, (Haizel *et al.,* 1997) as a loading reference. Total RNA (20ug per lane) was extracted from rosette leaves of adult plants.

Interestingly, the point mutant *sil1* results in similar, if not higher *TSI* expression compared with the splice site mutant *axe1-5*, but both mutants have lower *TSI* levels than *mom1*. While the possibly nuclear non-polyadenylated, 1250 nt long *TSI* fragment and the cytoplasmic, polyadenylated 2500 nt long RNA (Steimer *et al.,* 2000) accumulate to similar levels in *mom1,* the *HDA6* mutants predominantly express the shorter, non-polyadenylated fragment (*Figure 20A*).

Therefore, HDA6 is involved in transcriptional repression of pericentromeric repeats and certain transgenic loci, however it is not involved in co-suppression of endogenous copies of a transgene (Furner et al., 1998).

I.4.2. Effect of *HDA6* Mutations on Chromatin Structure at rDNA Repeats

Because the *HDA6* gene product has sequence homology with other nuclear proteins like Rpd3p and human HDAC1/2 shown to have histone deacetylase activity, we studied the effect of *HDA6* mutations on the nuclear distribution of histone H4 acetylation. Mesophyll protoplasts from Ler, the *sil1* mutant, DR5 and the *axe1-5* mutant were fixed, stained with an antibody detecting tetra-acetylated histone H4 (α-H4ac) and counterstained with DAPI. The DAPI-stained nuclei of mutants were indistinguishable from wild type. Chromatin containing tetra-acetylated histones was found exclusively in euchromatin in all wild-type nuclei (*Figure 21A* and *C*). However, nuclei of *axe1-5* and *sil1* mutant plants contained chromocenters that were intensively stained with the H4ac antibody. This effect was more pronounced in the *axe1-5* mutant than in the *sil1* mutant (*Figure 21B* and *D*, and Table 1, see below). The labeled chromocenters were always in close association with the nucleolus (*Figure 21B* and *D*, arrow). Layer-by-layer analysis of mutant nuclei revealed that the number of highly acetylated heterochromatic regions never exceeds 4 in one nucleus and comprises only part of the chromocenter (*Figure 21B* and *D*). The tight association of the highly acetylated chromocenters with the nucleolus, together with the proposed role in rRNA gene repression described for the *HDA6* homologue *RPD3* in yeast (Sandmeier *et al.,* 2002), suggested that these represent the rDNA loci. To examine a possible relationship between acetylated histones and rDNA, I combined immunodetection of modified histones with fluorescent *in situ* hybridization (FISH) for rDNA repeats. The rDNA loci of wild type and mutant nuclei are localized close to the nucleolus. However, while all chromocenters including those with the rDNA repeats were free of any H4ac signal in DR5 (*Figure 21E*), the double labeling technique revealed an overlap between the bright H4ac immunosignals and rDNA FISH signals in mutant nuclei (*Figure 21F*).

Therefore, the loss of functional HDA6 results in a drastic enrichment of histone acetylation specifically at rDNA repeats.

Figure 21

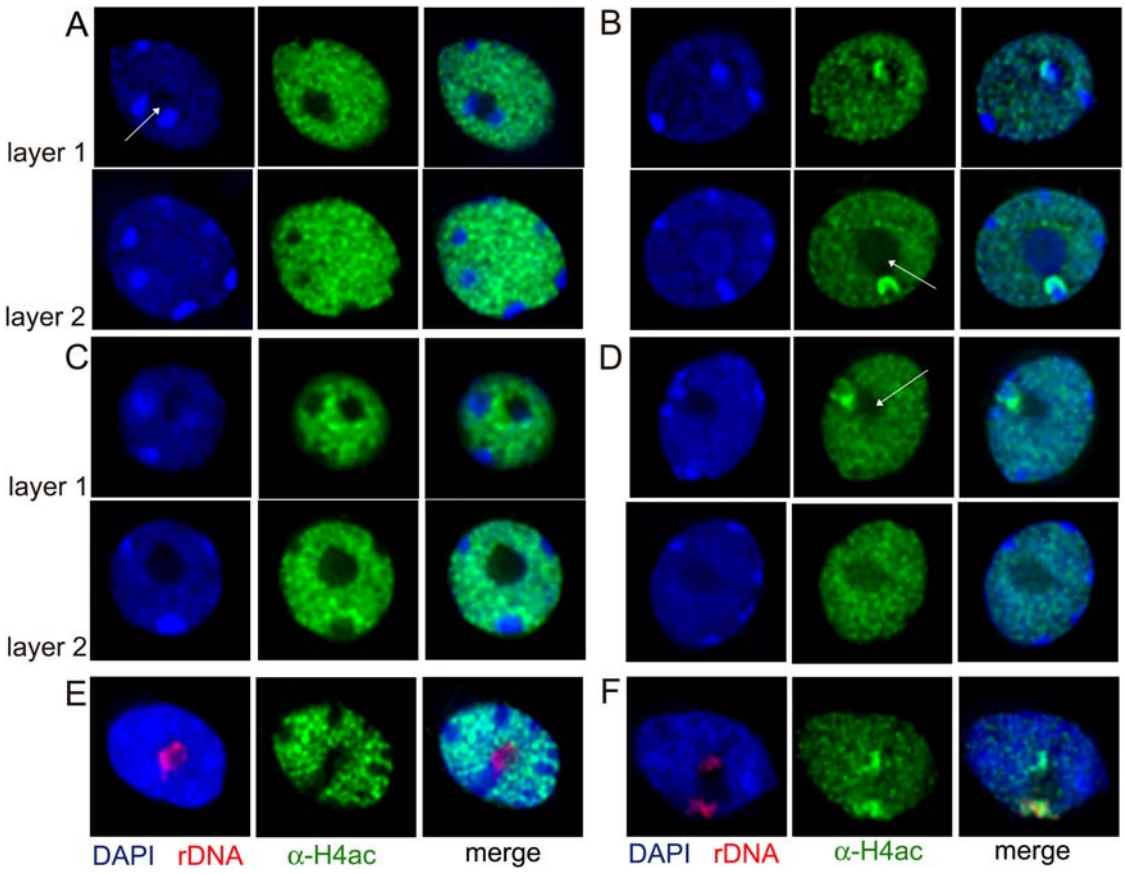

Figure 21. rDNA repeats are hyperacetylated in nuclei of HDA6 mutants
Distribution of histone H4 acetylation revealed by DAPI staining of DNA (blue, left panel) and immunodetection with an antibody specific for tetra-acetylated histone H4 (green, middle panel) in nuclei of control lines DR5 (**A**) and Ler (**C**) and in *axe1-5* (**B**) and *sil1* (**D**) mutant nuclei. Right panels show merged images. For each nucleus two layers were selected from deconvoluted image stacks, arrows mark the nucleolus. (**E**, **F**) Fluorescence *in situ* hybridization using rDNA repeats (red, left panel) following immunostaining with α-H4ac antibodies (green, middle panels) shows that the rDNA loci indeed are devoid of H4ac staining in wild type (**E**), but become highly enriched with H4Ac in mutant nuclei (**F**).

All *HDA6* alleles were originally isolated as mutations affecting loci other than rRNA genes. Intense H4ac immunosignals could indicate a global increase in histone acetylation that would appear more prominent at rDNA loci because these include long stretches of silent rRNA genes that are highly condensed in comparison to euchromatic regions (Pontes *et al.,* 2003). To test the possibility that reduced HDA6 activity affects histone acetylation levels globally, I isolated histones from DR5 and *axe1-5* plants and performed western blots. There is no obvious increase in tetra-acetylated histone H4 in mutant plants (*Figure 22A*). Also, the amount of methylation at lysine 4 of histone H3, another epigenetic mark for actively transcribed genes, is not significantly increased in the mutants (*Figure 22A*). Although the possibility that the HDA6 protein in *axe1-5* is still partially functional and sufficient to maintain a basal level of hypoacetylation cannot be excluded, it seems likely that HDA6 is not the major histone deacetylase in *Arabidopsis*, but may represent a member directed to specific targets, such as rDNA repeats or complex transgenes.

An increase in histone acetylation is often correlated with another specific modification – methylation at lysine residues at position 4 of histone H3 (H3K4, (Strahl and Allis, 2000). To investigate this correlation for the hyperactylated rDNA loci in *HDA6* mutants, I included antibodies specific for H3K4 methylation in my immunostaining experiments. All chromocenters in the wildtype are free of H3K4 methylation as described before, but I observed an enrichment of H3K4 methylation in the *axe1-5* and *sil1* mutants at the chromocenters presumably containing the rDNA (*Figure 22C* and *D*, lower panels). This change affects a significant number of nuclei in both mutants, although the proportion is lower in *sil1* (Table 1).

Table 1. Fraction of *HDA6* mutant nuclei with NOR-specific enrichment in acetylated histone H4 or methylated H3K4, respectively

	H4ac		H3K4met	
axe1-5	98%	n=100	62,4%	n=303
sil1	39.6%	n=306	19,1%	n=308

To confirm the local hyperacetylation at rDNA loci and the concomitant increase in H3K4 methylation at the molecular level I performed Chromatin Immunoprecipitation on 3-week

Figure 22

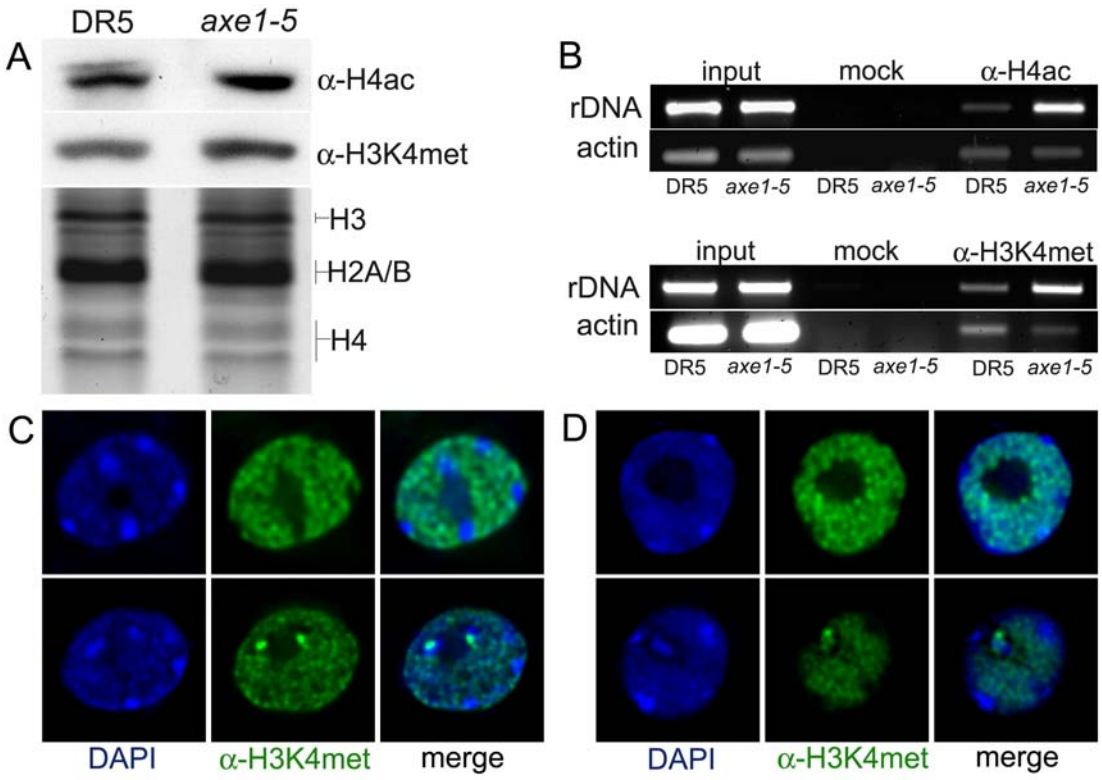

Figure 22. Changes in levels of H4ac and H3K4met are limited to specific loci in *HDA6* mutants

(**A**) Western Blot analysis detecting H4ac (upper panel), and H3K4met (middle panel) using α-H4ac and α-H3K4met antibodies, respectively, on protein extracts from wild type (DR5) and *axe1-5* mutant plants. Bottom panel: Coomassie staining shows equal protein loading. (**B**) Chromatin immunoprecipitation performed in the control line DR5 and the mutant allele *axe1-5* reveals an increase in H4ac and H3K4met at rDNA repeats. The *Actin2/7* gene is equally present in mutant and control precipitates. If the antibodies are omitted during the procedure (mock), neither target is amplified, while the equal strength of bands after PCR with the input fraction indicate equal amounts of chromatin prior to immunoprecipitation. (**C**, **D**) Distribution of histone H3 methylated at lysine K4 revealed by DAPI staining (blue, left panel) and immunodetection with an antibody specific for H3K4met (green, middle panel) in nuclei of control lines (upper row) DR5 (**C**), Ler (**D**) and mutants (lower row) *axe1-5* (**C**) and *sil1* (**D**). Right panels show merged images.

old soil-grown plants of DR5 and the mutant allele *axe1-5*. Amplification with primers specific for a 280bp region at the 5'end of the 25S rRNA gene showed that indeed rDNA repeats are enriched in both H4ac and H3K4met immunoprecipitates, compared to the control line DR5. These chromatin modifications at the *Actin2/7* gene, serving as reference

(Johnson et al., 2002; Tariq et al., 2003), remain unaffected by the *HDA6* mutation (*Figure 22B*). Therefore, the irregular histone acetylation in the *HDA6* mutants at rDNA-comprising chromocenters is correlated with an increase in H3K4 methylation.

Only a subset of rDNA repeats in eukaryotic cells is transcribed at a given time (McKnight and Miller, 1976; Morgan *et al.,* 1983; French *et al.,* 2003). The hyperacetylation of rDNA repeats in the *HDA6* mutants and the increased histone H3K4 methylation suggested that these changes might reflect an increase in rRNA transcription. However, comparison of rRNA levels relative to actin RNA using semi-quantitative RT-PCR (*Figure 23A*) or relative to total RNA using an S1 nuclease protection assay to detect pre-rRNAs initiated directly at the gene promoter (*Figure 23B*) did not reveal any differences between mutant and wild-type. However, potential up-regulation of ribosomal RNAs might be masked when normalized to total RNA because rRNA represents the major species of RNA.

Figure 23

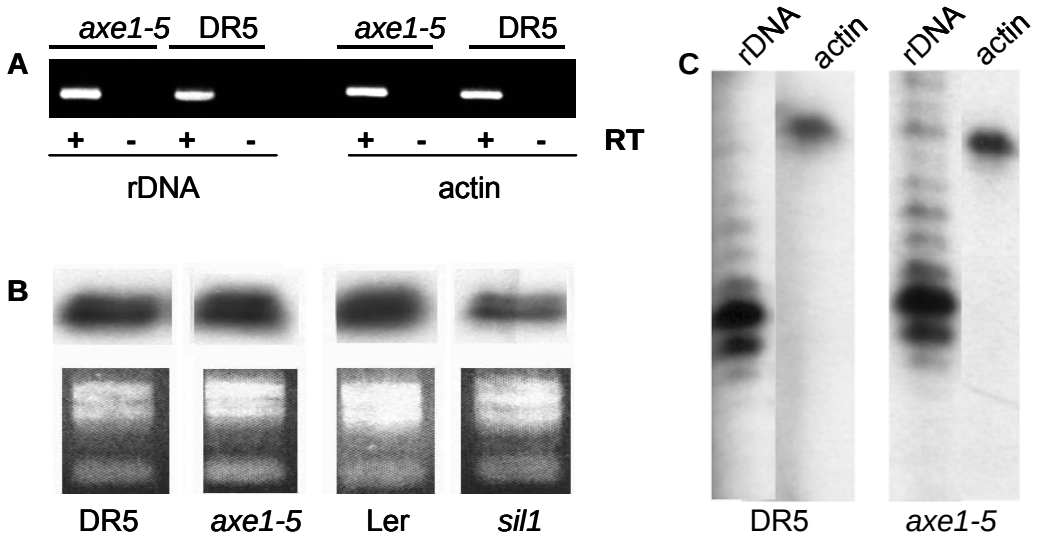

Figure 23. rDNA expression is not increased in HDA6 mutant plants
RT-PCR was performed on total RNA extracted from DR5 and *axe1-5* plants using primers specific for rDNA and actin (**A**, identical primers to those used in the ChIP experiments). Total RNA from control lines DR5 and Ler and mutants *axe1-5* and *sil1* was subjected to S1 nuclease protection using probes specific for the 5' end of pre-rRNA transcripts and compared with total RNA amounts, as seen from EtBr staining **(B)**. The signals obtained for rRNA of DR5 and *axe1-5* were normalized against signals obtained with probes specific for the protein-coding gene actin **(C)**.

Therefore, a subsequent S1 nuclease protection experiment compared rRNA transcript levels relative to the messenger RNA levels for actin (*Figure 23C*). The results of this experiment reveal that *axe1-5* mutant plants contain the same or even slightly reduced amounts of rRNA transcripts compared to wild type (*Figure 23C*), thus there is no indication for increased rRNA transcription concomitant with hyperacetylation at rDNA.

With the exception of the 5S RNA genes, rRNA genes of *Arabidopsis* are arranged in long tandem arrays comprising the two nucleolus organizer regions (NORs) on chromosome II and IV (*Figure 24A*) (Maluszynska and Heslop-Harrison, 1991). Both NORs adjoin the telomeres (*Figure 24A*) (Copenhaver and Pikaard, 1996).

Figure 24

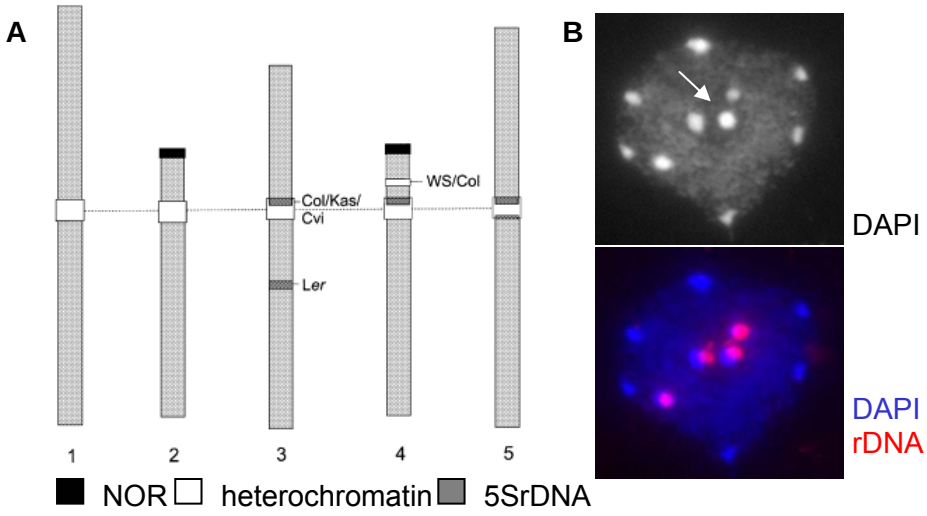

Figure 24. rDNA repeats are organized at the distal ends of chromosome II and IV

Scheme depicting the arrangement of constitutive heterochromatin, 5S rDNA and NOR (nucleolus organizer regions) on the five *A. thaliana* chromosomes (**A**). Interphase nuclear spread of wildtype Col stained with DAPI (black and white in the upper panel, blue in merged images in the lower panel) and fluorescent *in situ* hybridization with biotin-labeled probes for rDNA repeats. Chromocenters only comprising centromeric and pericentromeric repeats align at the nuclear periphery, while those containing the NORs build up the nucleolus (arrow), (**B**).

FISH with rDNA probes on wild type interphase nuclear spreads revealed the rDNA to be compactly organized in the chromocenter(s) close to the nucleolus, and only a few DNA repeats extend visibly into the nucleolus (*Figure 24B* and *25A,* right panels). No obvious change in appearance occurred in the point mutation allele *sil1* (data not shown). However, in the splice-site mutation *axe1-5* the tight organization was abolished. The rDNA appears less condensed, and rDNA enters the nucleolus and overlaps with adjacent euchromatin (*Figure 25A*, left panels). In contrast, the core centromeric regions, represented by the 180bp tandem repeats, do not become disorganized in the mutant (*Figure 25B*). This result appears distinct from the drastic decondensation of centromeric and pericentromeric repeats observed in *ddm1-5* mutants, in which rDNA containing chromocenters often remain relatively stable (*Figure 9*). The decondensation of rDNA repeats is correlated with the high acetylation of histone H4 and with an increase in histone H3K4 methylation, suggesting a specific role for the HDA6 deacetylase in the regulation of chromatin structure at particular loci such as the rDNA repeats.

Figure 25

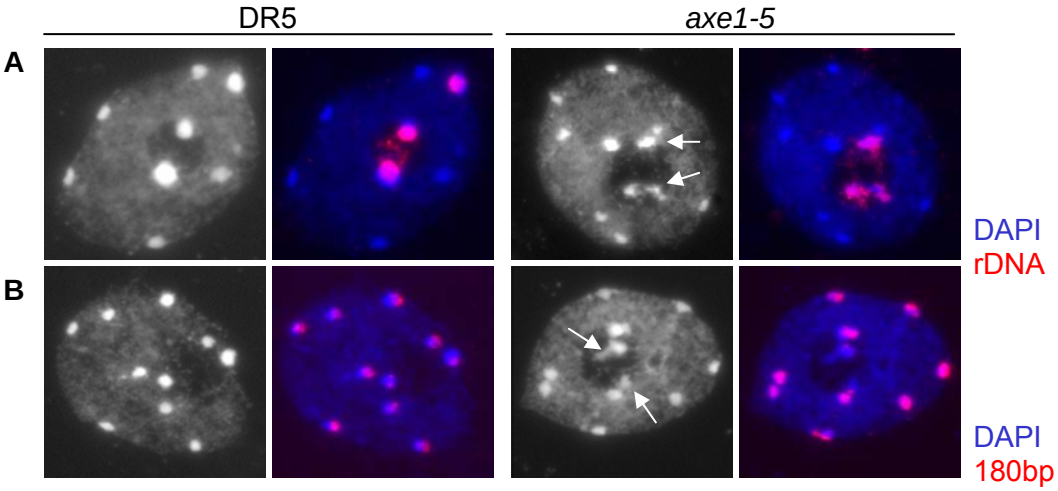

Figure 25. rDNA loci, but not chromocenters in general, are decondensed in *HDA6* mutant nuclei
Interphase nuclear spreads of control lines DR5 the *axe1-5* mutant stained with DAPI (black and white in left panel, blue in merged images on the right panel) and fluorescent *in situ* hybridization with biotin-labeled probes for rDNA repeats (**A**) and centromeric (180bp) repeats (**B**). Arrows in the black and white images point to decondensed rDNA repeats in mutant nuclei in (**A**) and (**B**).

Inhibition of histone deacetylases by TSA in *Neurospora crassa* results in reduced DNA methylation at specific, transgenic loci (Selker, 1998). No significant changes in DNA methylation levels of either transgene or rDNA was reported in the initial study of the *sil1* mutation (Furner *et al.,* 1998) or the *axe1* mutations (Murfett *et al.,* 2001). In contrast, the *rts1* and *rts2* alleles caused limited demethylation at the target site analyzed (Aufsatz *et al.,* 2002). I investigated whether the increased H4 acetylation at the rDNA loci in *HDA6* mutants was accompanied by changes in DNA methylation at these targets. I incubated DNA from wild-type plants (Columbia, Landsberg erecta), the transgenic line DR5 and the mutants *axe1-5* and *sil1* (devoid of the C-locus) with different methylation-sensitive restriction enzymes and performed Southern blot analysis with an rDNA probe. Clear changes in the methylation pattern between wild type and mutants were detected using *Cfo*I ($G^{m5}CGC$, *Figure 26A*). Other enzymes, which are also specifically inhibited by CG methylation, *Hpa*II ($C^{m5}CGG$) and *Mae*II ($A^{m5}CGT$) confirmed the rDNA hypomethylation (*Figure 26B*). The digest with the enzyme *Msp*I inhibited by CNG methylation and *Ava*II which is inhibited by either CG, CNG or CNN methylation (GGW ^{m5}CC, GGWC^{m5}C, *Figure 26B*) showed only minor reductions in cytosine methylation at the rDNA repeats. Though the changes in CG methylation are significant and distinct, the demethylation is much less pronounced than in DNA of *ddm1-5* (Jeddeloh *et al.,* 1999), used as demethylation control and strongly affected in methylation patterns at many repetitive sequences. To examine whether the mutations induce specifically rDNA demethylation or a more general genome-wide demethylation, Southern blots were reprobed for other potential candidate genes containing appropriate restriction sites. Suggested by the delay in flowering time in the *HDA6* mutants, the membrane with the *Cfo*I digest was hybridized with the promoter of the *FWA* gene (Saze *et al.,* 2003), a positive regulator of flowering (*Figure 26C*). We also analyzed the *Hpa*II digest for methylation changes at the (weakly expressed) *TSI* genes (*Figure 26D, E*) and at the 180bp centromeric repeats (*Figure 26F*). Only very subtle changes could be detected with the *FWA* and the *TSI* probes (*Figure 26E*), while the methylation at the 180bp repeats appeared unaffected by the *HDA6* mutations.

Figure 26

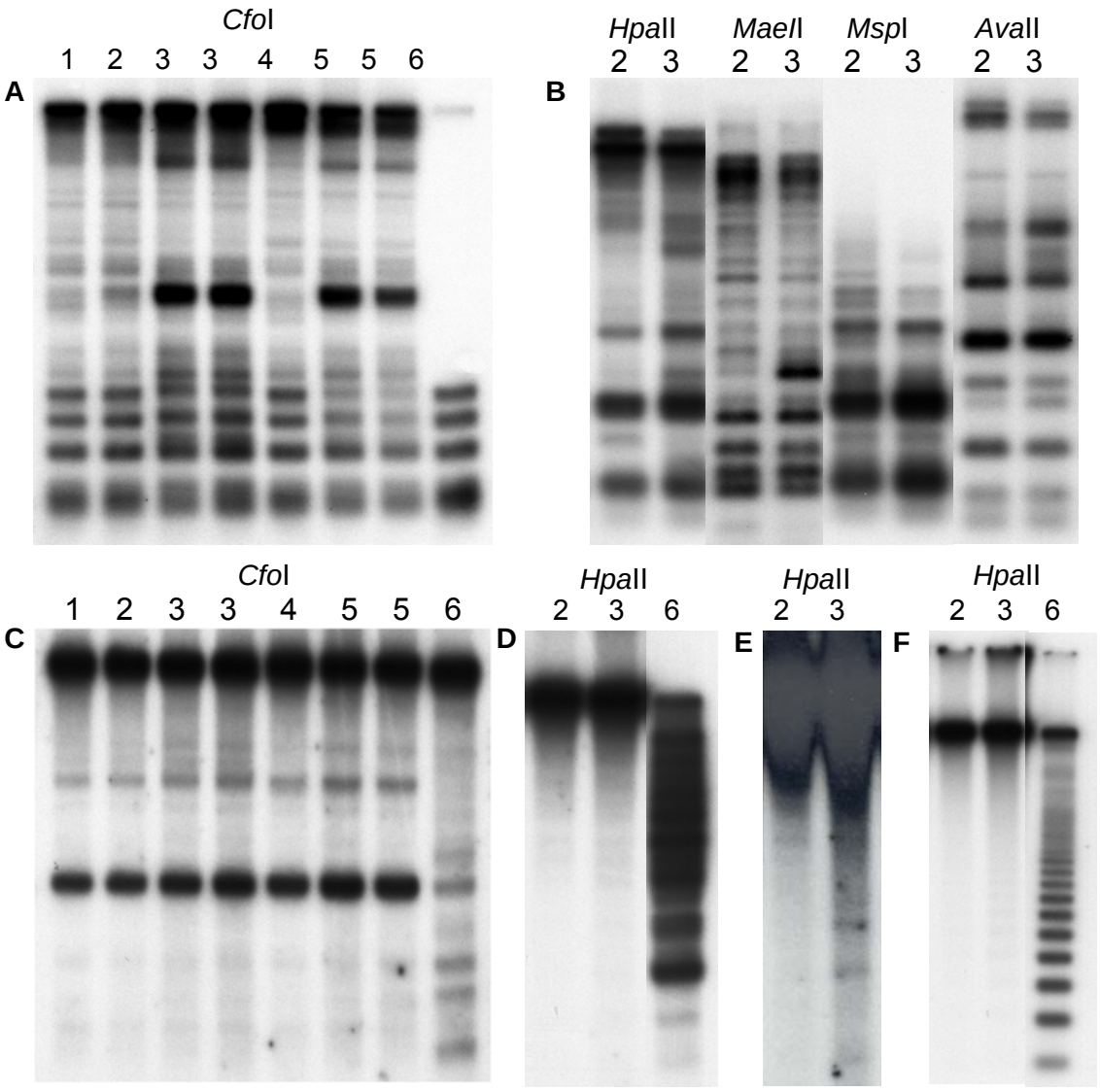

Figure 26. DNA methylation patterns at rDNA repeats are affected in *HDA6* mutants

Genomic DNA samples from wild type Columbia (Col, 1), Landsberg erecta (Ler, 4), the transgenic line DR5 (2), the *HDA6* mutant alleles *axe1-5* (3) and *sil1* (5), and from the DNA methylation mutant *ddm1-5* (6) (Jeddeloh *et al.* 1999) were analyzed. The DNA was digested with methylation-sensitive restriction enzymes *Cfo*I**,** *Hpa*II, *Mae*II, *Msp*I and *Ava*II, subjected to Southern blot analysis and probed with rDNA (Vongs *et al.,* 1993) **(A, B)**, a *FWA* probe (Saze *et al.,* 2003, **C**), the TSI probe (**D** and **E; E** showing a 4 day exposure of the blot shown in **D**) and the 180bp probe (**F**).

I.5 Chromatin Factors Involved in DNA Replication

Histone deposition after DNA replication is mediated by specialized histone chaperones. For example, the chromatin assembly factor-1 (CAF-1) preferentially associates with histones H3.H4, localizes to replication foci and is thought to assemble nucleosomes onto replicating DNA (Stillman, 1986). The association of CAF-I with the replication fork is mediated by its interaction with the proliferating cell nuclear antigen (PCNA) (Shibahara and Stillman, 1999). CAF-1 is conserved in eukaryotic organisms ranging from yeast to man. In *Arabidopsis thaliana* CAF-1 consists of three subunits, named p150, p60 and p48. Null mutations in both the p150 (*fas1-1*) and the p60 subunit (*fas2-2*) have been described (Kaya et al., 2001). *fas* mutants show distorted phyllotaxy and fasciation (thick and flattened stems and fused organs) and are sensitive to DNA damaging agents, revealing the implication in DNA repair mechanisms (Takeda et al., 2004). Recently, in a screen for mutants hypersensitive to Methyl Methane Sulfonate (MMS), a reagent mimicking DNA double strand breaks (DSBs), a novel mutant *bru1 (brushy)* was identified (Takeda et al., 2004), which also shows a fasciation phenotype. Three alleles were described; *bru1-1* carrying a deletion, leading to miss splicing and truncation of the C-terminus of the protein; *bru1-2,* in which a single amino acid in the N-terminal region is exchanged and *bru1-3* with a T-DNA insertion in the middle of the gene. The *BRU1* gene encodes a novel protein of 1311aa characterized by domains involved in protein-protein interaction and possibly DNA binding.

Even though *bru1* mutants are extremely sensitive to DNA damaging treatments, they are proficient not only in intra-chromosomal homologous recombination (HR), but also in non-homologous end joining (NHEJ). The sensitivity to MMS reflects probably a constitutively increased level of DSBs, possibly resulting from replication defects (Takeda et al., 2004).

Both *fas* and *bru1* mutants release transcriptional gene silencing in a stochastic fashion as was shown for two independent silenced transgenes (Takeda et al., 2004), but do not affect global DNA methylation. It was proposed that the CAF-1 complex ensures stable propagation of epigenetic states and maintenance of genome integrity by facilitating rapid reformation of chromatin structure after passage of the replication fork (Kaya et al., 2001). Even though BRU1 does not directly interact with the CAF-1 subunits (Takeda et al., 2004) it is likely to be involved in chromatin assembly and to contribute – together with the CAF-1 complex – to post-replicative stability of epigenetic states. In order to maintain the epigenetic information throughout cell division the histone code has to be transmitted to the daughter cells. Therefore, I investigated the impact of *fas* and *bru1* mutations on

Figure 27

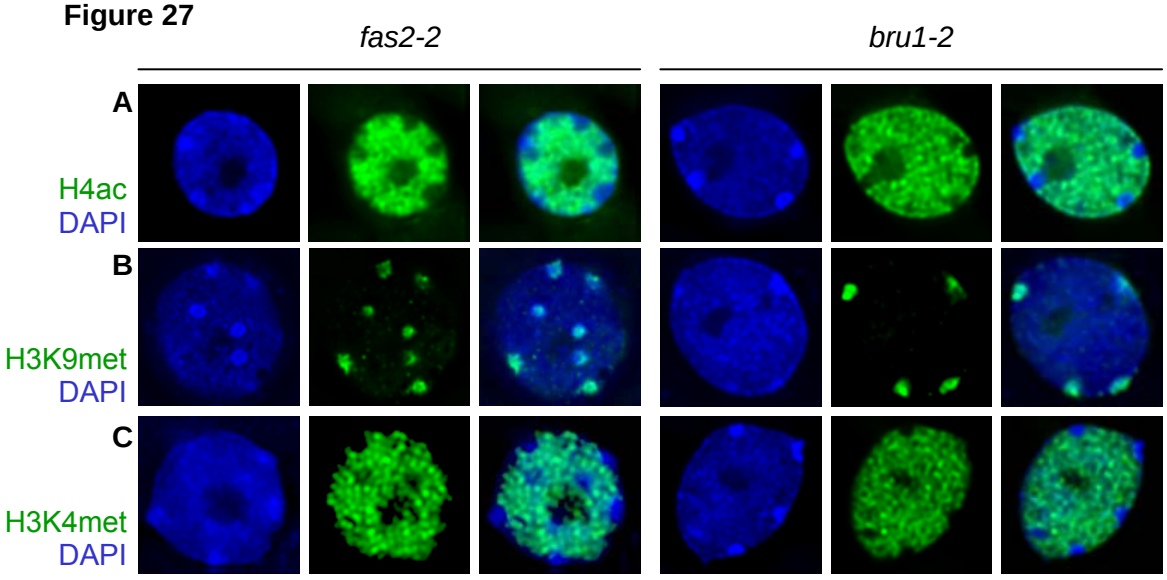

Figure 27. Histone modifications are not affected in *fas* and *bru1* mutants
Distribution of histone H4 acetylation (**A**), H3K9 (**B**) and H3K4 methylation (**C**) revealed by DAPI staining of DNA (blue, left panel) and immunodetection with an antibody specific for tetra-acetylated histone H4, H3K9dimet, and H3K4dimet (green, middle panel) in nuclei of the *fas2-2* and *bru1-2* mutants. Right panels show merged images.

patterns of histone modifications. I performed immunostaining with antibodies against tetra-acetylated H4, as well as against H3 methylated at K4 or K9. In brief, both mutants did not show any alteration in the pattern of these modifications (*Figure 27A-C*). Tetra-acetylated histone H4 and methylated histone H3 at K4 remained enriched in euchromatin. The chromocenters, clearly visible in the DAPI staining, were free of these two marks however enriched in methylated H3K9. One has to bear in mind, however, that the *bru1-2* allele used in this experiment still gives rise to a partially functional protein. In a subsequent approach I studied heterochromatin stability by FISH analysis using the 180bp repeats as probe. Several plants were selected for analysis showing a wide phenotype variation ranging from almost none to strong alterations. We performed a double-blind study, since the effect on heterochromatin stability was expected to be only marginal. Although the organization of centromeric heterochromatin in the majority of *bru1* nuclei was identical to wild type (*Figure 28A, C* and *E*), some nuclei exhibited decondensation of centromeric heterochromatin (*Figure 28B, D*). Altered heterochromatin organization was observed especially in plants showing strong fasciation and distorted leaf shapes. In *fas2-*

2 mutants the chromatin structure was not affected (*Figure 28F*). These observations and the fact that distorted heterochromatin organization was not observed in all plants and if detected, not in a very elevated number of nuclei, are in accordance with our observation of a stochastic release of transcriptional gene silencing observed in the *bru1* mutants.

Figure 28

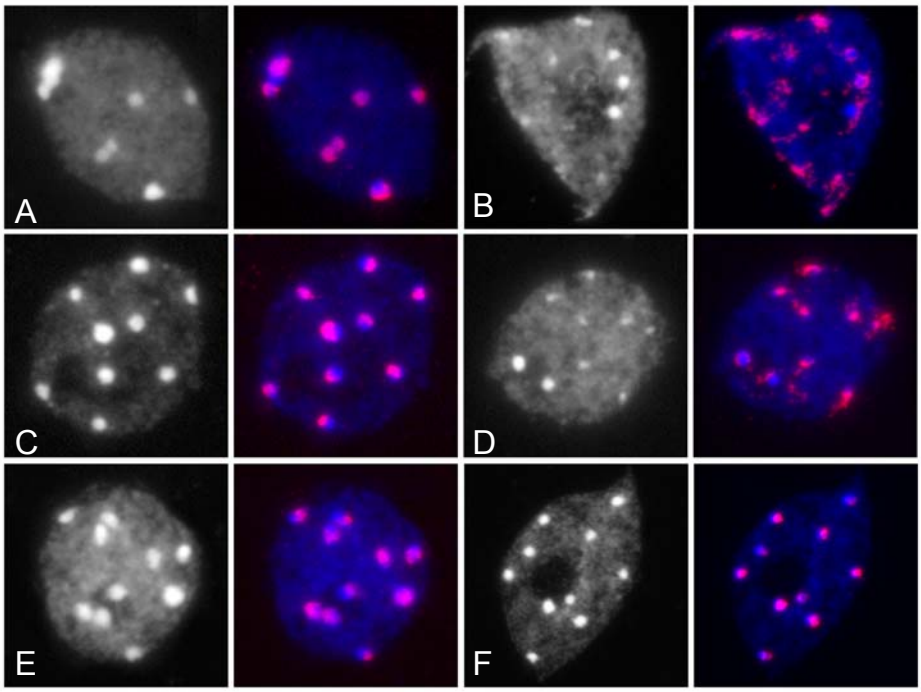

Figure 28. Chromatin organization in interphase nuclei of *bru1* and *fas2* mutants.
DAPI-stained nuclei (left panels) and FISH with a probe specific for 180bp centromeric repeats (right panels) visualizing the compaction of the centromeric DNA (red) in wild-type Ws (**A**), *bru1-1* (**B**), wild-type Col (**C**), *bru1-2* (**D**), wildtype No (**E**), and *fas2-2* (**F**). While most of the nuclei show wildtype structure, nuclei with affected chromocenter organization were selected here for demonstration.

II. Epistasis analysis of *MOM1* with *DDM1* and *HDA6*

Two different hypotheses have been proposed to explain the role of MOM1 in the maintenance of transcriptional gene silencing. MOM1 could act downstream of an already well-defined silencing pathway in *Arabidopsis* involving a concerted action of different chromatin modifications like DNA methylation, hypoacetylated histones and specific histone methylation marks. MOM1 could "read" these epigenetic marks and " translate" them into suppression of transcription. Another more interesting possibility is that MOM1 defines a novel previously uncharacterized level of epigenetic control acting independent of DNA methylation and histone modifications. To test these hypotheses, we examined the epistatic relationship between *mom1* and two transcriptional gene silencing mutants *ddm1* and *axe1* (see I.2 and I.4). If the two mutations contribute to the same mechanism linked directly or indirectly to DNA methylation and histone de-acetylation, the phenotype and effect on TGS of the double mutant would be expected to resemble that of the single mutants. In contrast, if the mutations were part of different or only partially convergent mechanisms, then the double mutant could display a stronger phenotype than either single mutant because of an additive or accelerated loss of silencing.

II.1. Analysis of the *mom1-1/ddm1-5* Double Mutant

For the creation of the *mom1-1/ddm1-5* double mutant, two alleles in the same genetic background were selected. Therefore, differences caused by factors other than these particular mutations or their epigenetic effects are rather unlikely. To avoid the secondary epigenetic effects seen in later inbred generations of *ddm1*, plants homozygous for *ddm1–5* were recovered from segregating heterozygotes before crossed to *mom1-1*. The two genes are on different chromosomes (chromosome5 and chromosome1 respectively) and therefore expected to segregate independently.

We genotyped and scored the phenotypes of 124 plants from five segregating populations. These consisted of 51 F2 plants derived from three F1 hybrids, 38 F3 plants from a parent homozygous for *mom1* and heterozygous for *ddm1*, and 35 F3 plants from a parent homozygous for *ddm1* and heterozygous for *mom1*. In total, 26 plants showed characteristic abnormalities in leaf morphology, namely, upward curling of the younger leaves parallel to the midrib, and growth retardation (*Figure 29*). All these plants had double mutant genotype (*mmdd*). The double mutants were observed with approximately

Figure 29

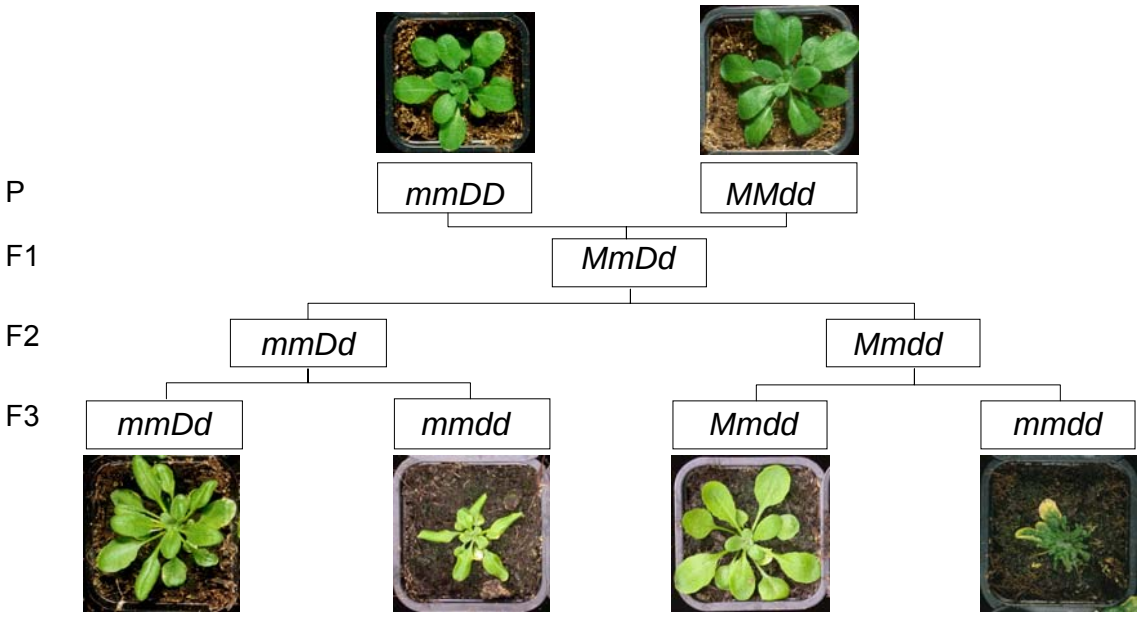

Figure 29. Phenotype of *mom1-1*, *ddm1-5* and double mutant plants. Plants homozygous for *mom1-1* or *ddm1-5* were crossed, the F1 generation selfed and plants selected homozygous for one and heterozygous for the other mutation (F2). These plants were selfed and the progeny analyzed. Double mutant plants are distinguished by their small size, distorted leaf shape, delay in development and strongly reduced seed set. The genotype of the plants was confirmed by PCR genotyping.

the expected frequency (6.25% in F2 and 25% in F3). The specific morphology was never seen in any stage of development among the 97 segregants from the same populations identified as wild type, heterozygous, or homozygous for any single mutation. Therefore, each gene seems to be haplosufficient, even in the absence of the other. However, in the double mutant, the loss of MOM1 that on its own provokes no phenotypic deviation causes immediate and severe developmental abnormalities.

Since *ddm1* affects DNA methylation (Vongs et al., 1993; Jeddeloh et al., 1999) and *mom1* interferes with the maintenance of transcriptional gene silencing without detectable methylation changes, we were interested to study the effect of the double mutant on DNA methylation. The degree of DNA methylation at CpG sites was analyzed within the *HPT* transgene and *TSI* repeats. Both sequences substantially lose methylation in *ddm1*, but remain hypermethylated in *mom1*. Methylation in the double mutant was reduced, but only to the level found in *ddm1* (Mittelsten Scheid et al., 2002).

Interestingly, *HPT* transcripts levels were increased in a more than additive fashion (*Figure 30A*). This finding suggests a synergistic action of the mutations on release of silencing of the transgenic target locus. Reactivation of TSI repeats was additive, and individual transcripts appeared even more abundant (*Figure 30B*). In summary, loss of both proteins in the double mutant leads to superimposed or even synergistic transcriptional reactivation of the studied templates, suggesting that DDM1 and MOM1 have a concerted action in silencing.

Figure 30

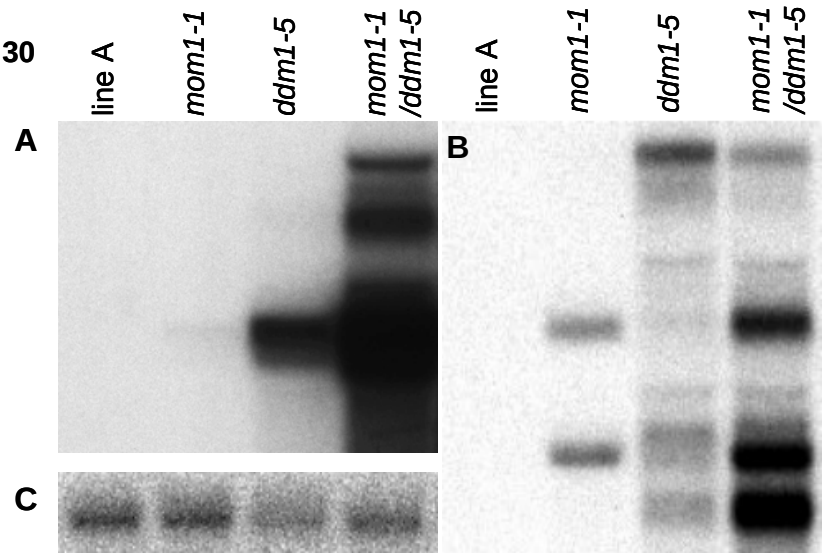

Figure 30. Analysis of *HPT* and *TSI* transcript levels in the double mutant

Northern blot of line A, *mom1*, *ddm1–5* and double mutant plants, hybridized with the *HPT* gene (**A**) and *TSI* (**B**). The blots were reprobed with Ran for loading control (**C**).

ddm1 strongly affects chromatin organization and histone modifications, while *mom1* reactivates silencing within a heterochromatic environment. Therefore, I expected the effect of the double mutant to be restricted to the nuclear phenotype seen in *ddm1* plants. I examined the effects of the double mutant on heterochromatin organization in interphase nuclei using fluorescence *in situ* hybridization (FISH). The hybridization with the 180bp probe revealed differences in heterochromatin distribution, which were grouped to five different types for quantification (*Figure 31*). In wild-type nuclei, the probe hybridizes to discrete, bright DAPI-stained chromocenters (*Figure 31*, type 1), sometimes a little smaller (*Figure 31*, type 2). Nuclei of *mom1* plants are indistinguishable from the wild type, as described; while most nuclei of *ddm1–5* mutants are either of type 2 or show an even stronger disintegration of chromocenters (*Figure 31*, types 3 and 4), indicating decondensation of the centromeric heterochromatin (see also I.3).

Figure 31

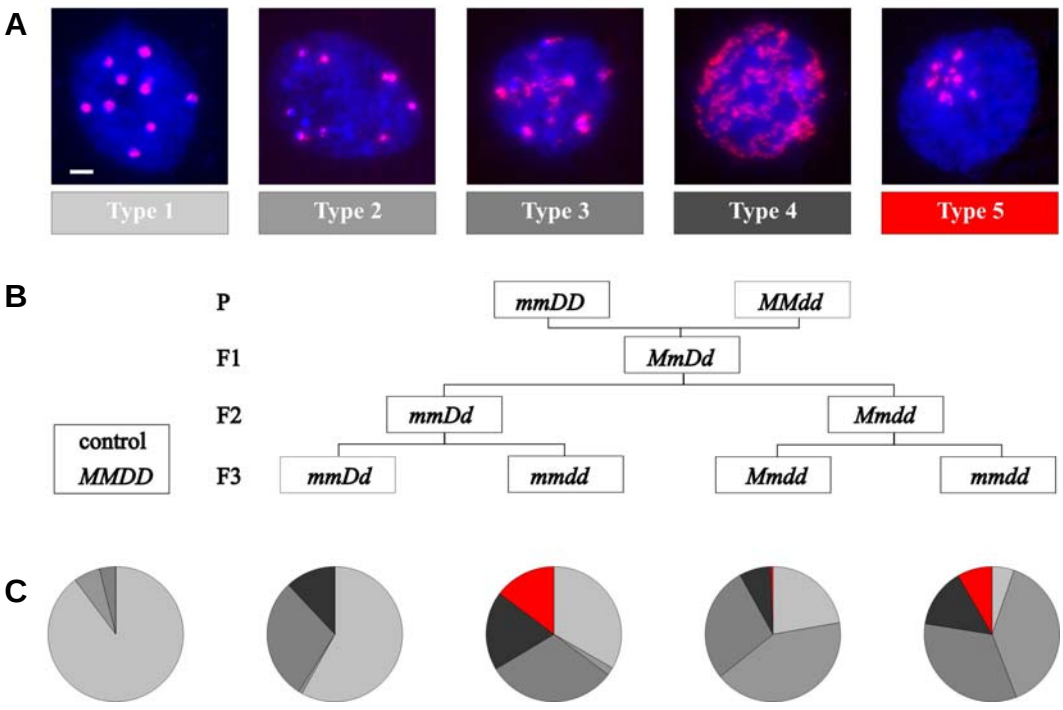

Figure 31. Chromatin organization in interphase nuclei of single and double mutants.
(**A**) Classification based on distribution of the pericentromeric heterochromatin (red, 180-bp repeats revealed by fluorescence *in situ* hybridization analysis; blue, DNA stained with DAPI. (**B**) Genetic pedigree of the plant material. (**C**) Representation of the five types of nuclei in different F3 genotypes. Results from 6 – 12 independent experiments are combined. Number of nuclei evaluated: *MMDD*, 829; mmDD, *1,002*; mmdd, *2,257*; *Mmdd*, 778; *mmdd*, 2,280.

Intriguingly, nuclei of double mutants exhibit structural peculiarities never observed in the single mutants. Not only do the chromocenters disintegrate, but they also have the tendency to aggregate (*Figure 31*, type 5). I compared the frequency of the different types of nuclei in double mutants and heterozygous controls segregating from F2 parents that were already homozygous for either *mom1* or *ddm1* (*Figure 31).* The presence of type 3 and 4 nuclei even in F3 of heterozygous *ddm1-5* is likely to be a heritage of the original parental *ddm1-5* plant. Type 5 nuclei occur only in double mutant plants, regardless which single mutation was homozygous already in the previous generation (*Figure 31*). The frequency of the heterochromatin aggregation characteristic for the double mutant seems to be correlated with the severity of developmental abnormalities of individual *mmdd* plants (*Figure 32*).

Figure 32

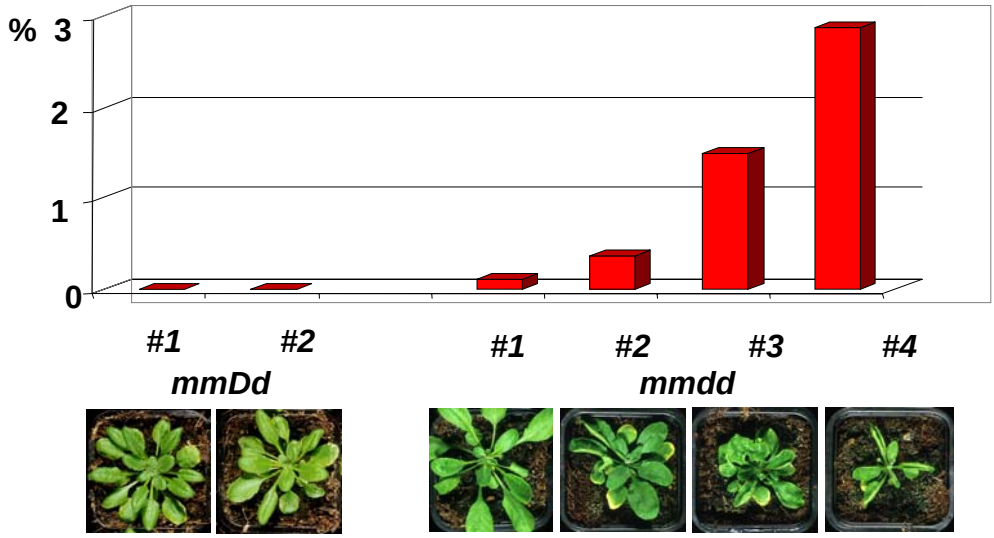

Figure 32. Correlation of frequency of type 5 nuclei with double mutant phenotypes
Plants with phenotypes progressive from #1 with a weak and delayed phenotype appearance, to #4 with an early and strong phenotype were analyzed for the frequency of type 5 nuclei. A minimum of 300 nuclei were scored for each of six plants with a phenotype as illustrated below.

In many nuclei of *ddm1-5* centromeric and pericentromeric heterochromatin undergoes decondensation, while the rDNA loci remain relatively compact (Probst et al., 2003), possibly creating an additional subnuclear region prone to gene inactivation. Therefore, I proposed that the chromocenter clustering in *mom1-1/ddm1-5* double mutants might take place around the nucleolus. Indeed, when fluorescence *in situ* hybridization was carried out with probes specific for telomeres (*Figure 33A, B*) that cluster around the nucleolus (Armstrong et al., 2001) or rDNA repeats (*Figure 33A*) I could show that indeed the chromocenter remnants assemble around this sub-nuclear compartment (*Figure 33B*).

Figure 33

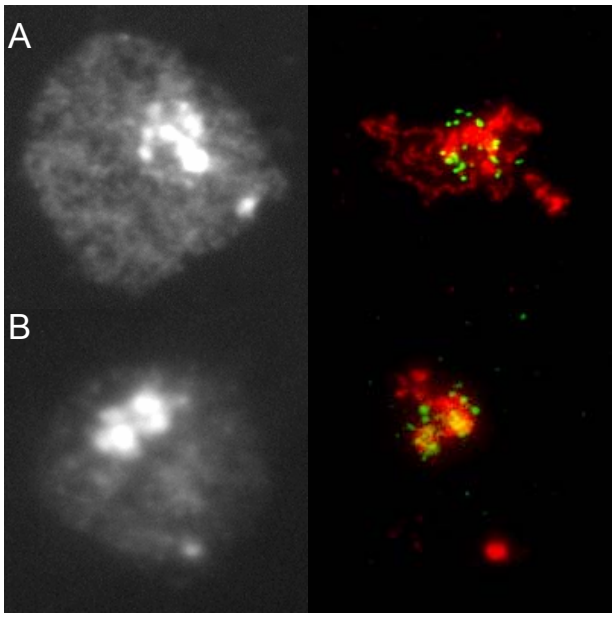

Figure 33. Aggregation of chromocenters in *mom1-1/ddm1-5* double mutants takes place in the peri-nucleolar region.
Interphase nuclear spreads of *mom1-1/dmm1-5* double mutants stained with DAPI (black and white in left panel) and fluorescent *in situ* hybridization with probes for 180bp repeats (red, **A**), rDNA (red, **B**) and telomeres (green in **A** and **B**, left panel).

II.2. Analysis of the *mom1-1/axe1-1* Double Mutant

The phenotype of the *mom1-1/ddm1-5* double mutant suggests that MOM1 defines an independent level of epigenetic control not linked to DNA methylation. Mutations in the *HDA6* gene reactivate several complex transgenic loci e.g. the C-locus (Furner et al., 1998) and the *GUS* locus in line L5 (Morel et al., 2000) and interfere with silencing of *TSI* repeats. This effect is probably due to increased histone H4 acetylation at the target loci and subsequently induced changes in H3 histone modifications, DNA methylation and chromatin structure (Aufsatz et al., 2002; Probst et al., 2004). Therefore, the analysis of the epistatic relationship between *mom1* and *axe1* mutations should confirm the existence of an independent pathway of epigenetic control defined by MOM1.

We chose to cross *mom1-1* to *axe1-1* (Murfett et al., 2001), since the point-mutation in this *HDA6* mutant allele destroys a *Msp*I site therefore allowing genotyping. The analysis of progeny of two selfed *Aamm* and one selfed *aaMm* plant suggested an under-representation of double mutant plants (3.7% observed instead of 25% expected). However the limited number of plants genotyped (27 plants) does not allow a final statement. Two double mutant lines (line 33 and line 36) were recovered from the F2 population (provided by Jane Murfett and Ortrun Mittelsten Scheid). I compared plants from the two double mutant lines to segregating siblings of the same population homozygous for one of the two mutations or wildtype for both genes (*aaMM*, *AAmm* and AAMM). While the single mutants did not show any phenotypic alterations, a variation of phenotypes was observed in the double mutant lines (*Figure 34*). The abnormalities range from variation in flowering time to reduced plant size and rolling of leaves (*Figure 34,* arrow). This observation suggested that MOM1 might operate at a level of epigenetic regulation not only independent of DDM1, but also of HDA6 function. To confirm this I extracted RNA from different plants of lines 33 and 36, the segregating single mutants and wildtype controls and performed Northern blot analysis with a *TSI* probe. In this assay no *TSI* expression was detected in the weak *axe1-1* mutant allele, in contrast to the *axe1-5* splice site mutation (I.4). Interestingly, *TSI* was reactivated in a more than additive fashion in each of the independent double mutant plants analyzed (*Figure 35*), however levels are still lower than observed in *ddm1-5* plants. Interestingly, both mutations have either no (Amedeo et al., 2000) or very subtle effects on the DNA methylation patterns at *TSI* loci as shown for the strong *HDA6* mutant allele, *axe1-5* (*Figure 26F*).

Figure 34

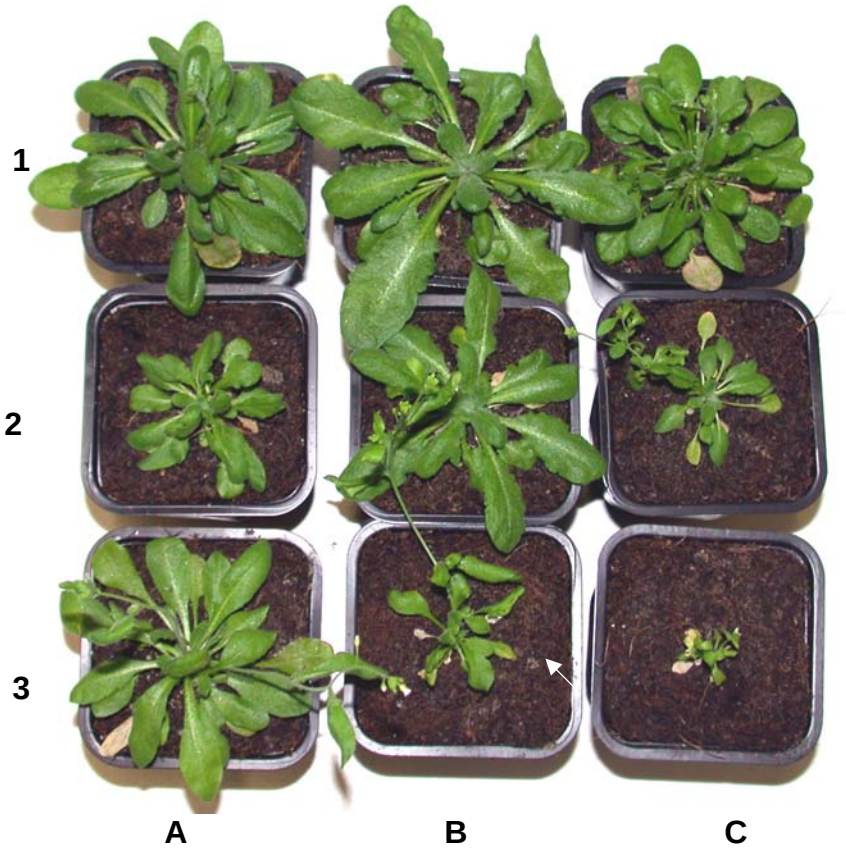

Figure 34. Phenotype of *axe1-1*, *mom1-1* and *axe1-1/mom1-1* double mutant plants.
Plants homozygous for *axe1-1* or *mom1-1* were crossed, the F1 generation selfed and plants selected homozygous for one or both mutations. The F3 generation is shown. *AAMM* (**1A**), *aaMM* (**1B**), *AAmm* (**1C**), *aamm* line 33 (**2A-C**) and *aamm* line 36 (**3A-C**).

In contrast to *mom1-1/ddm1-5* double mutants, a preliminary FISH experiment designed to study the nuclear phenotype in *mom1-1/axe1-1* double mutant plants versus single mutants did not reveal any abnormalities in heterochromatin organization (data not shown). Since *axe1-1* is a weak allele, the organization of rDNA repeats was not affected, as stated for the *sil1* mutation.

Figure 35

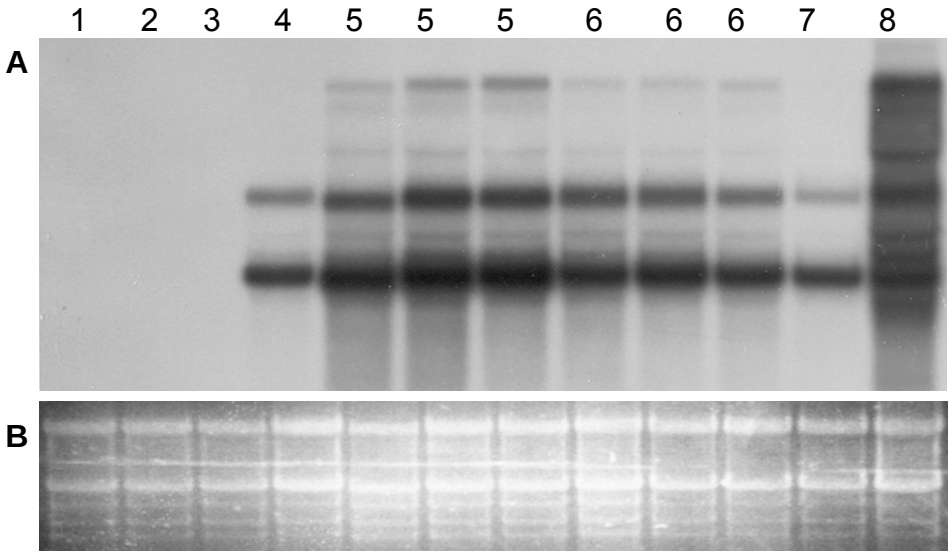

Figure 35. Analysis of *TSI* transcript levels in the axe1-*1/mom1-1* double mutant

Northern blot with RNA extracted from wt ZH (1), *AAMM (2)*, *aaMM (3)*, *Aamm (4),* independent plants of double mutant lines 33 (5) and 36 (6), the *mom1-1* mutant in line A background (7) and the *ddm1-5* mutant (8), hybridized with the TSI probe (**A**). Radiant Red counter stain of RNA prior to blotting shows equal loading (**B**).

6. DISCUSSION

I. Relationship between DNA Methylation and H3K9 Methylation

DNA methylation in *Arabidopsis thaliana* is essential for transcriptional gene silencing, transposon silencing and imprinting. Here I have studied the effects of several mutations in DNA methyltransferases and *DDM1*, a chromatin remodeling factor impaired in the maintenance of DNA methylation, on heterochromatin structure and patterns of histone modifications.

We tried to understand whether histone methylation or DNA methylation is the primary epigenetic modification, using a *met1* null mutant, well characterized for its erasure of DNA methylation (Saze et al., 2003). Contradicting hypotheses were coined whether DNA methylation would determine histone H3K9 methylation or whether the histone methylation would target DNA methylation.

The following evidence suggested that DNA methylation would be downstream of H3K9 methylation: *Neurospora* crassa mutations in the histone methyltransferase DIM5 abolish DNA methylation (Tamaru and Selker, 2001), while elimination of the DNA methylation in the dim2 DNA methyltransferase mutant does not affect H3K9 methylation (Kouzminova and Selker, 2001). In *kyp* mutant plants, carrying a mutation in the major histone methyltransferase KRYTONITE (*KYP*) (Jackson et al., 2002; Jackson et al., 2004), H3K9 methylation is lost, leading to reduced CpNpG methylation and release of transcriptional gene silencing (Jackson et al., 2002). Johnson et al (2002) studied H3K9 methylation at 180pb repeats and two retrotransposons in weak alleles of *met1* and *ddm1*. While mutations in *ddm1* were as effective in reducing H3K9 methylation as *kyp* at the target loci, H3K9 methylation was retained in *met1* and *cmt3* mutant plants. Instead a reverse relationship between the levels of transcriptional reactivation and levels of H3K9 methylation was found, explained by replication-independent exchange of methylated H3 at K9 for the H3.3 variant (Ahmad and Henikoff, 2002; Choi et al., 2002). In accord with the observation in *Arabidopsis*, cells derived from Dnmt1-/- or Dnmt3a/b -/- mice embryos show wildtype distribution of tri-methylated H3K9 at pericentromeric heterochromatin (Lehnertz et al., 2003). The authors stated that DNA methylation functions downstream of histone methylation. Yet, it was not taken into account that only weak methyltransferase mutant alleles in *Arabidopsis* were used (Choi et al., 2002) and that both Dnmt1 -/- and Dnmt3a/b -/- cell lines still retain certain levels of DNA methylation at major satellites

(Lehnertz et al., 2003). Further, *Neurospora* differs from higher organisms, since most DNA methylation is associated with repeat-induced point mutations (RIP) (Selker et al., 2002), is not essential and not preferentially localized at CpG nucleotides (Selker et al., 2003).

In contrast Soppe and coworkers suggested that DNA methylation directs histone methylation. This hypothesis was based on their observation that H3K9 methylation levels were reduced in both *ddm1* and *met1* mutants in immunostaining experiments (Soppe et al., 2002).

To solve this contradiction, the *met1-3* null mutant represented the ideal system, since no residual CpG methylation remains in the mutant, moreover CpNpG and asymmetric methylation levels are reduced (Saze et al., 2003). Additionally, *de novo* methylation in *Arabidopsis* was suggested to have only a marginal influence on total methylation levels (discussed below), which is in contrast to the situation in mammals. Using Chromatin IP and immunostaining experiments with the *met1-3* allele we demonstrated that methylation at CpG sites is required to epigenetically mark genomic regions for H3K9 methylation and not vice versa (Tariq et al., 2003). In contrast to the results obtained by Johnson et al. (2002) the complete erasure of CpG methylation in the *met1-3* allele abolished H3K9 methylation at 180bp repeats and the Ta2 retrotransposon. The recently discovered interaction between proteins recognizing CpG methylation (MeCP2, MBD1) and histone methyltransferases (Fujita et al., 2003; Fuks et al., 2003b) provides a mechanistic link between these two modifications. This pathway seems to be independent of transcriptional activity: We were unable to detect transcription from the 180bp repeats or a transposon located in the heterochromatic knob on chromosome 4 (At4g03870) by RT-PCR, but nevertheless observed loss of methylated H3K9 at these targets.

DNA methylation and histone deacetylation operate along a common mechanistic pathway to repress transcription. HDACs can be recruited via methyl-binding domain proteins (MBDs) (Bird and Wolffe, 1999) or via interaction with the DNA methyltransferases itself (Fuks et al., 2000). Enrichment in acetylated histones H4 in the *met1-3* mutant was observed only at those loci that became transcriptionally activated, but not at 180bp repeats. This suggests that HDACs can be recruited to the 180pb repeats by components other than those involved in DNA methylation to maintain the hypoacetylated state at hypomethylated centromeric DNA in *met1-3*.

The results from immunostaining experiments in *met1-3* nuclei and Western Blot analysis on the total histone fraction implied not a loss but a redistribution of H3K9 methylation marks on chromatin. Interestingly, total H3K9 methylation levels stay constant also in the

ddm1 mutant even though a significant reduction of this modification at many target sequences was observed (Gendrel et al., 2002). When the DNA methylation mark normally directing *KYP* to its target sequences is lost, it is possible that *KYP* methylates H3K9 at random throughout the genome or is directed towards novel sites determined by other features like DNA structure, acetylation status or the presence of homologous small RNAs.

II. DNA Methylation Defects and Heterochromatin Stability

In mice, deletions in either Dnmt1, the *de novo* methylases Dnmt3a/b or the *DDM1* homologue Lsh are lethal. In contrast, *Arabidopsis* can tolerate major disruptions in DNA methylation: *ddm1*-5 mutant plants, even though the accumulation of developmental phenotypes was observed, can be inbred for several generations; *met1* homozygous plants, even though recovered with low frequency, are viable and develop to maturity; and *cmt3* and *drm2* mutants do not show any phenotypes in our hands.

II.1 *drm2* and *cmt3* Mutants

In a preliminary experiment designed to investigate heterochromatin integrity, no significant cytological difference in heterochromatin structure between wildtype and the *cmt3* mutants was observed. Interestingly, however, these preliminary data suggested that loss of DRM2 function in *Arabidopsis* led to disturbed chromocenter structure in a significant number of nuclei. DRM2 is required for *de novo* methylation and initiation of silencing at the FWA locus (Cao et al., 2003). If an epigenetic *fwa* mutant with hypomethylated FWA promoter is transformed with an extra copy of the gene, the transgene becomes methylated and silenced in wildtype plants. However, the transformation into a drm1 *drm2* double mutant prevents *de novo* methylation (Cao et al., 2003). The initiation of silencing at the FWA locus requires the functional RNAi machinery that probably guides *de novo* methyltransferase activity (Chan et al., 2004). If this transformed double mutant is further backcrossed to a wildtype plant, the hypomethylated state of the FWA transgene is maintained even in the presence of functional DRM1 and DRM2, suggesting that during transformation or in the first generation the transgene must have been recognized as target, while it later escaped the surveillance system (Cao et al., 2003). The observation that in a *met1* or *ddm1* background re-methylation of all demethylated sequences occurs slowly and the fact that *drm1 drm2* double mutant plants

do not have phenotypic alterations imply that *de novo* methylation does not play a major role in control of total DNA methylation levels in *Arabidopsis*.

Our observation, however, suggests that constant *de novo* methylation activity might be required for stable heterochromatin formation. The presence of small RNAs detected with homology to pericentromeric (Xie et al., 2004) and 180bp repeats (Todd Blevins, personal communication) proposes that a similar mechanism as suggested for silencing of the *FWA* transgene might be operating in *Arabidopsis* to control heterochromatin structure and silencing, directing the *de novo* methyltransferase to specific targets. Humans carrying a mutation in the DNMT3b gene suffer from the rare ICF (for immunodeficiency, centromere instability and facial abnormalities) syndrome, which is in part characterized by extensive cytosine demethylation at satellite DNA, while the total content of 5methylCytosine was not measurably reduced (Xu et al., 1999). In mice it was shown that a Dnmt3b is involved in DNA methylation of major and minor satellites (Lehnertz et al., 2003). In *Arabidopsis* DRM2 and CMT3 seem to act redundantly in the maintenance of proper patterns of asymmetric and CpNpG methylation, even though DRM2 appears to participate in both maintenance and initiation of methylation states, dependent on the locus investigated (Cao and Jacobsen, 2002b). The different influence of *cmt3* or *drm2* on heterochromatic structure could also be explained by their specificity for methylation sites. While *cmt3* is predominantly impaired in DNA methylation at CpNpG sites and was proposed to have evolved as an additional epigenetic modification involved specifically in transposon control (Kato et al., 2003), *drm2* mutations affect DNA methylation in all sequence contexts including CpG sites (Cao and Jacobsen, 2002a).

II.2 *met1* loss-of-function Mutant

The partial-loss-of function mutant *met1-2* was shown to have chromocenter fractions reduced by ~25-30% compared to wildtype nuclei (Soppe et al., 2002). In our *MET1* complete loss of function mutant, in which not only CpG and H3K9 methylation at chromocenters are lost, but also CpNpG and asymmetric sites are affected, we expected a very drastic consequence for heterochromatin structure. Surprisingly, most of the nuclei showed wildtype heterochromatin structure with a tight arrangement of centromeric heterochromatin into chromocenters.

It must be mentioned, however, that a more statistical analysis as done for *cmt3* and *drm2* plants or a quantitative analysis of chromocenter size as performed in Soppe et al., 2002 was not done. This might have revealed more subtle differences in heterochromatin

organization between wildtype and *met1-3* mutants and might have resolved the discrepancy between the effect of *drm2* and *met1* mutants on heterochromatin structure described here. Nevertheless, we can conclude that at least in the majority of nuclei DNA and histone H3K9 methylation are dispensable for heterochromatin formation. In conformance with this, chromocenter structure remains unaffected in the *kyp* mutant (Jasencakova et al., 2003), and in mouse fibroblasts recovered from Dnmt1 -/- embryos no disturbance of pericentromeric heterochromatin was observed (Lehnertz et al., 2003). Interestingly, even in *dnmt1 dnmt3a dnmt3b* triple mutants pericentromeric heterochromatin remained intact (Wendy Bickmore, Alan Wolffe Chromatin Workshop, Heidelberg). Homozygous *met1-3* plants can be recovered only with very low frequency suggesting that under strong selective pressure only those plants able to compensate for the loss of DNA methylation both during embryo development and adult plant life can survive. In this respect it would be interesting to study the expression profile of *met1*-3 plants to investigate if other pathways of epigenetic control are differentially regulated to compensate for the abolished methylation based gene silencing pathway. The 180bp repeats in wildtype chromocenters are not only enriched in methylated H3K9, but also the centromere specific histone H3 variant HTR12 can be found in plant centromeric chromatin (Talbert et al., 2002). It would be interesting to investigate whether the binding of this histone H3 variant depends on DNA methylation or whether it can localize to 180bp repeats despite reduced CpG levels and therefore assure centromere function in *met1-3* mutants. In this respect it would be also of interest to compare the localization of HTR12 to centromeric chromatin in *met1* and *ddm1* mutants.

II.3 *ddm1* Mutants

In contrast to *met1*, mutants in *ddm1* reveal drastic changes in nuclear organization, as well as in patterns of DNA methylation and histone modifications. The strongest effects were observed in centromeric and pericentromeric regions as well as in previously hypermethylated transgenic neo-heterochromatin. This is in accordance with the observation reported previously that the *ddm1* mutation predominantly influences DNA and H3K9 methylation of centromeric regions (Choi et al., 2002). Comparable FISH and immunolocalization studies carried out with the *ddm1-2* allele (Soppe et al., 2003) revealed a significant reduction in chromocenter size and relocation of low-copy pericentromeric sequences away from the remaining chromocenters. The observed differences between this study and my observation are probably due to the nature of the

ddm1 allele. While the *ddm1-5* allele is likely to be a null allele, the *ddm1-2* allele has a G to A transition in the splice donor site of intron 11 leading to a premature translation termination (Jeddeloh et al, 1998). This allele may encode a partially functional protein, since the RNA is stable (Jeddeloh et al, 1998). Also the number of inbred generations and the ecotype background (line A versus Col/Ler) may influence the consequences of DDM1 deficiency. It has been well documented that the integrity of genomic methylation patterns during development requires chromatin remodeling factors (Jeddeloh et al., 1999; Dennis et al., 2001). The *ddm1* mutation affects both CpG and the plant specific CpNpG methylation. It was speculated that *DDM1* acts by facilitating the access of DNA methyltransferase MET1 to its substrate, thereby determining CpG methylation levels. Interestingly, despite the predominant effect of *ddm1* on DNA methylation at pericentromeric and centromeric heterochromatin, its *in vitro* ATPase activity was shown to be independent of the methylation status of the DNA substrate (Brzeski et al, 2003). CpNpG methylation levels might be controlled indirectly by DDM1 through changes in histone methylation (Gendrel et al., 2002), since the status of H3K9 methylation was reported to affect CpNpG methylation in *Neurospora* (Tamaru and Selker, 2001) and *Arabidopsis* (Jackson et al., 2002).

It can be hypothesized that the observed changes in chromatin structure may be indirectly caused by the loss of DNA methylation in the *ddm1* mutant. The fact that Soppe et al. reported a nuclear phenotype identical to *ddm1-2* in the hypomethylation mutant *met1* supports this hypothesis. However, our study of the complete loss-of-function allele *met1-3* (Saze et al., 2003) showed that DNA methylation and histone H3K9 methylation are dispensable for stable heterochromatin and chromocenter formation. Additionally, the mutation in *CMT3* did not significantly affect nuclear structure and resulted in phenotypically normal plants. However, we cannot exclude that the disturbed chromatin structure might in part be a result of the re-distribution of DNA methylation and the subsequent miss-regulation of gene expression reported for *ddm1* mutants (Miura et al., 2001).

While *ddm1* decreases H3K9 methylation at chromocenters, H3K4 methylation is still retained in euchromatin and does not become enriched at the chromocenter remnants (Results I.2.). Interestingly, mouse Lsh -/- cells retain the condensed pericentromeric heterochromatin structure (Yan et al., 2003a), even though Lsh deletion induced methylation defects at repetitive sequences similar to *ddm1* (Dennis et al., 2001). In these Lsh -/- cells H3K9 trimethylation is still preserved at pericentromeric heterochromatin, but the DAPI bright foci acquire both di- and trimethylation at H3K4 (Yan et al., 2003b). The

enrichment of H3K4 methylation seems to be a consequence of reduced CpG methylation at the pericentromeric repeats, since treatment with 5azadeoxyCytidine induced the same effect and the localization of Lsh to pericentromeric foci is independent of their DNA methylation status (Yan et al., 2003b). Interestingly, the disruption of heterochromatin by prolonged treatment with TSA, a histone de-acetylase inhibitor, prevented binding of Lsh to chromatin (Taddei et al., 2001; Yan et al., 2003a). What determines the heterochromatin state in *Arabidopsis* remains unclear. Since *met1* plants are viable and able to form chromocenters with wildtype structure one could argue that not the absolute amounts of H3K9 and H3K4 methylation, but the ratio between the two modifications and probably the degree of hypoacetylation determines heterochromatin structure. Either the loss of H3K9 in *met1* in the presence of low amounts of H3K4 methylation, or the increase in H3K4 methylation in the presence of wildtype levels of H3K9 observed in Lsh -/- and 5azadeoxyCytidine treated mammalian cells might be insufficient to disturb chromatin structure. Instead, the *ddm1* mutation in *Arabidopsis* might induce further changes in chromatin modifications for example histone acetylation changes specifically at H4K16 in heterochromatin (Soppe et al., 2002) that result in decondensation of heterochromatin while in *met1* hypoacetylated chromocenters are retained. An example, in which hyperacetylation can result in loosening of heterochromatin structure is the organization of rDNA repeats in the *Arabidopsis* HDA6 mutants (Results I.4).

III. DNA Replication – Assuring Maintenance of Epigenetic Modifications

The process of DNA assembly into nucleosomes behind the replication fork is likely the crucial time point either for maintenance and/or *de novo* establishment of epigenetic information. The targeting of Dnmt1/MET1 to replication foci and its preference for hemimethylated DNA explains how DNA methylation marks are set after separation of the parental and synthesis of the new strands. How histone modifications are placed onto newly assembled nucleosomes is not well characterized. It was previously assumed that the histone octamer on the parental strand disassembles into one H3.H4 tetramer and two H2A.H2B dimers upon passage of the replication fork, resulting in random distribution of the parental H3.H4 tetramer on the two daughter strands. Now, recent evidence suggests that during replication octamers are broken into H3.H4 dimers that are evenly distributed onto the daughter strands, allowing the parental half to serve as template to rebuilt the nucleosome with its covalent modifications identical to the parental strand (Korber and

Horz, 2004; Tagami et al., 2004). H3.H4 dimers are detected in a complex with the chromatin assembly factor CAF-1 and together with ASF1 (anti-silencing factor 1) in the replication-coupling assembly factor (RCAF). Both complexes are tightly coupled to DNA replication and repair (Tyler et al., 1999). Given its crucial role in histone assembly subsequent to passage of the replication fork, CAF-1 mutants in yeast have silencing defects at telomeres and mating type loci (Kaufman et al., 1997). In mouse, the interaction of CAF-1 with HP1α (Murzina et al., 1999) and MBD1 (Reese et al., 2003) suggests a role of CAF-1 in heterochromatin formation. We observed that *fas1* and *fas2* mutants, encoding the p150 and the p60 subunits of the CAF-1 complex, respectively, release transcriptional gene silencing of a transgene stochastically and affect silencing of pericentromeric repeats (Takeda et al., 2004). However, while in yeast replication errors resulting from mutations in CAF-1 or RCAF lead to spontaneous gross chromosomal rearrangements (Myung et al., 2003), we did not observe failure to maintain heterochromatin structure in our *Arabidopsis fas1* and *fas2* mutants. In contrast, some plants carrying a mutation in the novel *BRU1* gene exhibit disturbed heterochromatin organization of 180bp repeats in a significant number of nuclei. A disturbed chromocenter structure strongly correlated with those plants showing a strong fasciation phenotype. Because of its phenotypic similarities to *fas* (Kaya et al., 2001), *mre-11* (Bundock and Hooykaas, 2002) and *condensin* mutants (Siddiqui et al., 2003), we proposed that *BRU1* is involved in DNA replication and chromatin assembly. We also suggested that *BRU1* deficiency leads to an increase in double stranded breaks, impaired chromatin structure in some clonal lineages and release of silencing. The differences in the effect on heterochromatin structure between *fas* and *bru1* mutants are also reflected in the differential sensitivity of the two mutations to double strand breaks inducing mutagens (Takeda et al., 2004) and may be explained by functional redundancy between CAF-1 and the putative ASF1 chromatin assembly factor genes found in *Arabidopsis*. The release of transcriptional gene silencing in both *fas* and *bru1* mutants underlines the importance of DNA replication and subsequent chromatin assembly for inheritance of epigenetic states. In mice, CAF-1 mutations induce S-phase arrest in early and mid S-phase suggesting that CAF-1 and in *Arabidopsis* probably also *BRU1* function may be specifically required for replication of heterochromatic repeat regions that normally replicate late in S-phase (Hoek and Stillman, 2003).

In mouse, the DDM1 homologue, Lsh, was reported to localize to replication foci (Yan et al., 2003a) – but it is unclear what role DDM1 may play during or after passage of the replication fork. While Dnmt1 is associated with replication foci throughout the whole S-

phase, Lsh associates with replication foci only during late S-phase when replication of pericentromeric heterochromatin takes place. Lsh is not required for targeting of Dnmt1 to replication foci, since in Lsh -/- cells Dnmt1 can still be recruited to heterochromatic foci (Yan et al., 2003a). Instead, Lsh/*DDM1* may function in facilitating accessibility and increasing enzymatic activity of chromatin modifying enzymes. The difference between an early and late replicating replication fork could be envisaged as follows: Dnmt1 might be targeted to every replication fork via its interaction with PCNA and subsequently recruiting HDACs, HP1 and HMTases (Fuks et al., 2000; Fuks et al., 2003a). While Dnmt1 activity might be required to set methylation marks also in euchromatin, the activity of HDACs and HMTases and the recruitment of HP1 in euchromatin might not be desired. Specific targeting of Lsh/*DDM1* to pericentromeric heterochromatin could lead to enhanced enzymatic activities of the histone modifiers at these target sequences, suggesting that Lsh/DDM1 plays a decisive role in differentiating between euchromatic and heterochromatic chromatin. Interestingly, in those multicellular organisms that do not employ DNA methylation (*Drosophila*, *C. elegans*), no *DDM1* homologues were identified. Alternatively, replication through heterochromatin and post-replicative chromatin modifications as well as the assembly into a condensed structure might require chromatin remodeling activity rather than replication of euchromatic chromatin. Whether DDM1 behaves like its mammalian homologue Lsh in localizing predominantly to pericentromeric heterochromatin remains to be determined.

IV. Histone Deacetylation involved in TGS and Control of Heterochromatin Structure at rDNA Repeats

The *Arabidopsis* gene HDA6 is a putative histone deacetylase with significant homology to yeast RPD3 and mouse HDAC1. Seven different mutated alleles have been previously identified. The first five were isolated as recessive mutations increasing expression of transgenes with auxin-responsive promoters. Two additional alleles were recovered in a screen for interference with transcriptional silencing acting in trans via RNA-directed DNA methylation (Aufsatz et al., 2002). The *sil1* mutant was isolated as a modifier of transgene silencing (Furner et al., 1998) and is now shown to be another allele of HDA6. By crossing five of these alleles to a line having a well–characterized cis-transcriptionally silenced locus, release of silencing was observed, indicating that HDA6 is involved in epigenetic regulation. The HDA6 mutants also express non-coding RNA from endogenous repetitive

(*TSI*) templates (Steimer et al., 2000). This indicates that functional HDA6 is required to maintain transcriptional gene silencing at certain, probably repetitive target sequences. All of the HDA6 mutants analyzed accumulate less *TSI* transcripts than TGS mutants that affect global DNA methylation such as *met1* (Saze et al., 2003) or *ddm1* (Steimer et al., 2000). This could either be due to the fact that none of the *sil* or *axe* alleles are true null mutations or that there might be redundancy with other members of the HDAC family (Pandey et al., 2002). An interesting peculiarity of the HDA6 mutations is the predominant accumulation of the smaller, non-polyadenylated *TSI* transcript (compared to *mom1*, *ddm1* and *met1* mutants). The origin and/or the processing of the *TSI* transcript family are not yet well understood. Even though *TSI* repeats are present in the pericentromeric region of all five chromosomes, they are predominantly expressed from two genomic templates (Steimer et al., 2000). However, ectopic expression of *TSI* leads to the same pattern of *TSI* transcripts observed in *mom1*1 (Andrea Steimer, Dissertation) suggesting that the different transcripts are processed from a single precursor. Nevertheless, the observed pattern of *TSI* transcripts in *hda6* mutants might reflect release of expression from particular transcriptional initiation sites, transcription from templates lacking appropriate polyadenylation signals or ecotype differences of *TSI* expression patterns between Ler and Col. The changes of chromatin modifications at rDNA loci that also produce non-polyadenylated transcripts, suggest further studies to investigate whether HDA6 has a specific role in regulation of transcripts lacking this 3' end modification.

The known *HDA6* mutations occur throughout the coding region of the gene. With the exception of the glycine mutated in *sil1* that is not conserved in the yeast counterpart RPD3 all amino acid exchange mutations affect residues that are highly conserved between plant, animal and yeast HDACs (Murfett et al., 2001). Although the mutations cause different degrees of transcriptional reactivation, histone H4 acetylation and histone H3K4 methylation at rDNA loci, these differences are not directly correlated with either single amino acid exchanges or splice-site-mutations. HDA6 activity might be very sensitive to any structural changes of the protein.

Even though it cannot be excluded that HDA6 has an effect on acetylation of other, yet unidentified target proteins, the significant increase of histone acetylation at the rDNA loci in HDA6 mutants strongly suggests that HDA6 is indeed a functional histone deacetylase. Since the Western blot analysis indicated no significant increase in the total level of tetra-acetylated histone H4, HDA6 might remove acetyl residues only from specific targets, while other related family members are responsible for a more general control of histone deacetylation. HDAC genes form a large family, and many members were already shown

to be responsible for the reversible and dynamic acetylation changes of histone tails (Kurdistani and Grunstein, 2003). Both yeast RPD3 (Rundlett et al., 1998) and mouse HDAC1 (Doetzlhofer et al., 1999) are required for transcriptional repression of reporter genes, and RPD3 is involved in the deacetylation of large chromosomal domains throughout the yeast genome (Vogelauer et al., 2000; Kurdistani et al., 2002). The ten members of the RPD3/HDA1 gene family with complete HDAC domains in *Arabidopsis* (Pandey et al., 2002) show varying and tissue-specific expression levels. Evidence for their role in histone modification and gene regulation so far was limited to *HDA19* (synonyms AtRPD3A, AtHDA1), the closest homologue of HDA6 with detectable expression levels (Kunz et al., 2001). Other members are weakly expressed or have yet to be analyzed for their transcript levels (http://www.chromdb.org/). Transcripts from HDA19 are highly abundant in leaves, stem and flowers, and expression as a GAL4 fusion protein was shown to down-regulate a reporter gene (Deuring et al., 2000). Antisense-based down regulation of *HDA19* resulted in a ten-fold increase in tetra-acetylated histone 4 (Kunz et al., 2001). Therefore, HDA6 shares sequence homology and very likely enzymatic activity with its homologue HDA19, but seems to be responsible more for specific rather than for general deacetylation.

A knock-out of mouse HDAC1 leads to embryonic lethality due to severe proliferation defects (Lagger et al., 2002). Clr3 (for Cryptic loci regulator; RPD3-like) and Clr6 (HDAC1-like) HDACs in fission yeast are involved in maintenance of silent mating type and centromeric heterochromatin (Grewal et al., 1998), and mutants for *clr3* and *clr6* show defective mitotic segregation (Grewal et al., 1998). No *Arabidopsis* mutant affected in any other HDA gene has been described, but down-regulation of HDA19 by antisense RNA expression resulted in strong pleiotropic effects in transgenic plants, including some that are due to secondary deregulation of genes controlling development (Kunz et al., 2001). In contrast, HDA6 mutants do not have any drastic phenotype even after several generations of inbreeding (Furner et al., 1998; Murfett et al., 2001; Aufsatz et al., 2002), except a significant delay in flowering time. The fact that morphology is largely unaffected in all plants with a mutated HDA6 is further evidence that the regulatory role of this protein is restricted to very specific target genes.

The developmental transition in *Arabidopsis* from the vegetative to the reproductive phase is tightly regulated by several pathways, integrating environmental factors and internal signals, reviewed in (Putterill et al., 2004). Some of the key components involved in flowering control are regulated by epigenetic mechanisms. For example, the late flowering mutant *fwa-1* is due to ectopic FWA expression resulting from hypomethylation of the

direct repeats in the 5' region of the gene (Soppe et al., 2000). The autonomous and the vernalization pathway control flowering by repression of the MADS box transcription factor flowering locus C (FLC). During the vernalization response chromatin around the transcription start site and in the first intron of *FLC* becomes enriched in histone H3 hypoacetylated at K9 and K14 and hypermethylated at position K9 and K27 (Bastow et al., 2004; Sung and Amasino, 2004). These histone modifications require the function of VIN3, VRN1 and VRN2 and lead to downregulation of *FLC* expression. Another recent publication also describes the requirement of a novel protein FLD, a component of the autonomous pathway, for *FLC* repression (He et al., 2003). The human FLD homologue is associated with HDAC1/2 containing corepressor complexes and indeed an *fld* mutation leads to local H4 hyperacetylation at the *FLC* gene and to an increase in *FLC* mRNA levels (He et al., 2003).

The late flowering phenotype in *hda6* mutants could therefore be a result of misregulation of *FLC*. A preliminary experiment using semiquantitative RT-PCR revealed an increase of *FLC* transcripts relative to actin mRNA levels in the *axe1-5* mutant compared to DR5 plants (data not shown). Interestingly, overexpression of HDA6 as a GFP fusion protein under control of the 35S promoter leads to early flowering (Richard Lawrence, personal communication). Therefore, HDA6 is likely to control flowering via *FLC* expression, however if HDA6 acts redundantly with its close homologues HDA7, 9 or 19 or whether the effect on *FLC* expression is specific for HDA6 needs to be determined. In this respect it would be interesting to investigate the interaction between the autonomous and the vernalization pathway and to explore whether the hyperacetylation of H4 in *FLC* chromatin in *fld* mutants influences hypoacetylation and hypermethylation of H3 induced by the vernalization response.

Our FISH analysis on interphase chromosome spreads indicated that the organization of rRNA genes into chromocenters was affected in the HDA6 mutants. Interestingly, in *ddm1*-5 mutant nuclei mainly centromeric and pericentromeric repeats undergo decondensation, while in *axe1-5* nuclei specifically rDNA repeats were affected. Therefore histone deacetylation by HDA6 may be required to establish a heterochromatin-like structure at the rDNA repeats, while down-regulation of transcription may well be achieved also by other mechanisms like modulation of the initiation frequency at active, decondensed rRNA genes (Sandmeier et al., 2002; Grummt and Pikaard, 2003). The number of active rDNA repeats can be variable, as evident by ultrastructural analysis in *Drosophila*, Xenopus and yeast (McKnight and Miller, 1976; Morgan et al., 1983; French et al., 2003). A very drastic specific regulation of rRNA gene activity in numerous eukaryotes is known as nucleolar

dominance (Pikaard 2000a, b), a phenomenon observed upon the formation of genetic hybrids between related but different species, when one set of parental rDNA is suppressed while the other is active. Nucleolar dominance in interspecific hybrids of Brassica and *Arabidopsis* can be overcome by treatment with trichostatin A (TSA), a general inhibitor of histone deacetylation, or by the DNA methyltransferase inhibitor 5-azadeoxyCytidine (Chen and Pikaard, 1997). Suppressed rDNA in allotetraploid hybrids between *A. thaliana* and *A. arenosa* is also characterized by DNA and histone modifications characteristic for heterochromatin, and nucleolar dominance is released by the same inhibitors as in Brassica (Lawrence et al., 2004). rRNA silencing was further shown to depend on histone deacetylase HDT1, a member of the plant-specific class II HDAC family with nucleolar localization. Interference with HDT1 expression by RNAi technology caused expression of the otherwise suppressed *A. thaliana* rRNA and an increase in histone H3K4 methylation and loss of cytosine methylation at rDNA (Lawrence et al., 2004). In contrast, the changes of chromatin features at rDNA in the HDA6 mutants seem to occur without major changes in transcription rates. This suggests several layers of regulation: a general control of potential transcription via accessibility of the templates and a secondary control of actual transcription by polymerase loading or activity of the polymerase complex. The existence of additional rDNA loci in the allopolyploid hybrids might feed back on both regulatory systems while transcriptional activity in an inbred diploid background is unaffected even if functional HDA6 is missing. This assumption is further supported by the observation that RNAi-downregulation of HDA6 in allopolyploid hybrids does indeed interfere with the selective uniparental transcription of rDNA repeats (Lawrence and Pikaard, personal communication). One could ask why the extra level of rDNA control involving histone deacetylation exists if it plays no role in transcriptional regulation. Limiting the number of potential accessible genes could have the advantage of reducing DNA damage, restricting ingression of PolII transcription, enhancing ribosome assembly by concentrating it around fewer active genes and repressing recombination (Fritze et al., 1997; Cioci et al., 2003; Moss, 2004).

Similar effects of chemical or genetic interference with DNA methyltransferase or histone deacetylase in nucleolar dominance suggest that DNA methylation and hypoacetylation collaborate in gene silencing mechanisms at rDNA loci. TSA treatment resulted in derepression of two silenced loci in *Neurospora crassa* (Selker, 1998), and induced a specific reduction of DNA methylation at these two silenced loci, without affecting overall methylation levels. This suggests a re-enforcing relationship between acetylation and DNA methylation, although an actual histone hyperacetylation at the affected loci was not

demonstrated. It has been well established that DNA methylation can lead to the recruitment of HDACs (Feng and Zhang, 2001), but our data suggest that histone H4 hyperacetylation can also affect DNA methylation levels. We observed clear differences in CpG methylation of rDNA genes between wild type and *sil1*/*axe1-5* mutants, upon digestion with a number of methylation-sensitive enzymes. These differences were not observed previously in the *sil1* or *rts1* mutants (Furner et al., 1998; Aufsatz et al., 2002), possibly because they are most obvious with restriction enzymes *Cfo*I and *Mae*II that were not used in earlier studies. The reductions in rDNA methylation levels in *sil1*/*axe1-5* mutants, compared with wild-type plants, were much less than those observed in other DNA methylation mutants, such as *ddm1* and *hog1* (Furner et al., 1998; Jeddeloh et al., 1999). Further, we observed a more significant effect on cytosines followed by G residues than on cytosines in other contexts. This is in accordance with the results of Aufsatz and co-workers (2002), which used bisulfite sequencing to measure cytosine methylation levels in the promoter region silenced by RNA-directed transcriptional gene silencing. The highest reductions in methylation levels between mutant *rts1* and wild-type plants were observed in CpG sites, and a lesser effect was observed in CpNpG sites. Non-symmetrical CpNpN sites showed no significant decrease in cytosine methylation in the mutants. These results led Aufsatz and co-workers to propose a model for HDA6 function, in which HDA6 plays a role in reinforcing CpG methylation after primary and intermediate *de novo* CpNpG methylation by other components, thus establishing the silent state of the target gene. My results are consistent with this model, which might explain why the HDA6 mutations discovered to date show only moderate reactivation of silenced target genes. Since methylation of rDNA and centromeric repeats was not affected in *rts1* mutants, and the HDA6 gene had not been identified in other screens for DNA hypomethylation or TGS mutants, it was suggested that HDA6 might be specifically involved in RNA-directed pathways of gene silencing (Aufsatz et al., 2002). However, here I showed that the *sil1*/*axe1* mutants alleviate silencing of a well-characterized TGS locus and endogenous, transcriptionally silenced repeats, but also affect acetylation of histones and maintenance of chromatin structure at rDNA loci. These observations indicate that HDA6 is not restricted to its role in an RNA-dependent epigenetic regulation, but acts with a certain level of specificity on other selective targets. Hypoacetylation of rDNA repeats and DNA methylation can be also reinforced by methylation of histone H3K9. Interestingly, recent studies in fission yeast have revealed that a mutation in the *clr3* histone deacetylase impairs methylation of histone H3K9 (Nakayama et al., 2001). It will be interesting to investigate if *HDA6* mutants in *Arabidopsis* affect H3K9met on particular heterochromatic

targets or have additional effects on other histone modifications. In our immunostaining experiments we could not observe a clear reduction of H3K9 methylation at chromocenters close to the nucleolus (data not shown).

The recent identification of a nucleolar remodeling complex in mouse (Santoro et al., 2002) might allow connecting DNA methylation and histone acetylation activities at the rDNA locus on a biochemical basis. NoRC, consisting of the large nucleolar protein Tip5 and SNF2, can induce nucleosomal movement on chromatin templates *in vitro* that depends not only on ATP, but also specifically on the presence of the histone H4 tail (Strohner et al., 2001). Tip5 was shown to interact *in vitro* with the DNA methyltransferases DNMT1 and DNMT3b, as well as with the deacetylase HDAC1. Being recruited to acetylated histone H4 tails via the bromodomain of Tip5, the complex might establish a repressive state by means of histone and DNA modifications. Interestingly, the failure to deacetylate histones also abolished DNA methylation of transfected rRNA gene templates; therefore supporting our observation that histone deacetylation can be required to maintain wild-type DNA methylation levels. It remains to be seen whether a NoRC-like complex with HDA6 (and/or HDT1) as a component exists in plants, or whether some other mechanism controls the equilibrium between decondensed, active rDNA, and condensed, inactive rDNA repeats.

V. Transcriptional Control within a Heterochromatic Environment

Many *Arabidopsis* mutations interfering with the maintenance of transcriptional gene silencing (e.g. *met1*, *cmt3*, *hog1*, *ddm1*, *kyp1* and even *sil1*) affect DNA methylation levels. In contrast, the *mom1* mutation was shown by Southern Blot analysis and bisulfite sequencing to reactivate silencing from highly methylated transgenes and to preserve the DNA methylation pattern (Amedeo et al., 2000) at the reactivated target sequences as well as at 180bp and rDNA repeats. *TSI* repeats are found in the pericentromeric region of all five chromosomes (Steimer et al., 2000) and are tightly condensed into the chromocenters together with the extensive heterochromatic 180bp repeats regions in wildtype (*Figure 14C, D*). The transgenic *HPT* locus consists of at least 15 copies of the transformed plasmid carrying the hygromycine resistance gene and salmon sperm DNA used as carrier DNA during transformation (Mittelsten Scheid et al., 1991). FISH analysis showed that the locus has formed a small highly methylated, neo-heterochromatic knob, clearly visible as condensed region in DAPI stained nuclei (*Figure 14A, B*). Here I showed that the release

of transcriptional silencing of *TSI* and *HPT* loci in *mom1-1* mutant nuclei is not connected to detectable structural changes at the associated heterochromatic structure. Likewise the pattern of DNA methylation and the distribution of the three analyzed histone modifications are not altered in the mutant compared to wildtype. This is in striking contrast to the release of silencing observed in plants carrying the *ddm1* mutation, which reactivates silencing of a partly overlapping set of target genes (Jerzy Paszkowski, personal communication). The effect of the *mom1-1* mutation on histone modifications was also investigated at the 35S promoter and the *HPT* coding region using Chromatin Immunoprecipitation (Muhammed Tariq, Dissertation). The molecular analysis confirmed the results obtained by my cytological study, namely H3K9 and H3K4 methylation and H4 acetylation levels remained unaffected in the mutant.

Tethering a target locus into close vicinity of constitutive heterochromatin was described to be associated with transcriptional inactivation in mammalian cells (Belyaeva et al., 1997). In wheat, multiple transgenes integrated at far spaced sites have the tendency to colocalize during interphase. An increase in their transcriptional activity by 5-azadeoxyCytidine or TSA treatment leads to dispersion of the transgene sites (Santos et al., 2002). In *Drosophila* position-effect variegation (PEV) resulting from an insertion of heterochromatin into a euchromatic gene can cause aberrant association of the gene and its homologous copy with heterochromatin. This association with heterochromatic regions is affected by the chromosomal distance from heterochromatin (Csink and Henikoff, 1996). The chromosomal position of the *HPT* locus has not been mapped, however, an early prophase spread of line A revealed that it did not integrate close to the centromeres (*Figure 8*).

Given the evidence for spatial rearrangements of silenced loci in other organisms, we examined, whether the reactivation of silencing of the *HPT* locus in the *mom1-1* mutant might be associated with a change in nuclear localization in respect to chromocenters. Our results, using FISH on spread nuclei did not indicate a significant difference between line A and *mom1-1* regarding the two loci relative to each other or their association with constitutive heterochromatin. Nevertheless, it remains possible that a difference would be observed not on spread nuclei but on nuclei with a preserved three-dimensional structure.

In mammals the nuclear membrane or the region surrounding the nucleolus is populated by pericentromeric heterochromatin (Haaf and Schmid, 1991) and in yeast the nuclear periphery was shown to play a role in telomere silencing (Andrulis et al., 1998; Feuerbach et al., 2002). Since *MOM1* encodes a putative transmembrane domain its role could be envisaged in binding heterochromatin to the nuclear periphery. Concerning the *HPT* locus

a FISH analysis on formaldehyde nuclei was attempted, but it turned out to be technically demanding and was not pursued due to time limitations. However, DAPI staining of formaldehyde fixed nuclei did not reveal any difference in the localization of chromocenters when comparing line A and *mom1-1*. Chromocenters remained at the nuclear periphery, despite transcriptional reactivation of pericentromeric *TSI* repeats residing within the chromocenters. Additionally, immunostaining experiments using a GFP antibody to detect the MOM1-GFP fusion protein in our transgenic *Arabidopsis* lines did not reveal localization to the nuclear periphery, suggesting that at least a fraction of MOM1 protein is not anchored in the membrane.

The cytological investigation of the nuclear structure in *mom1-1* implies that release of TGS can be achieved without gross changes in chromatin structure, DNA methylation or histone modifications. Therefore, the epigenetic control mediated by MOM1 may present a novel yet undefined mechanism. Evidence for active genes residing within heterochromatin and resisting inactivation exists, e.g. some genes are expressed from the inactive X-chromosome (Carrel et al., 1999). Regulatory mechanisms for such genes are not well understood. Transcriptional activation in the *mom1-1* mutant, occurring without obvious signs of conversion into euchromatin, resembles such “heterochromatic transcription”. Interestingly, some of the *Drosophila* genes expressed from heterochromatin (Hilliker et al., 1980) have special characteristics since they need the heterochromatin environment for expression. HP1 is required for expression of two essential heterochromatic genes in *Drosophila* (Lu et al., 2000), suggesting that HP1 plays a role in the formation of a particular chromatin structure that interferes on one hand with the activation of euchromatic genes, but on the other hand might be necessary for expression of heterochromatic genes. Also DNA hypomethylation at a locus is not always implicated with an increase in transcription. For example the activation of the H-2K gene in teratocarcinoma cells requires an increase in DNA methylation (Tanaka et al., 1983; Tanaka et al., 1986). One hypothesis is that MOM1 contributes to the regulation of transcription in usually silent, heterochromatic regions of chromosomes and therefore might be involved in the control of genes that are resistant to silencing by the “conventional” epigenetic pathway including histone and DNA methylation and whose expression is even favored by heterochromatic chromatin. In this respect an interesting observation is the increase in DNA methylation, predominantly at CpNpG and asymmetric but as well at CpG sites, in the 35S promoter region of the *HPT* gene in *mom1-1* compared to line A as determined by bisulfite sequencing (Paolo Amedeo, Dissertation).

Northern Blot analysis revealed a predominant expression of MOM1 in flowers and young seedlings, and only low transcript levels in adult leaves, suggesting a role of MOM1 especially in proliferating tissue. Similar to DDM1 it could therefore be involved in the faithful reproduction of epigenetic states during mitotic or meiotic cell divisions. Depletion of MOM1 in a chemically inducible system showed, however, that MOM1 protein is required for maintenance of silencing of a multicopy GUS reporter gene also in non-replicating cells (Tariq et al., 2002). Such properties of MOM1 resemble yeast SIR2 and SIR3 proteins, likewise dynamic components of silent chromatin (Cheng and Gartenberg, 2000; Tariq et al., 2002). SIR proteins are specifically tethered to certain regions in the genome, namely telomeres and mating type loci. The MOM1-GFP fusion protein, however, is localized in speckles all over the euchromatic compartment, revealing no evidence for specific targeting to e.g. the pericentromeric heterochromatin or the nuclear membrane. Yet these observations are based on the detection of a GFP fusion protein, which, even though shown to repress *TSI* expression, may be not completely functional or mislocalized due to ectopic expression and the presence of the tag. Experiments to investigate the localization of the endogenous protein using a polyclonal antibody generated against the C-terminal part of the protein are ongoing. With this antibody the localization of MOM1 protein in different TGS mutants especially those impaired in DNA methylation can also be studied.

To date important characteristics of the MOM1 protein remain still vague. For example it is unknown whether MOM1 has the ability to interact with DNA or with nucleosomes, probably via its half helicase domain. Nevertheless, I assume that MOM1 interacts directly with chromatin and does not function e.g. by binding of transcriptional activators to render them unavailable for transcription initiation. Slight evidence for the binding to chromatin arose from immunostaining experiments of the MOM1-GFP line in comparison to a line expressing GFP alone (Todd Blevins, personal communication). GFP is a small protein that can pass through nuclear pores and accumulate in the cytoplasm as well as in the nucleus. While GFP can be seen clearly in the nucleus when intact cells are observed under blue fluorescent light, I detected no signal in the immunostaining experiments, suggesting that those proteins diffusing in the nucleoplasm might be removed during permeabilization of the fixed protoplasts. MOM1-GFP fusion proteins remain detectable when the cells are fixed and permeabilized under identical conditions. The direct binding of MOM1 protein to chromatin is the prerequisite to identify new targets of MOM1 dependent gene regulation. Experiments are ongoing to genome wide map the binding sites of MOM1 protein using a ChIP on CHIP approach: Chromatin crosslinked to the MOM1 protein will

be pulled using the GFP epitope. The recovered DNA will then be amplified and hybridized to an *Arabidopsis* microarray. The identification of at least one target sequence, which directly interacts with the MOM1 protein and which can be further used as positive control, is a requirement for this experiment. Therefore, I will initially test the hypothesis that in wildtype plants, MOM1 protein is indeed physically associated with either *TSI* or *HPT* loci when contributing to their transcriptional inactivation.

Several domains have been predicted to be part of the large MOM1 protein (Amedeo et al., 2000). The most significant similarity is found to the helicase domain of the SWI2/SNF2 chromatin remodeling factor, however this domain is truncated in MOM1. Therefore, we expect MOM1 to function in a complex possibly including a protein that would provide the second half of functional helicase domain. However, so far, *in silico* searches did not reveal any protein with these properties.

VI. MOM1 Defines a Novel Pathway of Epigenetic Regulation

To further characterize the role of MOM1 in relation to epigenetic mechanisms involving DNA and histone tail modifications we established double mutant lines of *mom1-1* with *ddm1* and *axe1* mutants. All three mutants reactivated transcriptional silencing of *TSI* repeats, although to different extends. The mutant *ddm1* interferes mainly with DNA methylation, while the axe1 mutants affect histone acetylation patterns. Both the *mom1-1/ddm1-5* and the *mom1-1/axe1-1* double mutant plants reactivated silencing at the *TSI* repeats synergistically. Additionally, the combination of two mutations led to a variation of strong phenotypes suggesting a mismanagement of a large number of genes normally kept under epigenetic control. These observations argue against the hypothesis that MOM1 acts downstream of epigenetic prints like DNA and histone modifications, but suggest that MOM1 defines a novel, previously uncharacterized level of epigenetic control. Although an indirect, epistatic interaction cannot be completely excluded, considering secondary epigenetic effects of the three mutations, a hypomorphic interaction at least in the *mom1-1/ddm1-5* double mutant is rather unlikely since *ddm1*–5 is expected to be a null allele. In addition, the synergistic effect on plant morphology and silencing release was not restricted to the *mom1-1/ddm1-5* double mutant, but was also found in the *mom1-1/axe1-1* double mutant. This also confirms that the observed effect is not specific for the loss of DDM1 function as chromatin remodeling factor, but rather due to general independence of MOM1 function of the histone and DNA code. In addition, the

requirement for MOM1 to silence *HPT* and *TSI* loci showed that the DNA methylation based silencing machinery is not always sufficient to assure a complete shutdown of transcription, but requires another, probably minor TGS pathway.

The analysis of double mutant plants provided the first demonstration of a phenotype for *mom1-1* mutant plants. So far no challenge of the mutant plant with different stimuli or stresses has revealed an aberration from the wildtype phenotype (Paolo Amedeo, Dissertation). Until now there was no evidence that the epigenetic pathway delineated by MOM1 would indeed be of functional relevance for the plant. However, by combination of the *mom1-1* mutation with mutants affecting DNA methylation and histone acetylation we showed that MOM1 defines a level of epigenetic control that prevents major impacts on the plant when alternative silencing pathway(s) are compromised.

Interestingly, however, in the *mom1-1/ddm1-5* double mutant plants, the phenotype was not restricted to aberrant plant morphology but also the nuclear architecture was affected. Only in *mom1-1/ddm1-5* double mutant plants and not in segregating siblings, which are heterozygous for one of the two mutations, was a clustering of chromocenters observed. This phenotype was also not found in the *mom1-1/axe1-1* double mutant. Nuclei with clustered chromocenters were also more abundant in progeny of a mother homozygous of the *mom1-1* and heterozygous for *ddm1* mutation, than in the progeny of a mother already homozygous for *ddm1*. The analysis of slides derived from different plants showed that either a plant contained a large number of extremely dispersed 180bp repeats or a high percentage of aggregating chromocenters, as if the two nuclear phenotypes would reflect two ways to respond to a loss of DNA methylation and of the DNA methylation-independent pathway represented by *mom1-1*.

Centromeres, telomeres, constitutively heterochromatic regions and NORs are proposed to provide a structural framework for the nuclear architecture. Especially the centromeres may behave as structural centers for chromatin organization in interphase favoring the creation of functional compartments for essential nuclear processes such as gene expression (Manuelidis, 1990). The centromere position in interphase nuclei of mammals seems to be cell type specific and to change during cell cycle and differentiation (Manuelidis, 1990; Ferguson and Ward, 1992). Centromeres of human and mouse lymphocyte nuclei localize to the nuclear periphery (Weierich et al., 2003), but also around the nucleolus (Haaf and Schmid, 1991). Both subcompartments are also characterized by late replicating chromatin. In human lymphocytes, centromeres close to the nucleolus predominately belong to chromosomes containing NORs (Alcobia et al., 2000). In addition, centromeres in mammalian nuclei tend to cluster in chromocenters (Haaf and Schmid,

1991). The associations between heterochromatic chromosome regions could be mediated by similar chemical properties of the chromatin in these regions, e.g. highly concentration of simple sequence DNA or proteins specifically associated with constitutive heterochromatin (Marcand et al., 1996). Specific combinations of centromeres found in chromocenters seem to depend again on the cell type (Alcobia et al., 2000). In *Arabidopsis*, centromere clustering also takes place revealing a variation of chromocenter numbers ranging form four to ten (Fransz et al., 2002). A reduction in the chromocenter number to one or two containing the NORs was observed in mesophyll cells when transformed into protoplasts, probably accompanied by major changes in gene expression predicted to occur during protoplast isolation (Paul Fransz, personal communication).

However, the centromere clustering observed in the *mom1-1/ddm1-5* double mutant plants appears to be distinct, since it affects all chromocenters (*Figure 31* and *33A*) or all except one chromocenter, which comprises a NOR (*Figure 33B*). In addition the clustering of the chromocenters seems to take place around the nucleolus. Why would the centromere clustering happen around this nuclear subcompartment? Those *ddm1*-5 nuclei that show strongly affected heterochromatin organization can retain relatively compact NORs (*Figure 9*). One could speculate that chromatin structure at NORs is regulated by a mechanism not or less dependent on *DDM1* function. It is possible that chromocenter clustering around the NORs, which at least partly retained their heterochromatic structure, would help to keep a repressive chromatin environment required for the regulation of gene expression. Conversely, the clustering of centromeres may be a result of the intrinsic property of repetitive DNA. While in wildtype the chromocenters are organized at the nuclear periphery by a mechanism dependent on DNA methylation and possibly MOM1 function, clustering could be induced in the double mutant if the mountings that under normal conditions tie the chromocenters to the periphery are absent. No information is yet available that would elucidate the nature of these attachment sites at the nuclear periphery.

In mammals, interaction of chromatin with the nuclear lamina, a scaffold-like network of protein filaments surrounding the nucleus, could provide such an anchoring point. For example histones were reported to interact with the nuclear lamins via their C-terminal tails (Taniura et al., 1995) and the lamin B receptor (LBR) was found to interact with the chromodomain protein HP1 (Ye et al., 1997), which in turn is specifically enriched in pericentromeric heterochromatin domains. The *Arabidopsis* genome however, does not encode homologues to nuclear lamins, suggesting that plants have evolved a nuclear membrane with a unique protein composition. MAR binding filament-like protein 1 (MFP1),

a protein with similarities to myosin, tropomyosin and intermediated filament proteins, locates to the nuclear envelope and is a possible component of a nuclear substructure that might connect the nuclear envelope and the internal nuclear matrix in *Arabidopsis* (Meier et al., 1996; Gindullis and Meier, 1999).

Centromere clustering involving all centromeres has been described for interphase cells of the yeast *S. cerevisia*, the centromeres arrange in a circle at one pole of the nucleus however opposite of the nucleolus (Jin et al., 2000). The configuration in yeast, similar to the Rabl configuration, could be a relict of anaphase, however it was found to be reconstituted even in the absence of anaphase, when disrupted experimentally, and to require stabilization by a microtubule-dependent process (Jin et al., 2000). If the chromocenter clustering in the *mom1-1/ddm1-5* double mutant is a relict of the nuclear division, reflecting a failure to redistribute the chromocenters to the nuclear periphery after the division was completed, or if this structure is actively established to serve a function, remains to be determined.

Interestingly, this aggregation was not only observed in *mom1-1/ddm1-5* double mutants, but also in one line homozygous for *met1-3*. Preliminary experiments suggested that there is no further increase in this nuclear phenotype in a *mom1-1/met1-3* double mutant (data not shown). This would suggest that either the nuclear phenotype is not a direct consequence of the *mom1/ddm1* or *met1* mutation but that they indirectly determine expression of a downstream target responsible for the changes in nuclear architecture. Alternatively MOM1 function could only be required if residual levels of DNA methylation remain.

VII. Conclusions

In this work I have analyzed several *Arabidopsis* mutants impaired in the maintenance of transcriptional gene silencing for their impact on DNA and histone modifications as well as nuclear organization. One aspect revealed by this study is that several epigenetic prints namely DNA methylation, histone tail acetylation and methylation collaborate to establish an active or inactive state of the underlying genes and display distinct effects on nuclear structure. While inactivation of a transgene array can result in the formation of heterochromatin as shown for the *HPT* locus, the reactivation of transcription can be achieved by different mechanisms. A cytological visible disturbance of higher order chromatin structure as shown for the *ddm1* mutant is not required for transcriptional

reactivation in the *mom1* mutant. But the amount of *HPT* transcript produced in *mom1* and *ddm1* differs substantially, suggesting that the loosening of chromatin structure can contribute to achieve high transcription levels, probably by establishing further points of contact for the transcription machinery. In this line cytological studies of a large transgenic locus in human cells have shown that the onset of transcription precedes noticeable changes in higher order chromatin structure (Janicki et al., 2004). The study of the *HDA6* mutant alleles, however, has revealed that loosening of chromatin structure not necessarily entails an increase in transcription, implying the presence of additional mechanisms to assure gene activation and repression.

Regarding all possible epigenetic imprints, special importance is accorded to DNA methylation. CpG methylation determines histone H3K9 methylation and thereby probably defines a more condensed chromatin structure in *Arabidopsis*. A fundamental distinction between plants and animals is the lack of genome-wide resetting of methylation for example during germ cell development in plants. While in mammals the creation of germ cells occurs early in development, the reproductive tissue of plants arises from the shoot apical meristem during transition to flowering after a more or less extensive vegetative phase. If epigenetic modifications like DNA methylation change the phenotype so, that it performs better under certain environmental conditions, a change can become meiotically stable. This bears the possibility to transmit acquired adaptation to the progeny. A crucial parameter for successful reproduction of a plant is the onset of flowering, and flowering time is indeed at least partially under epigenetic control.

So far gene regulation by histone tail modifications and RNA-directed gene silencing are mechanisms common to all organisms investigated to date, while DNA methylation is not conserved in all organisms. However, in those eukaryotes applying this modification it is an important part of epigenetic regulation and genome evolution. However, in addition to those elements occurring transkingdom-wide, MOM1 of *Arabidopsis* seems to delineate a previously uncharacterized, methylation-independent epigenetic pathway controlling heritable patterns of gene expression.

7. ACKNOWLEDGEMENTS

First of all I would like to express my gratitude to both my PhD supervisor Dr. Jerzy Paszkowski and to Dr. Ortrun Mittelsten Scheid for their enthusiasm, encouragement and patience they have granted me during my PhD thesis. I am indebted to Sally Adams, Karin Afsar, Marian Caikowski, Sonia Guimil, Jacek Lichota, Susanne Lienhard, Yoshiki Habu, Moez Hanin, Uta Paskowski, Jon Reinders, Chotika Smathajitt, Shin Takeda, Muhammed Tariq and Roman Ulm whom I had the pleasure to work with. They created a great atmosphere in the laboratory and I profited from many fruitful discussions and collaborations. All my colleagues taught me a lot and stimulated my development both as scientist and human being. Special thanks also go to the members of my thesis committee, Dr. Barbara Hohn and Dr. Lukas Landmann, for their advice and support. Dr. Paul Fransz helped me tremendously by sharing his technical expertise, in the same way I owe thanks to Dr. Hanna Weiss for her support. Further I thank Drs. Herve Vaucheret, Jane Murfett, Ian Furner, Craig Pikaard and their research groups for the excellent collaboration on the HDA6 mutant project. Last but not least I would like to thank my parents and grand parents, my sister and Ilja Boschke for their constant support, encouragement and love.

8. REFERENCES

Abranches, R., Beven, A.F., Aragon-Alcaide, L., and Shaw, P.J. (1998). Transcription sites are not correlated with chromosome territories in wheat nuclei. *J Cell Biol* **143**, 5-12.

Ahmad, K., and Henikoff, S. (2002). The histone variant H3.3 marks active chromatin by replication-independent nucleosome assembly. *Mol Cell* **9**, 1191-1200.

Ahringer, J. (2000). NuRD and SIN3 histone deacetylase complexes in Development. *Trends Genet* **16**, 351-356.

Alexandrova, O., Solovei, I., Cremer, T., and David, C.N. (2003). Replication labeling patterns and chromosome territories typical of mammalian nuclei are conserved in the early metazoan Hydra. *Chromosoma* **112**, 190-200.

Allfrey, V.G., Faulkner, R.M., and Mirsky, A.E. (1964). Acetylation and methylation of histones and their possible role in the regulation of RNA synthesis. *Proc Natl Acad Sci USA* **51**, 786-794.

Amedeo, P., Habu, Y., Afsar, K., Scheid, O.M., and Paszkowski, J. (2000). Disruption of the plant gene MOM releases transcriptional silencing of methylated genes. *Nature* **405**, 203-206.

Andrulis, E.D., Neiman, A.M., Zappulla, D.C., and Sternglanz, R. (1998). Perinuclear localization of chromatin facilitates transcriptional silencing. *Nature* **394**, 592-595.

ArabidopsisGenomeInitiative. (2000). Analysis of the genome sequence of the flowering plant *Arabidopsis thaliana*. *Nature* **408**, 796-815.

Armstrong, S.J., Franklin, F.C., and Jones, G.H. (2001). Nucleolus-associated telomere clustering and pairing precede meiotic chromosome synapsis in *Arabidopsis thaliana*. *J Cell Sci* **114**, 4207-4217.

Attwood, J.T., Yung, R.L., and Richardson, B.C. (2002). DNA methylation and the regulation of gene transcription. *Cell Mol Life Sci* **59**, 241-257.

Aufsatz, W., Mette, M.F., Van Der Winden, J., Matzke, M., and Matzke, A.J. (2002). HDA6, a putative histone deacetylase needed to enhance DNA methylation induced by double-stranded RNA. *Embo J* **21**, 6832-6841.

Bannister, A.J., Zegerman, P., Partridge, J.F., Miska, E.A., Thomas, J.O., Allshire, R.C., and Kouzarides, T. (2001). Selective recognition of methylated lysine 9 on histone H3 by the HP1 chromo domain. *Nature* **410**, 120-124.

Bartee, L., Malagnac, F., and Bender, J. (2001). *Arabidopsis* cmt3 chromomethylase mutations block non-CG methylation and silencing of an endogenous gene. *Genes Dev* **15**, 1753-1758.

Bastow, R., Mylne, J.S., Lister, C., Lippman, Z., Martienssen, R.A., and Dean, C. (2004). Vernalization requires epigenetic silencing of FLC by histone methylation. *Nature* **427**, 164-167.

Beisel, C., Imhof, A., Greene, J., Kremmer, E., and Sauer, F. (2002). Histone methylation by the Drosophila epigenetic transcriptional regulator Ash1. *Nature* **419**, 857-862.

Belyaev, N.D., Houben, A., Baranczewski, P., and Schubert, I. (1997). Histone H4 acetylation in plant heterochromatin is altered during the cell cycle. *Chromosoma* **106**, 193-197.

Bender, J. (2004). DNA Methylation and Epigenetics. *Annu Rev Plant Physiol Plant Mol Biol* **55**, 41-68.

Berger, S.L. (2002). Histone modifications in transcriptional regulation. *Curr Opin Genet Dev* **12**, 142-148.

Bird, A.P., and Wolffe, A.P. (1999). Methylation-induced repression--belts, braces, and chromatin. *Cell* **99**, 451-454.

Braunstein, M., Sobel, R.E., Allis, C.D., Turner, B.M., and Broach, J.R. (1996). Efficient transcriptional silencing in Saccharomyces cerevisiae requires a heterochromatin histone acetylation pattern. *Mol Cell Biol* **16**, 4349-4356.

Brown, K.E., Guest, S.S., Smale, S.T., Hahm, K., Merkenschlager, M., and Fisher, A.G. (1997). Association of transcriptionally silent genes with Ikaros complexes at centromeric heterochromatin. *Cell* **91**, 845-854.

Burgers, W.A., Fuks, F., and Kouzarides, T. (2002). DNA methyltransferases get connected to chromatin. *Trends Genet* **18**, 275-277.

Cao, X., and Jacobsen, S.E. (2002a). Role of the *Arabidopsis* DRM Methyltransferases in De Novo DNA Methylation and Gene Silencing. *Curr Biol* **12**, 1138-1144.

Cao, X., and Jacobsen, S.E. (2002b). Locus-specific control of asymmetric and CpNpG methylation by the DRM and CMT3 methyltransferase genes. *Proc Natl Acad Sci USA* **99** Suppl 4, 16491-16498.

Chen, Z.J., and Pikaard, C.S. (1997). Epigenetic silencing of RNA polymerase I transcription: a role for DNA methylation and histone modification in nucleolar dominance. *Genes Dev* **11**, 2124-2136.

Chikashige, Y., Kinoshita, N., Nakaseko, Y., Matsumoto, T., Murakami, S., Niwa, O., and Yanagida, M. (1989). Composite motifs and repeat symmetry in S. pombe centromeres: direct analysis by integration of NotI restriction sites. *Cell* **57**, 739-751.

Choi, Y., Gehring, M., Johnson, L., Hannon, M., Harada, J.J., Goldberg, R.B., Jacobsen, S.E., and Fischer, R.L. (2002). DEMETER, a DNA glycosylase domain protein, is required for endosperm gene imprinting and seed viability in arabidopsis. *Cell* **110**, 33-42.

Choo, K.H. (2001). Domain organization at the centromere and neocentromere. *Dev Cell* **1**, 165-177.

Cloix, C., Tutois, S., Mathieu, O., Cuvillier, C., Espagnol, M.C., Picard, G., and Tourmente, S. (2000). Analysis of 5S rDNA arrays in *Arabidopsis thaliana*: physical mapping and chromosome-specific polymorphisms. *Genome Res* **10**, 679-690.

Comings, D.E. (1968). The rationale for an ordered arrangement of chromatin in the interphase nucleus. *Am J Hum Genet* **20**, 440-460.

Comings, D.E. (1980). Arrangement of chromatin in the nucleus. *Hum Genet* 53, 131-143.

Copenhaver, G.P., and Pikaard, C.S. (1996). RFLP and physical mapping with an rDNA-specific endonuclease reveals that nucleolus organizer regions of *Arabidopsis thaliana* adjoin the telomeres on chromosomes 2 and 4. *Plant J* **9**, 259-272.

Csink, A.K., and Henikoff, S. (1996). Genetic modification of heterochromatic association and nuclear organization in Drosophila. *Nature* **381**, 529-531.

Dorer, D.R., and Henikoff, S. (1994). Expansions of transgene repeats cause heterochromatin formation and gene silencing in Drosophila. *Cell* **77**, 993-1002.

Fagard, M., Boutet, S., Morel, J.B., Bellini, C., and Vaucheret, H. (2000). AGO1, QDE-2, and RDE-1 are related proteins required for post-transcriptional gene silencing in plants, quelling in fungi, and RNA interference in animals. *Proc Natl Acad Sci USA* **97**, 11650-11654.

Feil, R., and Khosla, S. (1999). Genomic imprinting in mammals: an interplay between chromatin and DNA methylation? *Trends Genet* **15**, 431-435.

Feuerbach, F., Galy, V., Trelles-Sticken, E., Fromont-Racine, M., Jacquier, A., Gilson, E., Olivo-Marin, J.C., Scherthan, H., and Nehrbass, U. (2002). Nuclear architecture and spatial positioning help establish transcriptional states of telomeres in yeast. *Nat Cell Biol* **4**, 214-221.

Finnegan, E.J., Peacock, W.J., and Dennis, E.S. (1996). Reduced DNA methylation in *Arabidopsis thaliana* results in abnormal plant *Development* . *Proc Natl Acad Sci USA* **93**, 8449-8454.

Fischle, W., Wang, Y., Jacobs, S.A., Kim, Y., Allis, C.D., and Khorasanizadeh, S. (2003). Molecular basis for the discrimination of repressive methyl-lysine marks in histone H3 by Polycomb and HP1 chromodomains. *Genes Dev* **17**, 1870-1881.

Francastel, C., Magis, W., and Groudine, M. (2001). Nuclear relocation of a transactivator subunit precedes target gene activation. *Proc Natl Acad Sci USA* **98**, 12120-12125.

Fransz, P., Armstrong, S., Alonso-Blanco, C., Fischer, T.C., Torres-Ruiz, R.A., and Jones, G. (1998). Cytogenetics for the model system *Arabidopsis thaliana. Plant J* **13**, 867-876.

Fransz, P., De Jong, J.H., Lysak, M., Castiglione, M.R., and Schubert, I. (2002). Interphase chromosomes in *Arabidopsis* are organized as well defined chromocenters from which euchromatin loops emanate. *Proc Natl Acad Sci USA* **99**, 14584-14589.

Fransz, P.F., Armstrong, S., de Jong, J.H., Parnell, L.D., van Drunen, C., Dean, C., Zabel, P., Bisseling, T., and Jones, G.H. (2000). Integrated cytogenetic map of chromosome arm 4S of A. thaliana: structural organization of heterochromatic knob and centromere region. *Cell* **100**, 367-376.

French, S.L., Osheim, Y.N., Cioci, F., Nomura, M., and Beyer, A.L. (2003). In exponentially growing Saccharomyces cerevisiae cells, rRNA synthesis is determined by the summed RNA polymerase I loading rate rather than by the number of active genes. *Mol Cell Biol* **23**, 1558-1568.

Fuks, F., Burgers, W.A., Brehm, A., Hughes-Davies, L., and Kouzarides, T. (2000). DNA methyltransferase Dnmt1 associates with histone deacetylase activity. *Nat Genet* **24**, 88-91.

Fuks, F., Hurd, P.J., Deplus, R., and Kouzarides, T. (2003). The DNA methyltransferases associate with HP1 and the SUV39H1 histone methyltransferase. *Nucleic Acids Res* **31**, 2305-2312.

Fuks, F., Hurd, P.J., Wolf, D., Nan, X., Bird, A.P. and Kouzarides, T. (2003) The Methyl-CpG-binding protein MeCP2 links DNA methylation to histone methylation. *J Biol Chem* **278**, 4035-4040.

Furner, I.J., Sheikh, M.A., and Collett, C.E. (1998). Gene silencing and homology-dependent gene silencing in Arabidopsis: genetic modifiers and DNA methylation. *Genetics* **149**, 651-662.

Galy, V., Olivo-Marin, J.C., Scherthan, H., Doye, V., Rascalou, N., and Nehrbass, U. (2000). Nuclear pore complexes in the organization of silent telomeric chromatin. *Nature* **403**, 108-112.

Gendrel, A.V., Lippman, Z., Yordan, C., Colot, V., and Martienssen, R.A. (2002). Dependence of heterochromatic histone H3 methylation patterns on the *Arabidopsis* gene DDM1. *Science* **297**, 1871-1873.

Gerbi, S.A., and Bielinsky, A.K. (2002). DNA replication and chromatin. *Curr Opin Genet Dev* **12**, 243-248.

Gerlich, D., Beaudouin, J., Kalbfuss, B., Daigle, N., Eils, R., and Ellenberg, J. (2003). Global chromosome positions are transmitted through mitosis in mammalian cells. *Cell* **112**, 751-764.

Grant, P.A., Sterner, D.E., Duggan, L.J., Workman, J.L., and Berger, S.L. (1998). The SAGA unfolds: convergence of transcription regulators in chromatin-modifying complexes. *Trends Cell Biol* **8**, 193-197.

Haaf, T., and Schmid, M. (1989). Centromeric association and non-random distribution of centromeres in human tumour cells. *Hum Genet* 81, 137-143.

Hamilton, A.J., and Baulcombe, D.C. (1999). A species of small antisense RNA in posttranscriptional gene silencing in plants. *Science* **286**, 950-952.

Haupt, W., Fischer, T.C., Winderl, S., Fransz, P., and Torres-Ruiz, R.A. (2001). The centromere1 (CEN1) region of *Arabidopsis thaliana*: architecture and functional impact of chromatin. *Plant J* **27**, 285-296.

Heard, E., Clerc, P., and Avner, P. (1997). X-chromosome inactivation in mammals. *Annu Rev Genet* **31**, 571-610.

Hecht, A., Laroche, T., Strahl-Bolsinger, S., Gasser, S.M., and Grunstein, M. (1995). Histone H3 and H4 N-termini interact with SIR3 and SIR4 proteins: a molecular model for the formation of heterochromatin in yeast. *Cell* **80**, 583-592.

Heitz, E. (1928). Das Heterochromatin der Moose. *Jahrb. Wiss. Bot* **69**, 762-818.

Henikoff, S., Ahmad, K., Platero, J.S., and van Steensel, B. (2000). Heterochromatic deposition of centromeric histone H3-like proteins. *Proc Natl Acad Sci USA* **97**, 716-721.

Heslop-Harrison, J.S., Brandes, A., and Schwarzacher, T. (2003). Tandemly repeated DNA sequences and centromeric *Chromosoma*l regions of *Arabidopsis* species. *Chromosome Res* **11**, 241-253.

Hochstrasser, M., Mathog, D., Gruenbaum, Y., Saumweber, H., and Sedat, J.W. (1986). Spatial organization of chromosomes in the salivary gland nuclei of Drosophila melanogaster. *J Cell Biol* **102**, 112-123.

Jackson, J.P., Johnson, L., Jasencakova, Z., Zhang, X., PerezBurgos, L., Singh, P.B., Cheng, X., Schubert, I., Jenuwein, T., and Jacobsen, S.E. (2004). Dimethylation of histone H3 lysine 9 is a critical mark for DNA methylation and gene silencing in *Arabidopsis thaliana*. *Chromosoma* **112**, 308-315.

Jackson, J.P., Lindroth, A.M., Cao, X., and Jacobsen, S.E. (2002). Control of CpNpG DNA methylation by the KRYPTONITE histone H3 methyltransferase. *Nature* **416**, 556-560.

Janicki, S.M., Tsukamoto, T., Salghetti, S.E., Tansey, W.P., Sachidanandam, R., Prasanth, K.V., Ried, T., Shav-Tal, Y., Bertrand, E., Singer, R.H., and Spector, D.L. (2004). From silencing to gene expression: real-time analysis in single cells. *Cell* **116**, 683-698.

Jasencakova, Z., Meister, A., Walter, J., Turner, B.M., and Schubert, I. (2000). Histone H4 acetylation of euchromatin and heterochromatin is cell cycle dependent and correlated with replication rather than with transcription. *Plant Cell* **12**, 2087-2100.

Jasencakova, Z., Soppe, W.J., Meister, A., Gernand, D., Turner, B.M., and Schubert, I. (2003). Histone modifications in Arabidopsis- high methylation of H3 lysine 9 is dispensable for constitutive heterochromatin. *Plant J* **33**, 471-480.

Jeddeloh, J.A., Stokes, T.L., and Richards, E.J. (1999). Maintenance of genomic methylation requires a SWI2/SNF2-like protein. *Nat Genet* **22**, 94-97.

Jenuwein, T., and Allis, C.D. (2001). Translating the histone code. *Science* **293**, 1074-1080.

Jeppesen, P., and Turner, B.M. (1993). The inactive X chromosome in female mammals is distinguished by a lack of histone H4 acetylation, a cytogenetic marker for gene expression. *Cell* **74**, 281-289.

Jin, Q., Trelles-Sticken, E., Scherthan, H., and Loidl, J. (1998). Yeast nuclei display prominent centromere clustering that is reduced in nondividing cells and in meiotic prophase. *J Cell Biol* 141, 21-29.

Johnson, L., Cao, X., and Jacobsen, S. (2002). Interplay between two epigenetic marks. DNA methylation and histone H3 lysine 9 methylation. *Curr Biol* **12**, 1360-1367.

Jones, P.L., Veenstra, G.J., Wade, P.A., Vermaak, D., Kass, S.U., Landsberger, N., Strouboulis, J., and Wolffe, A.P. (1998). Methylated DNA and MeCP2 recruit histone deacetylase to repress transcription. *Nat Genet* **19**, 187-191.

Kakutani, T., Munakata, K., Richards, E.J., and Hirochika, H. (1999). Meiotically and mitotically stable inheritance of DNA hypomethylation induced by ddm1 mutation of *Arabidopsis thaliana. Genetics* **151**, 831-838.

Kankel, M.W., Ramsey, D.E., Stokes, T.L., Flowers, S.K., Haag, J.R., Jeddeloh, J.A., Riddle, N.C., Verbsky, M.L., and Richards, E.J. (2003). *Arabidopsis* MET1 cytosine methyltransferase mutants*. Genetics* **163**, 1109-1122.

Kaya, H., Shibahara, K.I., Taoka, K.I., Iwabuchi, M., Stillman, B., and Araki, T. (2001). FASCIATA genes for chromatin assembly factor-1 in *Arabidopsis* maintain the cellular organization of apical meristems*. Cell* **104**, 131-142.

Koornneef, M., Fransz, P., and de Jong, H. (2003). Cytogenetic tools for *Arabidopsis* thaliana*. Chromosome Res* **11**, 183-194.

Kumekawa, N., Hosouchi, T., Tsuruoka, H., and Kotani, H. (2000). The size and sequence organization of the centromeric region of *Arabidopsis thaliana* chromosome 5*. DNA Res* **7**, 315-321.

Kurdistani, S.K., and Grunstein, M. (2003). Histone acetylation and deacetylation in yeast*. Nat Rev Mol Cell Biol* **4**, 276-284.

Lachner, M., O'Carroll, D., Rea, S., Mechtler, K., and Jenuwein, T. (2001). Methylation of histone H3 lysine 9 creates a binding site for HP1 proteins. *Nature* **410**, 116-120.

Lehnertz, B., Ueda, Y., Derijck, A.A., Braunschweig, U., Perez-Burgos, L., Kubicek, S., Chen, T., Li, E., Jenuwein, T., and Peters, A.H. (2003). Suv39h-mediated histone H3 lysine 9 methylation directs DNA methylation to major satellite repeats at pericentric heterochromatin. *Curr Biol* **13**, 1192-1200.

Lei, H., Oh, S.P., Okano, M., Juttermann, R., Goss, K.A., Jaenisch, R., and Li, E. (1996). De novo DNA cytosine methyltransferase activities in mouse embryonic stem cells. *Development* **122**, 3195-3205.

Leonhardt, H., Page, A.W., Weier, H.U., and Bestor, T.H. (1992). A targeting sequence directs DNA methyltransferase to sites of DNA replication in mammalian nuclei*. Cell* **71**, 865-873.

Leyser, H.M.O., and Furner, I.J. (1992). Charcterisation of three shoot apical meristem mutants of *Arabidopsis thaliana*. *Development* **116**, 397-403.

Lindroth, A.M., Cao, X., Jackson, J.P., Zilberman, D., McCallum, C.M., Henikoff, S., and Jacobsen, S.E. (2001). Requirement of CHROMOMETHYLASE3 for maintenance of CpXpG methylation*. Science* **292**, 2077-2080.

Lo, W.S., Trievel, R.C., Rojas, J.R., Duggan, L., Hsu, J.Y., Allis, C.D., Marmorstein, R., and Berger, S.L. (2000). Phosphorylation of serine 10 in histone H3 is functionally linked in vitro and in vivo to Gcn5-mediated acetylation at lysine 14. *Mol Cell* **5**, 917-926.

Luger, K., Mader, A.W., Richmond, R.K., Sargent, D.F., and Richmond, T.J. (1997). Crystal structure of the nucleosome core particle at 2.8 A resolution. *Nature* **389**, 251-260.

Lusser, A., Brosch, G., Loidl, A., Haas, H., and Loidl, P. (1997). Identification of maize histone deacetylase HD2 as an acidic nucleolar phosphoprotein*. Science* **277**, 88-91.

Lysak, M.A., Fransz, P.F., Ali, H.B., and Schubert, I. (2001). Chromosome painting in *Arabidopsis thaliana. Plant J* **28**, 689-697.

Maluszynska, J., and Heslop-Harrison, J.S. (1991). Localization of tandemly repeated DNA sequences in *Arabidopsis thaliana. Plant J* **1**, 159-166.

Martienssen, R.A., and Colot, V. (2001). DNA methylation and epigenetic inheritance

in plants and filamentous fungi. *Science* **293**, 1070-1074.
Masson, J., and Paskowski, D.J. (1992). The culture response of *Arabidopsis* thaliana protoplasts is determined by the growth conditions of the donor plants. *Plant J* **2**, 829-833.
Mayr, C., Jasencakova, Z., Meister, A., Schubert, I., and Zink, D. (2003). Comparative analysis of the functional genome architecture of animal and *Plant Cell* nuclei. *Chromosome Res* **11**, 471-484.
McKnight, S.L., and Miller, O.L., Jr. (1976). Ultrastructural patterns of RNA synthesis during early embryogenesis of Drosophila melanogaster. *Cell* **8**, 305-319.
Mette, M.F., Aufsatz, W., van der Winden, J., Matzke, M.A., and Matzke, A.J. (2000). Transcriptional silencing and promoter methylation triggered by double-stranded RNA. *Embo J* **19**, 5194-5201.
Miklos, G.L., and Cotsell, J.N. (1990). Chromosome structure at interfaces between major chromatin types: alpha- and beta-heterochromatin. *Bioessays* **12**, 1-6.
Mittelsten Scheid, O., Afsar, K., and Paszkowski, J. (1998). Release of epigenetic gene silencing by trans-acting mutations in Arabidopsis. *Proc Natl Acad Sci USA* **95**, 632-637.
Mittelsten Scheid, O., Paszkowski, J., and Potrykus, I. (1991). Reversible inactivation of a transgene in *Arabidopsis thaliana*. *Mol Gen Genet* **228**, 104-112.
Mittelsten Scheid, O., Probst, A.V., Afsar, K., and Paszkowski, J. (2002). Two regulatory levels of transcriptional gene silencing in Arabidopsis. *Proc Natl Acad Sci USA* **99**, 13659-13662.
Morel, J.B., Mourrain, P., Beclin, C., and Vaucheret, H. (2000). DNA methylation and chromatin structure affect transcriptional and post-transcriptional transgene silencing in Arabidopsis. *Curr Biol* **10**, 1591-1594.
Morgan, G.T., Reeder, R.H., and Bakken, A.H. (1983). Transcription in cloned spacers of Xenopus laevis ribosomal DNA. *Proc Natl Acad Sci USA* **80**, 6490-6494.
Murfett, J., Wang, X.J., Hagen, G., and Guilfoyle, T.J. (2001). Identification of *Arabidopsis* histone deacetylase HDA6 mutants that affect transgene expression. *Plant Cell* **13**, 1047-1061.
Nagele, R.G., Velasco, A.Q., Anderson, W.J., McMahon, D.J., Thomson, Z., Fazekas, J., Wind, K., and Lee, H. (2001). Telomere associations in interphase nuclei: possible role in maintenance of interphase chromosome topology. *J Cell Sci* **114**, 377-388.
Ng, H.H., Robert, F., Young, R.A., and Struhl, K. (2003). Targeted recruitment of Set1 histone methylase by elongating Pol II provides a localized mark and memory of recent transcriptional activity. *Mol Cell* **11**, 709-719.
Okano, M., Bell, D.W., Haber, D.A., and Li, E. (1999). DNA methyltransferases Dnmt3a and Dnmt3b are essential for de novo methylation and mammalian *Development . Cell* **99**, 247-257.
Pandey, R., Muller, A., Napoli, C.A., Selinger, D.A., Pikaard, C.S., Richards, E.J., Bender, J., Mount, D.W., and Jorgensen, R.A. (2002). Analysis of histone acetyltransferase and histone deacetylase families of *Arabidopsis thaliana* suggests functional diversification of chromatin modification among multicellular eukaryotes. *Nucleic Acids Res* **30**, 5036-5055.
Peters, A.H., O'Carroll, D., Scherthan, H., Mechtler, K., Sauer, S., Schofer, C., Weipoltshammer, K., Pagani, M., Lachner, M., Kohlmaier, A., Opravil, S., Doyle, M., Sibilia, M., and Jenuwein, T. (2001). Loss of the Suv39h histone methyltransferases impairs mammalian heterochromatin and genome stability. *Cell* **107**, 323-337.
Probst, A.V., Fagard, M., Proux, F., Mourrain, P., Boutet, S., Earley, K., Lawrence,

R.J., Pikaard, C.S., Murfett, J., Furner, I., Vaucheret, H., and Mittelsten Scheid, O. (2004). *Arabidopsis* histone deacetylase HDA6 is required for maintenance of transcriptional gene silencing and determines nuclear organization of rDNA repeats. *Plant Cell* **16**, 1021-1034.

Probst, A.V., Fransz, P.F., Paszkowski, J., and Mittelsten Scheid, O. (2003). Two means of transcriptional reactivation within heterochromatin. *Plant J* **33**, 743-749.

Rabl, C. (1885). Uber Zellteilung. *Morphol. Jahrbuch*. **10**, 214-330.

Rea, S., Eisenhaber, F., O'Carroll, D., Strahl, B.D., Sun, Z.W., Schmid, M., Opravil, S., Mechtler, K., Ponting, C.P., Allis, C.D., and Jenuwein, T. (2000). Regulation of chromatin structure by site-specific histone H3 methyltransferases. *Nature* **406**, 593-599.

Reik, W., Dean, W., and Walter, J. (2001). Epigenetic reprogramming in mammalian *Development . Science* **293**, 1089-1093.

Rountree, M.R., Bachman, K.E., and Baylin, S.B. (2000). DNMT1 binds HDAC2 and a new co-repressor, DMAP1, to form a complex at replication foci. *Nat Genet* **25**, 269-277.

Sadoni, N., Langer, S., Fauth, C., Bernardi, G., Cremer, T., Turner, B.M., and Zink, D. (1999). Nuclear organization of mammalian genomes. Polar chromosome territories build up functionally distinct higher order compartments. *J Cell Biol* **146**, 1211-1226.

Sandmeier, J.J., French, S., Osheim, Y., Cheung, W.L., Gallo, C.M., Beyer, A.L., and Smith, J.S. (2002). RPD3 is required for the inactivation of yeast ribosomal DNA genes in stationary phase. *Embo J* **21**, 4959-4968.

Santisteban, M.S., Kalashnikova, T., and Smith, M.M. (2000). Histone H2A.Z regulats transcription and is partially redundant with nucleosome remodeling complexes. *Cell* **103**, 411-422.

Santos-Rosa, H., Schneider, R., Bannister, A.J., Sherriff, J., Bernstein, B.E., Emre, N.C., Schreiber, S.L., Mellor, J., and Kouzarides, T. (2002). Active genes are tri-methylated at K4 of histone H3. *Nature* **419**, 407-411.

Saze, H., Mittelsten Scheid, O., and Paszkowski, J. (2003). Maintenance of CpG methylation is essential for epigenetic inheritance during plant gametogenesis. *Nat Genet* **34**, 65-69.

Schermelleh, L., Solovei, I., Zink, D., and Cremer, T. (2001). Two-color fluorescence labeling of early and mid-to-late replicating chromatin in living cells. *Chromosome Res* **9**, 77-80.

Schramke, V., and Allshire, R. (2003). Hairpin RNAs and retrotransposon LTRs effect RNAi and chromatin-based gene silencing. *Science* **301**, 1069-1074.

Schubeler, D., Scalzo, D., Kooperberg, C., van Steensel, B., Delrow, J., and Groudine, M. (2002). Genome-wide DNA replication profile for Drosophila melanogaster: a link between transcription and replication timing. *Nat Genet* **32**, 438-442.

Schwarzacher, H.G., and Wachtler, F. (1983). Nucleolus organizer regions and nucleoli. *Hum Genet* **63**, 89-99.

Selker, E.U. (1998). Trichostatin A causes selective loss of DNA methylation in Neurospora. *Proc Natl Acad Sci USA* **95**, 9430-9435.

Selker, E.U., Tountas, N.A., Cross, S.H., Margolin, B.S., Murphy, J.G., Bird, A.P., and Freitag, M. (2003). The methylated component of the Neurospora crassa genome. *Nature* **422**, 893-897.

Shibahara, K., and Stillman, B. (1999). Replication-dependent marking of DNA by PCNA facilitates CAF-1-coupled inheritance of chromatin. *Cell* **96**, 575-585.

Sijen, T., Vijn, I., Rebocho, A., van Blokland, R., Roelofs, D., Mol, J.N., and Kooter,

J.M. (2001). Transcriptional and posttranscriptional gene silencing are mechanistically related. *Curr Biol* **11**, 436-440.

Sobel, R.E., Cook, R.G., Perry, C.A., Annunziato, A.T., and Allis, C.D. (1995). Conservation of deposition-related acetylation sites in newly synthesized histones H3 and H4. *Proc Natl Acad Sci USA* **92**, 1237-1241.

Soppe, W.J., Jasencakova, Z., Houben, A., Kakutani, T., Meister, A., Huang, M.S., Jacobsen, S.E., Schubert, I., and Fransz, P.F. (2002). DNA methylation controls histone H3 lysine 9 methylation and heterochromatin assembly in Arabidopsis. *Embo J* **21**, 6549-6559.

Spector, D.L. (2001). Nuclear domains. *J Cell Sci* 114, 2891-2893.

Steimer, A., Amedeo, P., Afsar, K., Fransz, P., Mittelsten Scheid, O., and Paszkowski, J. (2000). Endogenous targets of transcriptional gene silencing in Arabidopsis. *Plant Cell* **12**, 1165-1178.

Sterner, D.E., and Berger, S.L. (2000). Acetylation of histones and transcription-related factors. Microbiol Mol Biol Rev **64**, 435-459.

Stillman, B. (1986). Chromatin assembly during SV40 DNA replication in vitro*. Cell* **45**, 555-565.

Strahl, B.D., and Allis, C.D. (2000). The language of covalent histone modifications. *Nature* **403**, 41-45.

Sullivan, K.F., Hechenberger, M., and Masri, K. (1994). Human CENP-A contains a histone H3 related histone fold domain that is required for targeting to the centromere. *J Cell Biol* **127**, 581-592.

Tachibana, M., Sugimoto, K., Nozaki, M., Ueda, J., Ohta, T., Ohki, M., Fukuda, M., Takeda, N., Niida, H., Kato, H., and Shinkai, Y. (2002). G9a histone methyltransferase plays a dominant role in euchromatic histone H3 lysine 9 methylation and is essential for early embryogenesis. *Genes Dev* **16**, 1779-1791.

Takahashi, K., Chen, E.S., and Yanagida, M. (2000). Requirement of Mis6 centromere connector for localizing a CENP-A-like protein in fission yeast*. Science* **288**, 2215-2219.

Takeda, S., Tadele, Z., Hofmann, I., Probst, A.V., Angelis, K.J., Kaya, H., Araki, T., Mengiste, T., Scheid, O.M., Shibahara, K., Scheel, D., and Paszkowski, J. (2004). BRU1, a novel link between responses to DNA damage and epigenetic gene silencing in Arabidopsis. *Genes Dev* **18**, 782-793.

Talbert, P.B., Masuelli, R., Tyagi, A.P., Comai, L., and Henikoff, S. (2002). Centromeric localization and adaptive evolution of an *Arabidopsis* histone H3 variant. *Plant Cell* **14**, 1053-1066.

Tanabe, H., Muller, S., Neusser, M., von Hase, J., Calcagno, E., Cremer, M., Solovei, I., Cremer, C., and Cremer, T. (2002). Evolutionary conservation of chromosome territory arrangements in cell nuclei from higher primates. *Proc Natl Acad Sci USA* **99**, 4424-4429.

Tariq, M., Saze, H., Probst, A.V., Lichota, J., Habu, Y., and Paszkowski, J. (2003). Erasure of CpG methylation in *Arabidopsis* alters patterns of histone H3 methylation in heterochromatin. *Proc Natl Acad Sci USA* **100**, 8823-8827.

Tian, L., and Chen, Z.J. (2001). Blocking histone deacetylation in *Arabidopsis* induces pleiotropic effects on plant gene regulation and *Development* . *Proc Natl Acad Sci USA* **98**, 200-205.

Turner, B.M., Birley, A.J., and Lavender, J. (1992). Histone H4 isoforms acetylated at specific lysine residues define individual chromosomes and chromatin domains in Drosophila polytene nuclei*. Cell* **69**, 375-384.

Verdel, A., Jia, S., Gerber, S., Sugiyama, T., Gygi, S., Grewal, S.I., and Moazed, D.

(2004). RNAi-mediated targeting of heterochromatin by the RITS complex. *Science* **303**, 672-676.

Vertino, P.M., Sekowski, J.A., Coll, J.M., Applegren, N., Han, S., Hickey, R.J., and Malkas, L.H. (2002). DNMT1 is a component of a multiprotein DNA replication complex. *Cell* Cycle **1**, 416-423.

Volpe, T.A., Kidner, C., Hall, I.M., Teng, G., Grewal, S.I., and Martienssen, R.A. (2002). Regulation of heterochromatic silencing and histone H3 lysine-9 methylation by RNAi. *Science* **297**, 1833-1837.

Volpi, E.V., Chevret, E., Jones, T., Vatcheva, R., Williamson, J., Beck, S., Campbell, R.D., Goldsworthy, M., Powis, S.H., Ragoussis, J., Trowsdale, J., and Sheer, D. (2000). Large-scale chromatin organization of the major histocompatibility complex and other regions of human chromosome 6 and its response to interferon in interphase nuclei. *J Cell Sci* **113** (Pt 9), 1565-1576.

Vongs, A., Kakutani, T., Martienssen, R.A., and Richards, E.J. (1993). *Arabidopsis* thaliana DNA methylation mutants. *Science* **260**, 1926-1928.

Wei, Y., Yu, L., Bowen, J., Gorovsky, M.A., and Allis, C.D. (1999). Phosphorylation of histone H3 is required for proper chromosome condensation and segregation. *Cell* **97**, 99-109.

Wu, K., Malik, K., Tian, L., Brown, D., and Miki, B. (2000). Functional analysis of a RPD3 histone deacetylase homologue in *Arabidopsis thaliana*. *Plant Mol Biol* **44**, 167-176.

Xie, Z., Kasschau, K.D., and Carrington, J.C. (2003). Negative feedback regulation of Dicer-Like1 in *Arabidopsis* by microRNA-guided mRNA degradation. *Curr Biol* **13**, 784-789.

Yan, L., Loukoianov, A., Blechl, A., Tranquilli, G., Ramakrishna, W., SanMiguel, P., Bennetzen, J.L., Echenique, V., and Dubcovsky, J. (2004). The wheat VRN2 gene is a flowering repressor down-regulated by vernalization. *Science* **303**, 1640-1644.

Yan, Q., Huang, J., Fan, T., Zhu, H., and Muegge, K. (2003). Lsh, a modulator of CpG methylation, is crucial for normal histone methylation. *Embo J* **22**, 5154-5162.

Yang, X.J., and Seto, E. (2003). Collaborative spirit of histone deacetylases in regulating chromatin structure and gene expression. *Curr Opin Genet Dev* **13**, 143-153.

You, A., Tong, J.K., Grozinger, C.M., and Schreiber, S.L. (2001). CoREST is an integral component of the CoREST- human histone deacetylase complex. *Proc Natl Acad Sci USA* **98**, 1454-1458.

Zegerman, P., Canas, B., Pappin, D., and Kouzarides, T. (2002). Histone H3 lysine 4 methylation disrupts binding of nucleosome remodeling and deacetylase (NuRD) repressor complex. *J Biol Chem* **277**, 11621-11624.

Zhang, Y., and Reinberg, D. (2001). Transcription regulation by histone methylation: interplay between different covalent modifications of the core histone tails. *Genes Dev* **15**, 2343-2360.

Zhou, Y.B., Gerchman, S.E., Ramakrishnan, V., Travers, A., and Muyldermans, S. (1998). Position and orientation of the globular domain of linker histone H5 on the nucleosome. *Nature* **395**, 402-405.

Zilberman, D., Cao, X., and Jacobsen, S.E. (2003). ARGONAUTE4 control of locus-specific siRNA accumulation and DNA and histone methylation. *Science* **299**, 716-719.